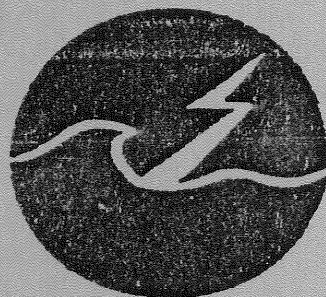


THE GROUP FOR WAVE ENERGY RESEARCH

CHALMERS UNIVERSITY OF TECHNOLOGY



WAVE - POWER BUOYS

Model Experiments;

efficiency and hydrodynamic coefficients.

Lars Bergdahl

Nils Mårtensson

ISSN 0280-5987

REPORT GR:55

GÖTEBORG

FEBRUARY 1984

WAVE-POWER BUOYS

Model Experiments; efficiency and
hydrodynamic coefficients.

Lars Bergdahl

Nils Mårtensson

PREFACE

This work was performed as a part of the Swedish wave energy research programme. The work was supported by the Swedish Energy Research Commission (EFN).

Chalmers, February 1984

Lars Bergdahl

Nils Mårtensson

SUMMARY

Model tests with a wave-power buoy, diameter 300 mm, was performed in a wave-basin (18.3 x 9.3 x 0.8 m) in irregular unidirectional waves. Amplitude respons functions, capture width ratio as a function of frequency and total capture width ratio were measured for two different spectra and for buoy weights from 5 kg to 16 kg and varying external damping (power take off).

The experimental results show that it is important that the diameter and draft of the buoy is adjusted to the wave spectrum for the tested passive system.

Mean values for added mass and added damping was calculated by a regression technique for each experiment. Nondimensional graphs are presented for these quantities. The graphs can be used for the design of prototype buoys.

LIST OF CONTENTS

1.	INTRODUCTION	1
2.	LABORATORY TESTS	
2.1	Objective	2
2.2	Experimental Arrangements	2
2.3	Wave Spectra	3
2.4	Measuring Equipment	5
3.	THEORY	
3.1	Hydrodynamic Model	6
3.2	Analysis	8
4.	EXPERIMENTAL RESULTS	
4.1	Capture Width Ratio	12
4.2	Evaluation of Frequency Independent Hydrodynamic Coefficients	16
4.3	Nondimensional Relations for the Frequency Independent Hydrodynamic Coefficients	18
5.	CONCLUSIONS	24
	References	25
	Appendix A1 Diagrams of buoy response	

1. INTRODUCTION

Since 1976 the Group for Wave Energy Research in Gothenburg has studied the utilization of wave energy from Swedish coastal waters. This work has partly been presented at two international symposia 1979 in Göteborg, Sweden, and 1982 in Trondheim, Norway.

The work has covered many aspects; hydrodynamics, model experiments, field tests, electrical generation, connection to main grid, wave characteristics, power fluctuations and the construction of wave power plants.

Below model tests of wave energy buoys in irregular waves are accounted for.

The presented experiments were performed 1980 and 1981, but were not completely evaluated until recently.

2. LABORATORY TESTS

2.1 Objective

Model tests with a wave power buoy were performed in pseudo-random long-crested sea in a wave tank. For a given sea state and buoy diameter the mass and external damping were varied in order to tune the buoy to the spectrum and get out the most power from the waves. Hydrodynamic coefficients for a simple scaling to prototype sizes were also searched for.

2.2 Experimental Arrangements

The experiments were performed in a wave tank with the measures 18.3 x 9.3 x 0.8 m (length x breadth x depth). The water depth was kept at 0.67 m.

The wave tank was equipped with a wave generator of the plunger type. The plunger motions were brought about with a hydraulic servo cylinder, steered either in a sine motion or in any other prescribed motion if fed with a punched tape.

See Figure 1.

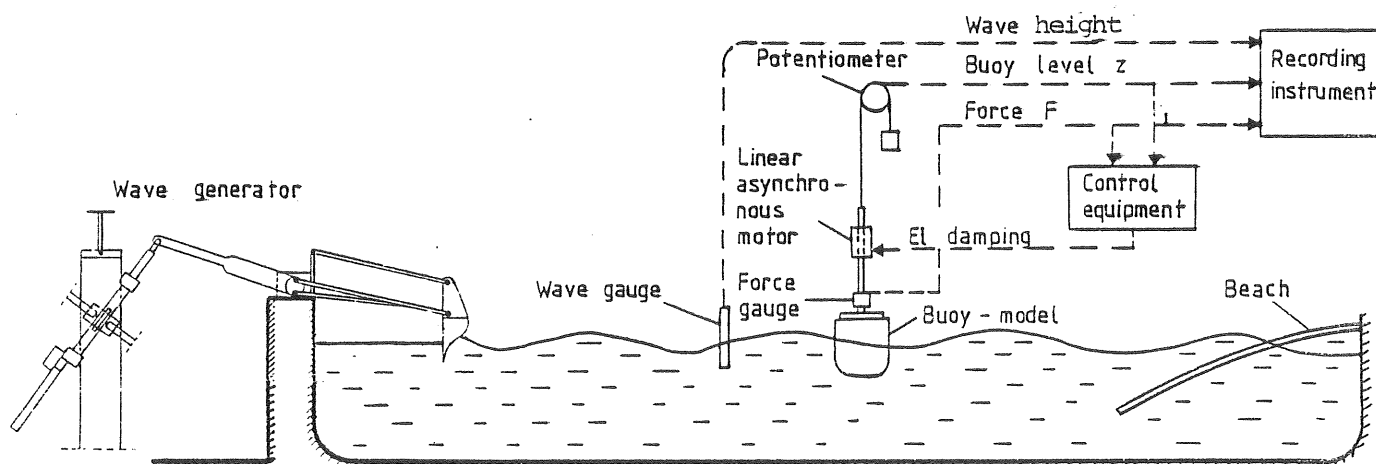
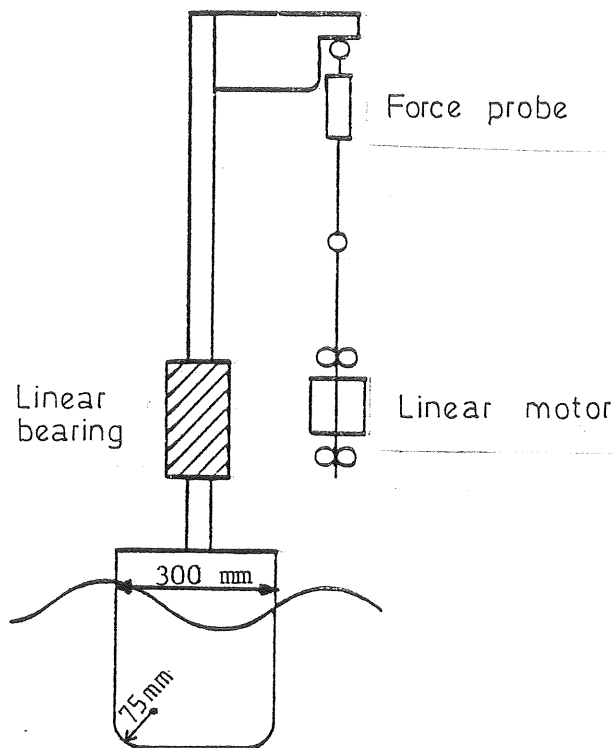


Figure 1. Experimental arrangements in the wave tank.



The modelled point absorber consisted of a vertical circular cylinder with a rounded bottom edge. It was tested in heave motion, and its power take-off was simulated with a linear motor, which was steered as to give a breaking force directly proportional to its heave velocity. Its constant of proportionality could be varied over a wide range. The experimental rig is sketched in Figure 2.

Figure 2. Experimental rig and buoy shape.

2.3 Wave Spectra

Two different wave spectra were used in the experiments. One had the spectrum width $\epsilon = 0.5$ and is called spectrum G0 below. The other had the spectrum with $\epsilon = 0.3$ and is called spectrum G4 below.

The shape of the latter spectrum was closest to a PM spectrum. Measured examples of the spectra are given in Figure 3.

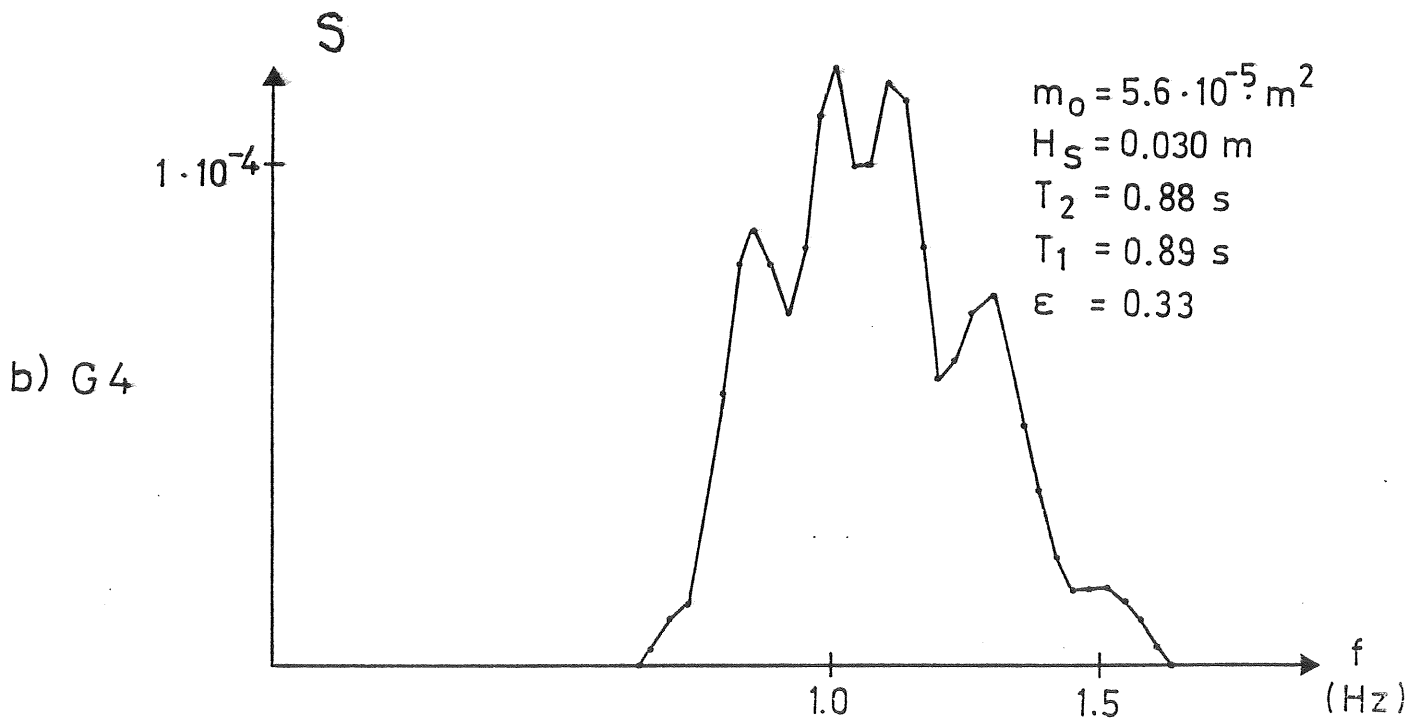
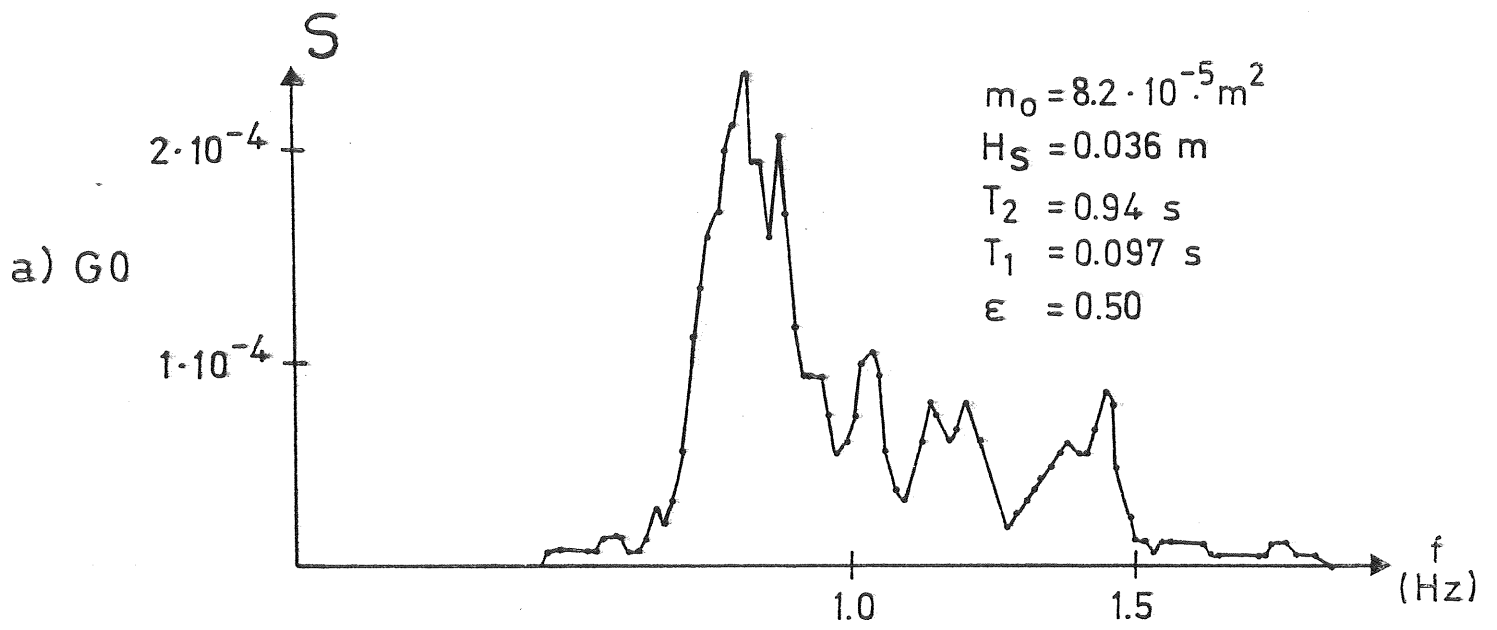


Figure 3. Examples of measured wave spectra.

2.4 Measuring Equipment

The measuring equipment consisted of probes with amplifiers and filters for measuring the waves (e.g. water level), buoy position and breaking force. The vertical position of the buoy was differentiated in an electronic filter to yield the velocity.

The signals of buoy velocity and breaking force were fed to the damping regulator for the buoy. The wave, buoy position buoy velocity and breaking force signals were recorded by a desk computer (Compucorp 625 Mark II) for subsequent analysis.

3. THEORY

3.1 Hydrodynamic model

The analysis and discussion of experimental results make use of the following simple mathematical model for the vertical motion of the buoy in regular waves. The oscillating system is also assumed to be linear and thus the principle of superposition is used for parts of the evaluation.

In a regular wave

$$\zeta(t) = \zeta_0 \cos \omega t \quad (1)$$

the heave motion is expressed as a second order differential equation

$$(m+a)\ddot{z} + (b+b_1)\dot{z} + cz = F_0 \cos(\omega t + \varphi) \quad (2)$$

where

$$F_0 = \zeta_0 \left\{ (c - a\omega^2)^2 + (b\omega)^2 \right\}^{1/2} e^{-kD} \quad (3)$$

is the driving force of the waves and

$\zeta(t)$	water level at the time t
ζ	wave amplitude
t	time
ω	angular frequency of the wave
m	accelerated masses
a	added mass
z	Position of the buoy
b	hydrodynamic damping
b_1	external damping of generator and functional forces
c	Hydrostatic restoring stiffness
k	wave number
D	draft of the buoy
φ	phase angle of the driving force

The spring constant c is

$$c = \rho g A \quad (4)$$

Where A is the cross-sectional area in the waterline and ρ is the density of the water.

Assuming that all coefficients are constant with respect to time, the following solution is obtained.

$$z(t) = z_0 \cdot \cos(\omega t + \psi) \quad (5)$$

where

$$\frac{z_0}{\zeta_0} = Y = \left[\frac{(c - a\omega^2)^2 + (b\omega)^2}{(c - (m+a)\omega^2)^2 + (b+b_1)^2 \omega^2} \right]^{1/2} e^{-kD} \quad (6)$$

ψ is the phase angle between the heave and the water surface. Y is usually called the amplitude response ratio.

The hydrodynamic factors a and b are, properly speaking, functions of the frequency of the oscillations, the shape and displacement of the buoy, the water depth and the boundaries of the horizontal plane.

Usually two dimensionless quantities μ and ϵ are defined as

$$\mu(\omega) = a / (\rho V) \quad (7)$$

$$\epsilon(\omega) = b / (\rho V \omega) \quad (8)$$

where V is the volume of the displacement.

The mean power take-off in regular waves is

$$P = (\rho^2 z_O^2 b_1^2) / 2 \quad (9)$$

This expression can be related to the mean power per unit length of wave front

$$p = \rho \cdot g^2 \cdot \zeta_O^2 / (4\omega) \quad (10)$$

by introducing the capture width ratio

$$\eta = P / (2pr) = \frac{b_1 \omega^3 Y^2}{\rho g^2 r} \quad (11)$$

where r is the radius of the buoy.

3.2 Analysis

The programme in the desk computer performed a fast fourier transform of the measured signals of wave and buoy position simultaneously. Examples of calculated wave and buoy spectra are given in Figur 4a and b.

The spectral moments m_{-1} to m_4 were calculated for the water surface level and buoy position. The n :th spectral moment is defined as

$$m_n = \int f^n S(f) df \quad (12)$$

where S is the spectrum
 f the frequency (in Herz)
 and n an integer.

H_S was thereafter given as

$$H_S = 4 m_0^{1/2} \quad (13)$$

The zero-crossing period T_z was not measured but the periods

$$T_1 = m_0/m_1 \quad (14)$$

and $T_2 = (m_0/m_2)^{1/2} \quad (15)$

were calculated instead, and the following inequality was assumed to be valid

$$T_2 < T_z < T_1 \quad (16)$$

The spectrum width was calculated as

$$\epsilon = (1 - m_2^2 / (m_0 m_4))^{1/2} \quad (17)$$

a) Wave Spectrum

$$\begin{aligned}
 m_{-1} &= 5.16 \cdot 10^{-5} \text{ m}^2 \text{ s} \\
 m_0 &= 5.66 \cdot 10^{-5} \text{ m}^2 \\
 m_1 &= 6.48 \cdot 10^{-5} \text{ m}^2 / \text{s} \\
 m_2 &= 7.47 \cdot 10^{-5} \text{ m}^2 / \text{s}^2 \\
 m_4 &= 1.11 \cdot 10^{-4} \text{ m}^2 / \text{s}^4 \\
 H_s &= 3.0 \cdot 10^{-2} \text{ m} \\
 0.871 < T_z < 0.884 \text{ s} \\
 \epsilon &= 0.32
 \end{aligned}$$

b) Buoy Spectrum

$$\begin{aligned}
 m_{-1} &= 7.48 \cdot 10^{-5} \text{ m}^2 \text{ s} \\
 m_0 &= 7.72 \cdot 10^{-5} \text{ m}^2 \\
 m_1 &= 8.10 \cdot 10^{-5} \text{ m}^2 / \text{s} \\
 m_2 &= 8.61 \cdot 10^{-5} \text{ m}^2 / \text{s}^2 \\
 m_4 &= 1.02 \cdot 10^{-4} \text{ m}^2 / \text{s}^4 \\
 H_s &= 3.5 \cdot 10^{-2} \text{ m} \\
 0.947 < T_z < 0.954 \text{ s} \\
 \epsilon &= 0.23
 \end{aligned}$$

c) Amplitude Responsed) Capture Width Ratio

Total capture width ratio
 $\eta_{\text{tot}} = 0.27$.
 Captured power 0.032 W

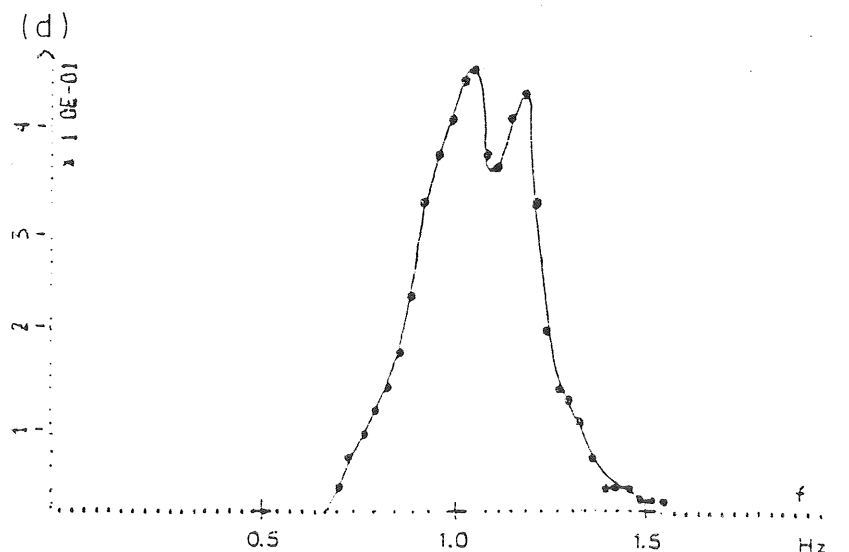
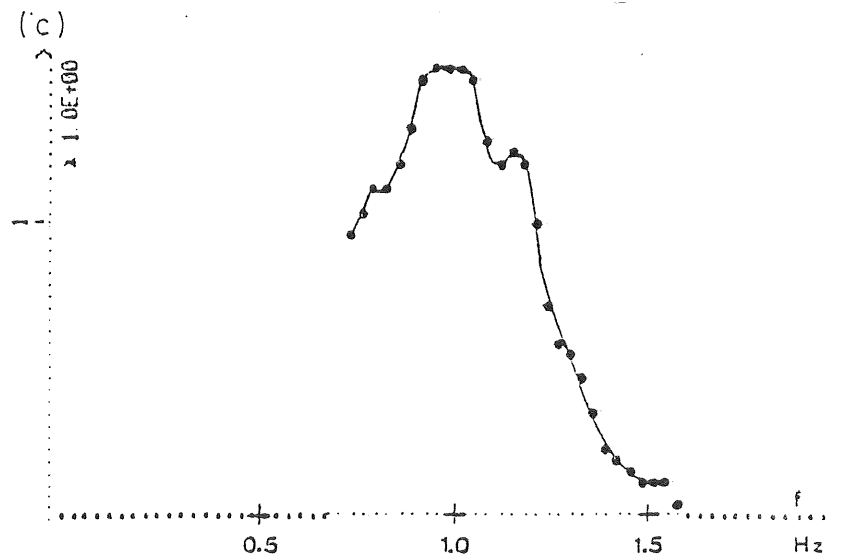
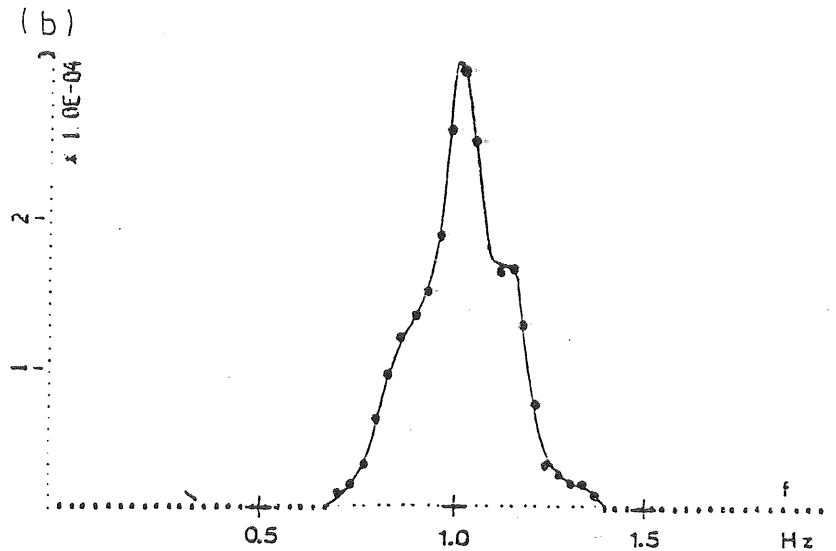
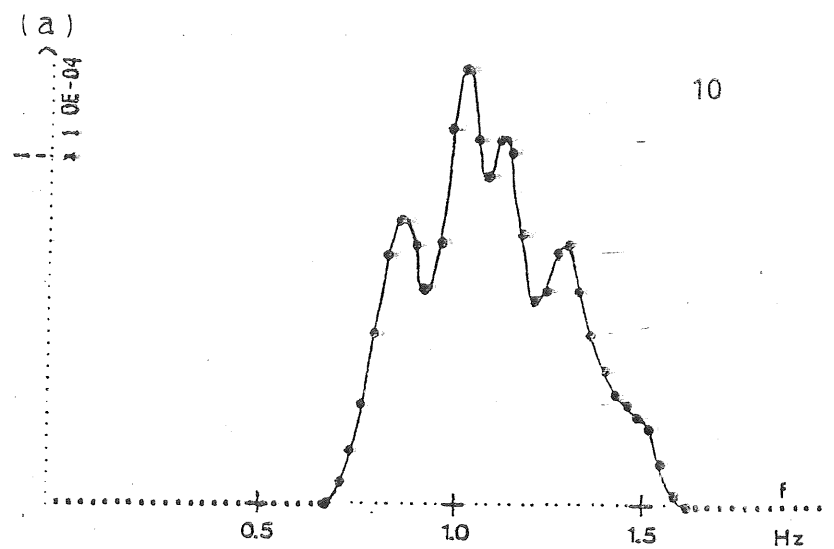


Figure 4. Example of an automatically evaluated experiment. Random sea.
 Date 80-10-29 No 2
 Spectrum G4. Mass 10 kg
 Ext. damping 18 Ns/m

The amplitude response $Y(\omega)$ was subsequently formed as

$$Y(\omega) = \frac{\widehat{X^*(\omega) \cdot Z(\omega)}}{\widehat{X^*(\omega) \cdot X(\omega)}}$$

where X and Z are the complex raw spectra of wave and buoy position. The "roofs" indicate smoothing and the asterisk complex conjugate. The use of the ratio between the products above instead of the simple ratio $Y = \widehat{Z(\omega)} / \widehat{X(\omega)}$ gives an efficient filtering of noise contained in only one of the signals. A calculated amplitude response is shown in Figure 4c.

The calculated amplitude response curve was thereafter used for calculating the capture width ratio η as a function of frequency by Eq. (11). The capture width ratio as a function of frequency is shown in Figure 4d.

Finally a total capture width ratio, in the actual experiment, was calculated as

$$\eta_{\text{tot}} = \frac{\int \eta(\omega) S(\omega) / \omega \, d\omega}{\int S(\omega) / \omega \, d\omega}$$

where $S(\omega)$ is the wave spectrum.

For some few experiments the captured energy (the numerator above) was also calculated as the time average of the product of breaking force and buoy velocity. The results were nearly identical.

4. EXPERIMENTAL RESULTS

4.1 Capture Width Ratio (Efficiency)

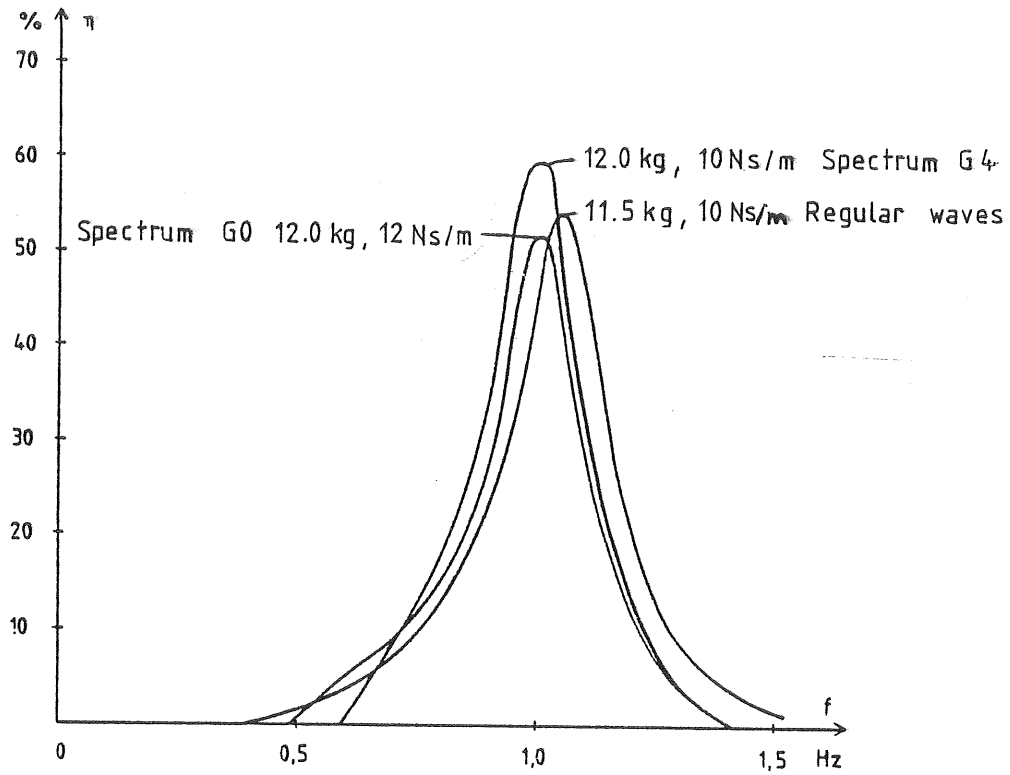
The buoy was tested in the two described wave conditions. Its diameter was kept constant (300 mm) but its mass was varied from 4 to 16 kg which is equivalent to an average draft of 0.06 to 0.23 m. The external damping was varied between 5 and 30 Ns/m.

In order to show the degree of accordance between old experiments in regular sinusoidal waves and the experiments in the two different wave spectra, the capture width ratio for three comparable experiments are shown in Figure 5.

A comparison between the experiments with the two spectra shows a good agreement as to the frequency position of the graphs of the capture width ratio. In comparison with the corresponding experiments in regular waves the maxima seem to have been translated a little towards lower frequencies. The difference is, however, not significant with respect to inaccuracies in the analyses.

At low damping (Figure 5a) the graphs of the capture width ratio show good agreement between the experiments in regular waves and the experiments in waves of both wave spectra. At higher damping (Figure 5b) the difference between the experiments in regular waves and the experiments in random waves seems to be greater.

a) External damping $b_1 = 10 \text{ Ns/m}$



b) External damping $b_1 = 16 \text{ Ns/m}$

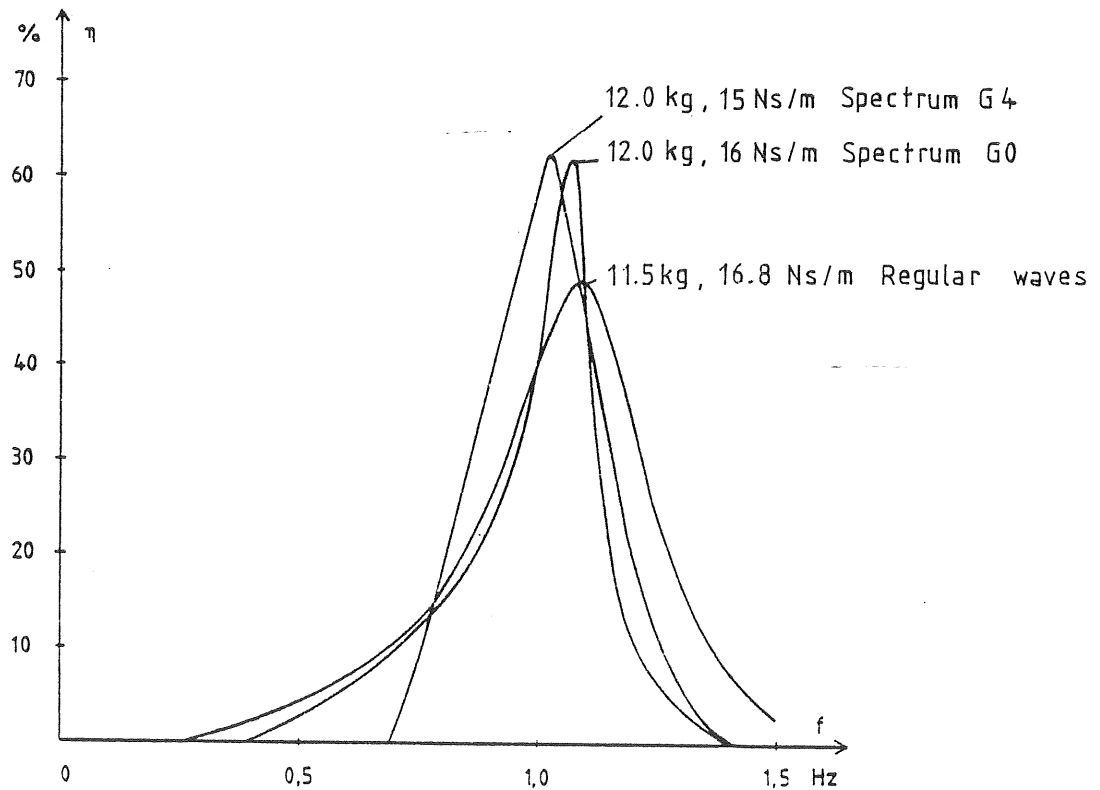


Figure 5 Capture width ratio as a function of frequency for approximately the same mass and damping in regular waves and in waves with the spectra G0 and G4.

The total capture width ratios as functions of mass and external damping for the wave power buoy in the two pseudo-random seas are illustrated in Figure 6 for spectrum G0 and in Figure 7 for spectrum G4.

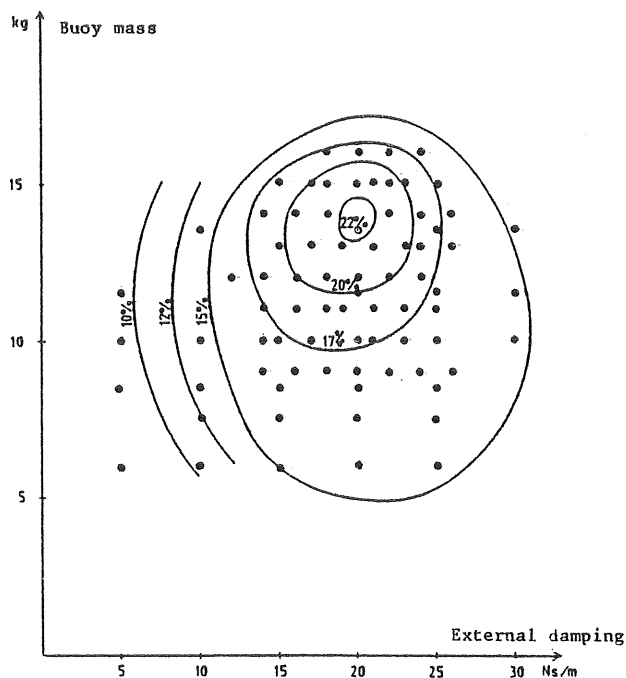


Fig 6. Contours of total capture width ratio as a function of mass and damping. Spectrum G0.

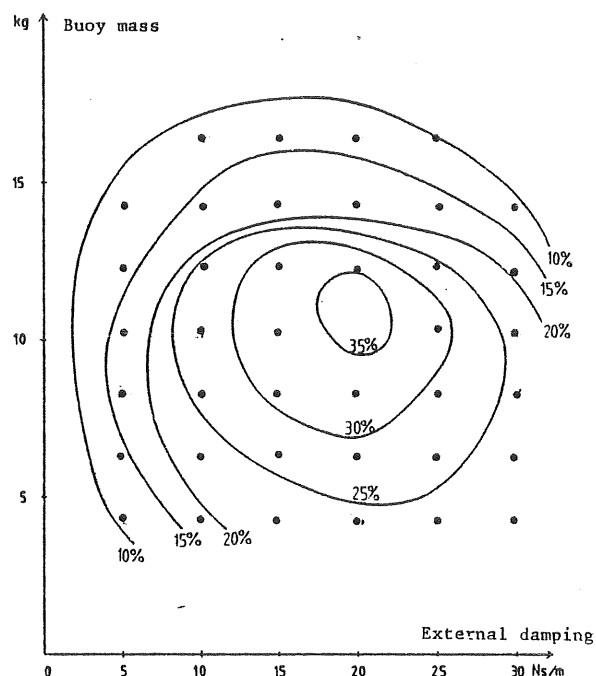


Fig 7. Contours of total capture width ratio as a function of mass and damping. Spectrum G4

Every experiment is represented by a point indicating a certain combination of mass and damping. For every such point the capture width ratio was measured. Contours for levels of equal total capture width ratio were approximately drawn between the measured points.

The difference of capture width, between the two different spectra, depends on the spectral shapes and the location of the spectra along the frequency axis. As the diameter of the buoy was kept constant ($\phi = 300$ mm) there was only a limited possibility to tune the buoy by changing mass and damping.

Spectrum G0 was the wider spectrum (see Figure 3a) but contained a narrow maximum within its lower range of frequencies. In order to increase the capture width at such low frequencies the mass of the buoy was increased. The total capture width ratio had a maximum ($\eta_{\text{tot}} = 22\%$) for a mass of 14 kg and a damping of 20 Ns/m. (See Figure 6), which implies that it would have been more efficient to increase the diameter of the buoy in the given spectrum.

The spectrum G4 was better adapted to the buoy with respect to frequency. Therefore the total capture width ratio had a maximum for a lower mass (11 kg) than for spectrum G0. The spectrum G4 was also more narrow. The combined effect was that the total capture width ratio was found to be higher ($\eta_{\text{tot}} = 36\%$). The optimal damping was found to be equal for both spectrum (20 Ns/m).

4.2 Evaluation of Frequency Independent Hydrodynamic Coefficients.

In the experiments the capture width ratio was calculated by using the measured amplitude response, and for comparison by direct integration of breaking force times velocity. For the scaling up of devices to full scale and for evaluating their capture width ratio in prototype seas, however, the amplitude response function Eq.(6) has been used by the Wave Energy Group in Gothenburg. In that work the quantities μ and ϵ (Eq. 7 and 8) have been assumed constant for each condition.

In order to evaluate average frequency independent μ and ϵ from the experiments, the best fit of Eq.(6) to the experimental points was searched in the meaning of the method of least squares by minimizing the function.

$$S(\mu, \epsilon) = \sum_i (Y(\omega_i, \mu, \epsilon) - \tilde{Y}_i(\omega_i))^2$$

where $Y(\omega_i, \mu, \epsilon)$ is the theoretical function Eq.(6) and \tilde{Y}_i is the experimental value for the frequency ω_i .

The minimization was performed with the help of a FORTRAN programme that utilizes the method of Davidon-Fletcher-Powell (Eriksson (1974)).

In Figure 8a and 8b two examples are shown where the fitted curve, experimental points and the resulting values of μ and ϵ are shown.

Figure 8a shows a reasonably good fit between experimental points and the approximate theoretical function Eq.(6). In Fig. 8b where the buoy was strongly damped the fit is still reasonable but the values of μ and ϵ are unrealistic. Generally, experimental functions, where $Y < 1$ for all frequencies, give strange values. In such cases the efficiency is also very small and therefore they are of less interest.

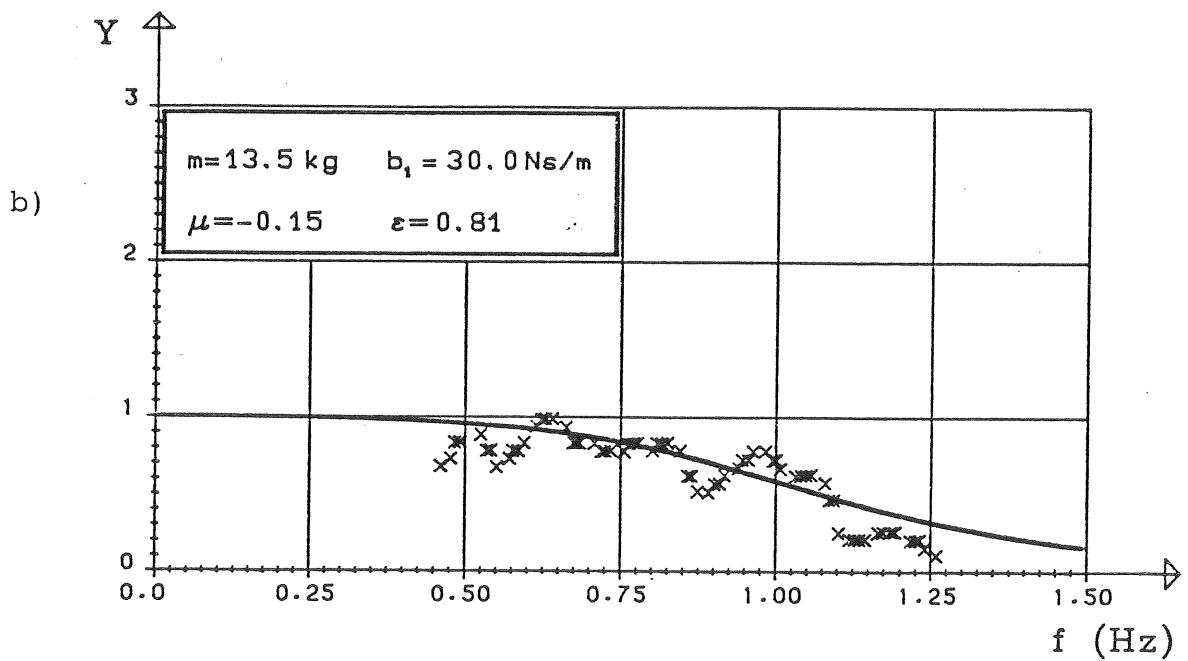
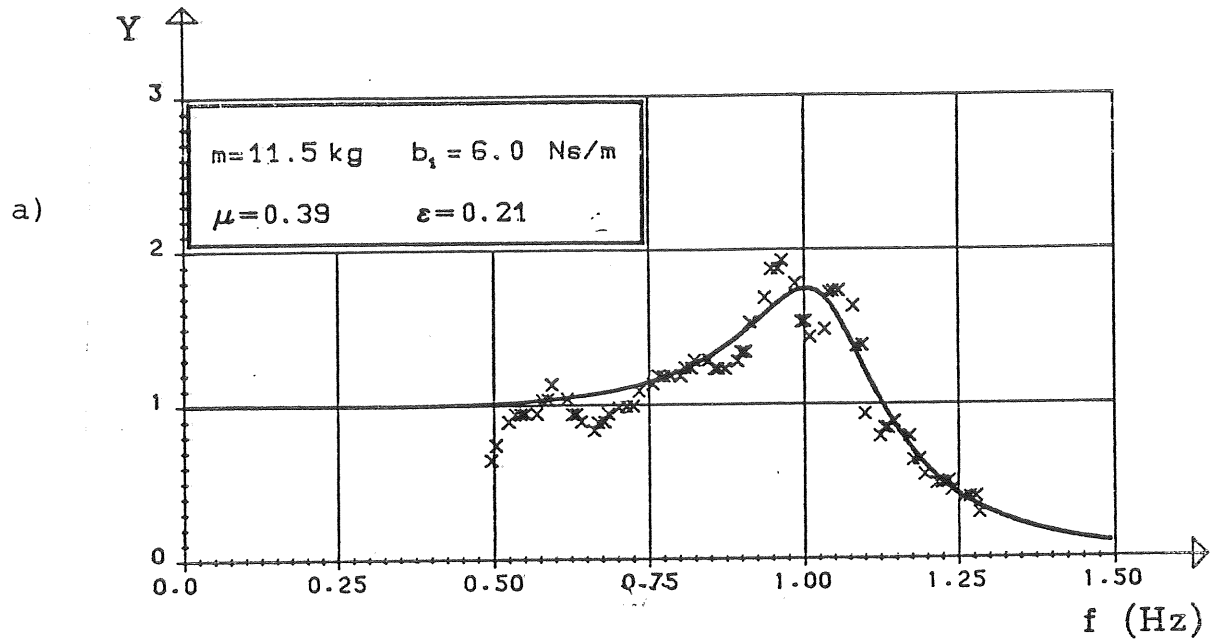


Figure 8 Examples of fits between experimental and theoretical amplitude responses.

4.3 Non-dimensional Relations for the Frequency Independent Hydrodynamic Coefficients.

The frequency independent (see above) hydrodynamic coefficients μ and ϵ were plotted as functions of several non-dimensional quantities. It was found that the added mass gave the most well defined curves if it was normalized against the mass of half a sphere of water $\hat{m} = \rho 2\pi r^3/3$ rather than against the mass of the displaced volume. To this end a new quantity $\hat{\mu}$ was defined;

$$\hat{\mu} = a/\hat{m} = \mu m/\hat{m} \quad (20)$$

In the first figures below $\hat{\mu}$ and ϵ are plotted as functions of the ratio between the external damping and mass times the formal natural frequency ω_N^* , which here is defined $\sqrt{c/m}$.

$$\Omega = \frac{b_1}{m \omega_N^*} \quad (21)$$

This representation is convenient because then $\hat{\mu}$ and ϵ can be read explicitly from the diagrams. For $\hat{\mu}$ this was also the best representation. For ϵ an alternative is shown further below.

In Figure 9a and b all the experimental values are plotted, and in Figure 10a and b all points with the amplitude ratio $Y \leq 1$ for all frequencies are excluded. The latter figures yield more well defined functions.

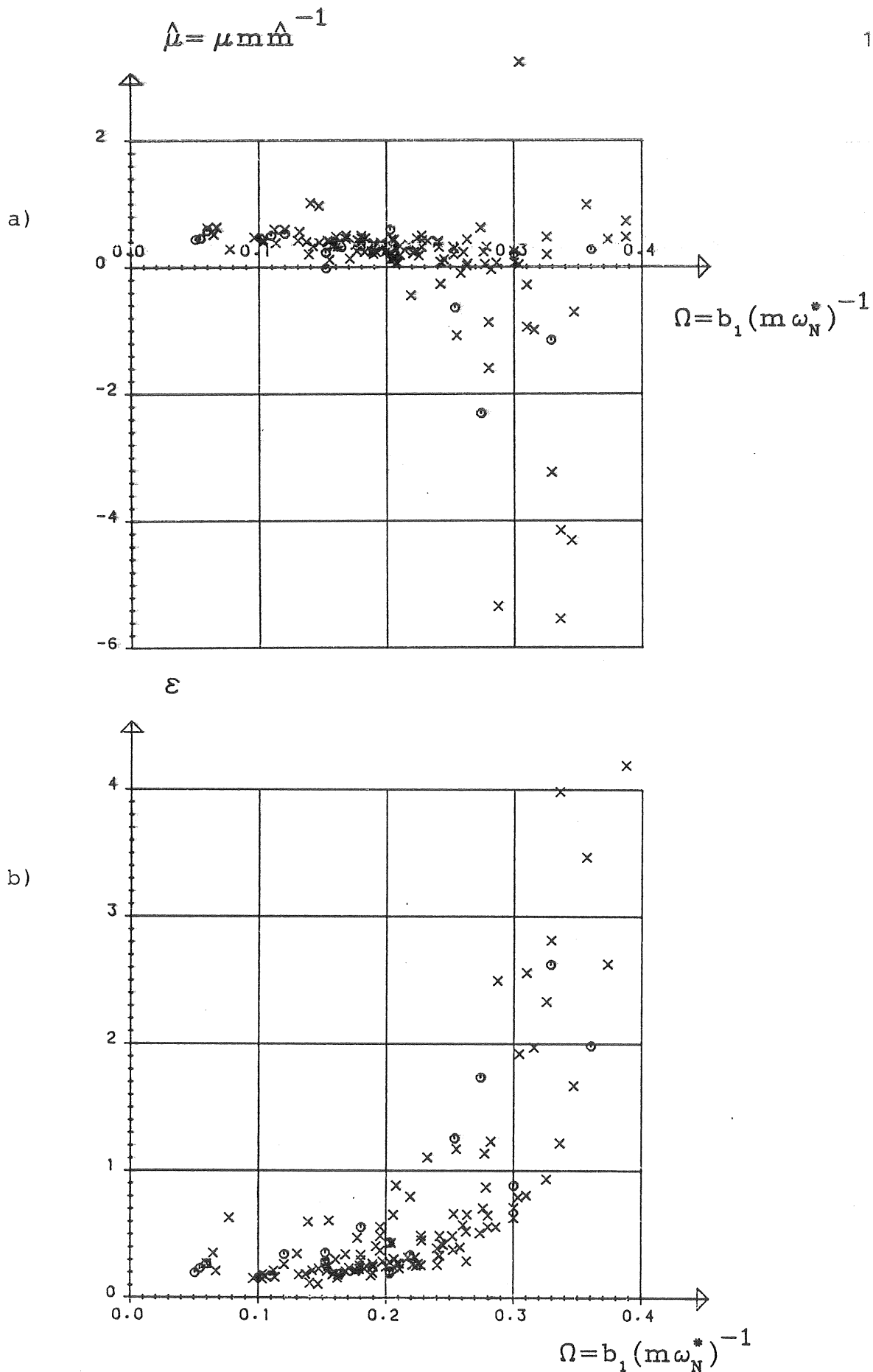


Figure 9. $\hat{\mu}$ and ε as functions of the dimensionless external damping Ω . All experiments. Marks; x - spectrum G0 and o - spectrum G4.

In Figure 11a and b fitted least squares polynomials are drawn. For $\hat{\mu}$ no significant improvement in the fitting was gained for higher order polynomials than for the chosen first order. As can be seen in Figure 11a, $\hat{\mu}$ was fitted to the selected points from Figure 10a. This was done because the values of $\hat{\mu}$ were very scattered for higher Ω . For ϵ a fourth order polynomial was chosen for the same reason as for $\hat{\mu}$'s polynomial. ϵ , however, was fitted to all experimental points because of the nice asymptotic values of ϵ for high Ω (see Fig.12)

The polynomials are for the normalized added mass;

$$\hat{\mu} = -1.9 \Omega + 0.66 \quad (22)$$

and for the hydrodynamic damping;

$$\epsilon = 1000 \Omega^4 - 380 \Omega^3 + 27\Omega^2 + 3\Omega \quad (23)$$

here $\Omega = b_1 (m \cdot \omega_N^*)^{-1}$

and $\omega_N^* = (c/m)^{1/2}$

where m is mass of the buoy

b_1 is external damping

$c = \rho g A$; buoy stiffness.

In Figure 13 an implicit relation for ϵ is plotted. This implicit relation gives a good fit because ϵ is plotted against the inverse of the sum of mass and added mass and because ϵ is contained in the independent variable as $b = \epsilon m(1+\mu) \omega_N^*$. This last regression curve has the equation

$$\epsilon = 0.07 \Omega^2 + 0.68 \Omega \quad (24)$$

with $\Omega = (b+b_1) (m(1+\mu) \omega_N^*)^{-1}$

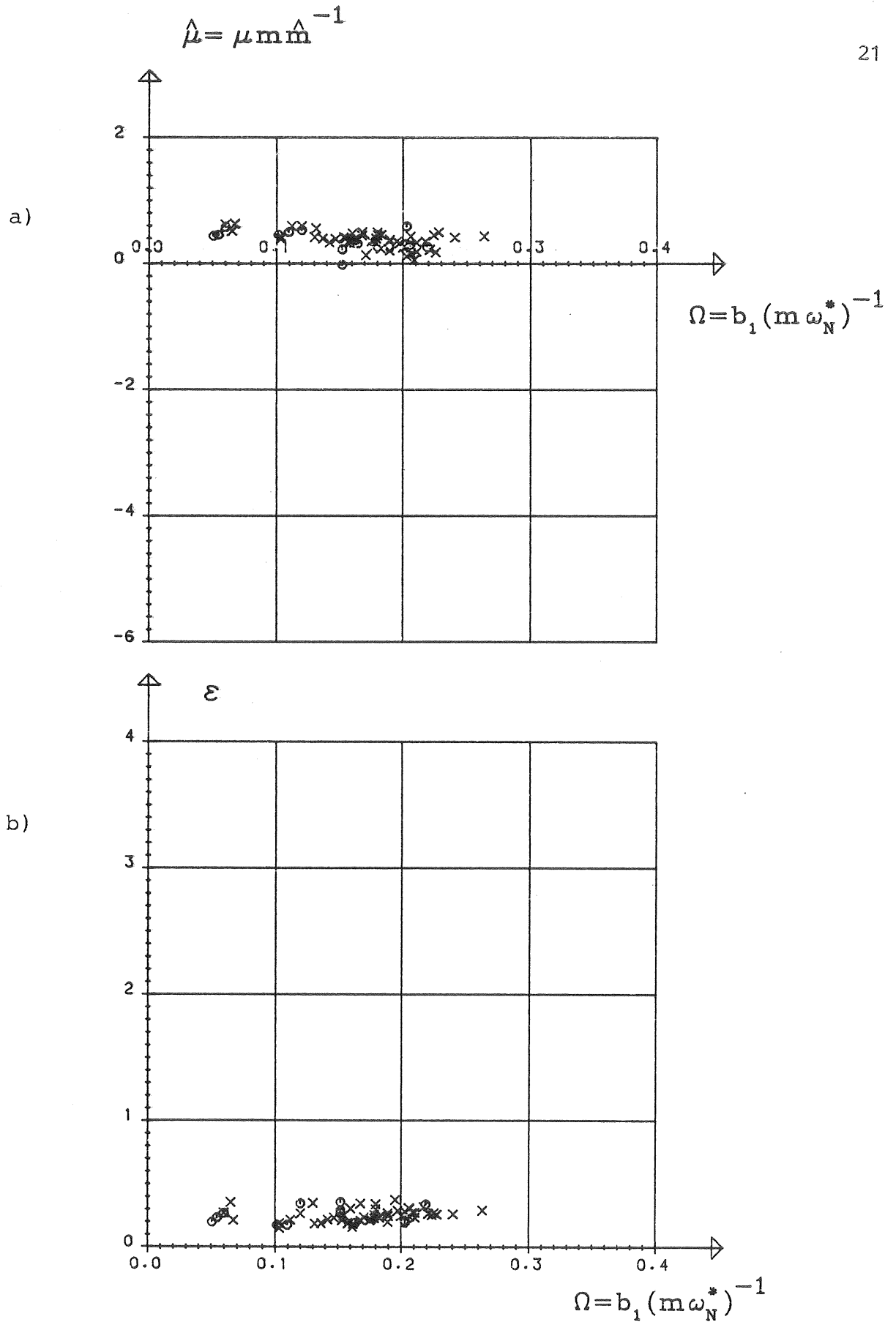


Figure 10 $\hat{\mu}$ and ε as functions of the dimensionless external damping Ω . Experiments selected with amplitude respons greater than one.

Marks; x - spectrum G0 and o - spectrum G4.

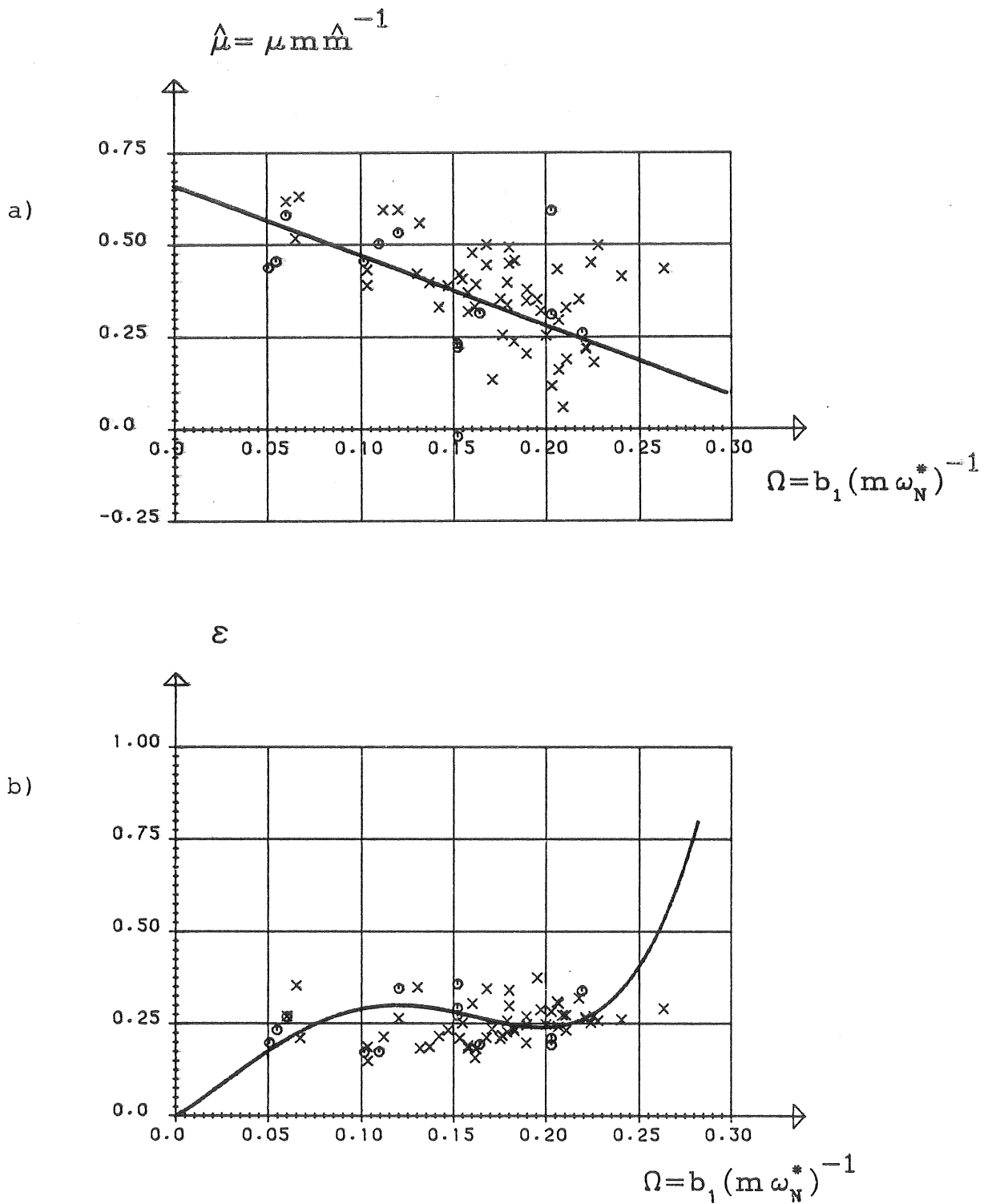


Figure 11. $\hat{\mu}$ and ε as functions of the dimensionless external damping Ω . Selected experiments and regression curves.

Marks; x - spectrum G0 and o - spectrum G4.

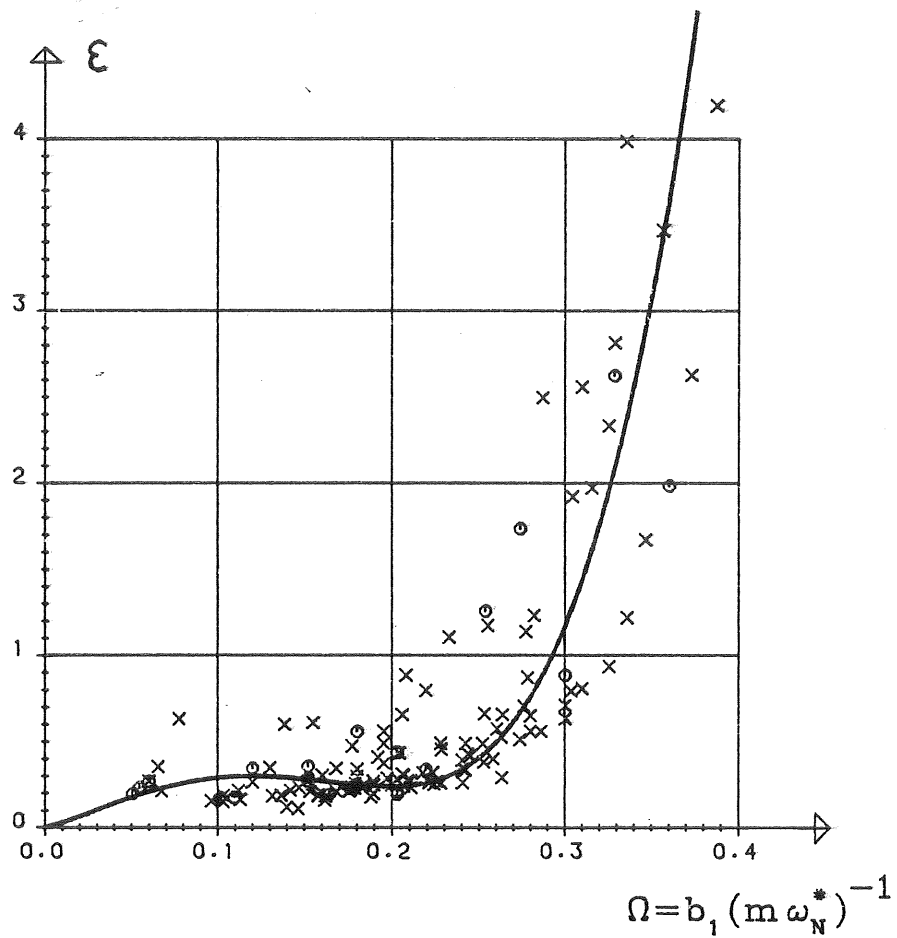


Fig. 12. ε as a function of the dimensionless external damping Ω .
All experiments. Marks; x - spectrum G0 and o - spectrum G4.

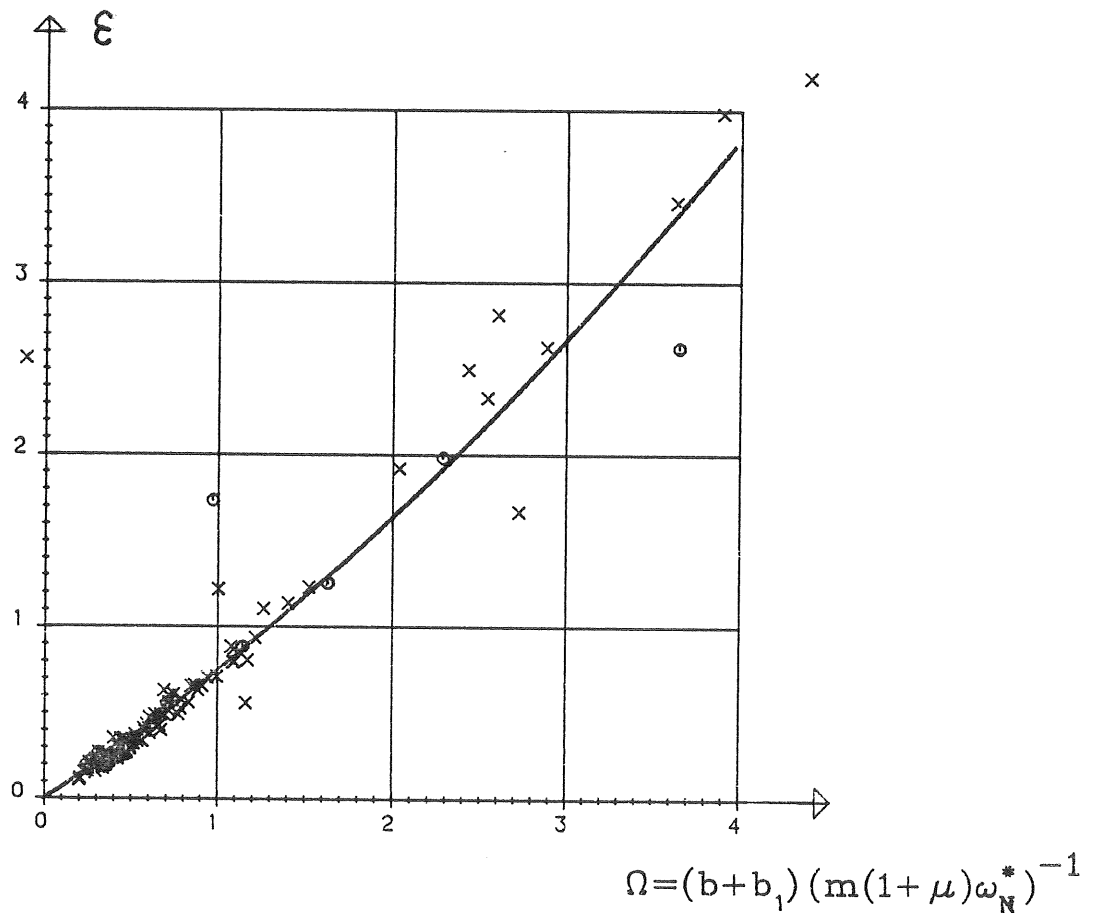


Fig. 13. ε as a function of the dimensionless external damping Ω .
All experiments. Marks; x - spectrum G0 and o - spectrum G4.

5. CONCLUSIONS

In the experiments the mass and external damping of a wave power buoy were systematically varied to get out as much power as possible in two different pseudo random long-crested seas. The diameter of the buoy was kept constant.

The experiments showed that it is important to choose a proper diameter when designing a buoy. The diameter must be adapted to the expected wave spectra. A badly chosen diameter can only to a limited degree be compensated for by changing the ballast of the buoy. A buoy with a small weight compared to its diameter will, for example, be heaving close to the water surface, and therefore its stroke and phase lag will be physically restricted. A buoy with a great weight compared to its diameter will get a deep draft and therefore the exciting wave force will get small. The latter fact was enhanced in the rather shallow (0.67 m) wave tank.

The calculated regression functions or more directly the diagrams can be used for choosing reasonable mean values of added mass and hydrodynamic damping ¹⁾ for wave power buoys within a wide range of sizes and with substantial power take off.

1) Hydrodynamic damping is here the sum of viscous and radiation damping. No separation is possible because of the averaging procedures. The viscous damping is supposed to be small compared to the radiation damping because of the rounded shape and the smooth surface of the experimental buoy.

References

Bergdahl et al (1979). The Swedish wave energy research programme. Symposium of wave energy utilization, Chalmers University of Technology, Göteborg, Sweden, 30 Oct-1 Nov. 1979, p.222-252

Bergdahl, Olsson, Sörman (1980). Wave-Power Buoys. Model experiments of energy absorption in regular waves in a wide basin. The Group for Wave Energy Research, Report GR:24 Göteborg 80-03-30. (In Swedish).

Bergdahl, Olsson, Sörman (1981): Wave-Power Buoys. Model experiments of energy absorption in irregular waves in a wide basin. The Group for Wave Energy Research, Report GR:32, Göteborg 81-03-30 (In Swedish)

Box, Hunter and Hunter (1978): Statistics for experimenters. John Wiley Sons, New York, USA

Brigham, E O (1973). The Fast Fourier Transform, Prentice Hall, Englewood Cliffs, N.Y.

Claeson et al (1982). Contribution to the theory and experience of energy production and transmission from the buoy concept. 2nd International Symposium on Wave Energy Utilization. The Norwegian Institute of Technology, Trondheim, Norway, June 22-24 1982 p.345-370.

Eriksson, G. (1974). Numerical Analysis Advanced Course. Dep. of Computer Sciences, Lunds Institute of Technology, Lund, Sweden.

Havelock, T. (1955): Waves Due to a Floating Sphere Making Periodic Heaving Oscillations. Proceedings of the Royal Society of London, A-231, p 1-7.

APPENDIX

A. Diagrams of buoy response

In the following diagrams the experimental results are plotted together with the fitted line. The fitting is done with the Davidon-Fletcher-Powell method (see Eriksson (1974)).

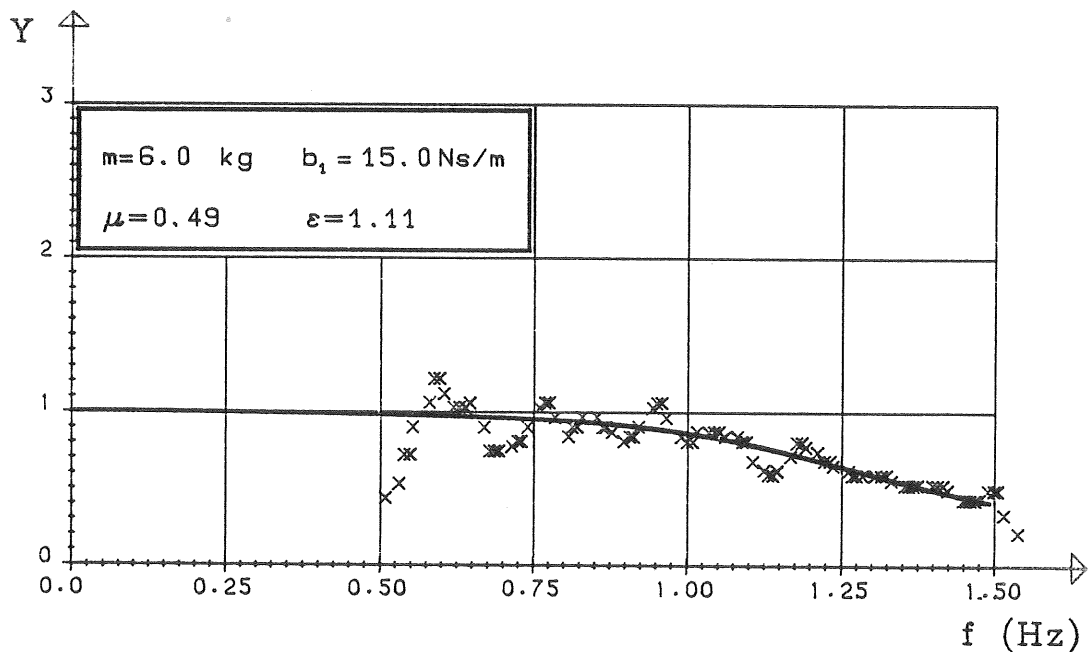
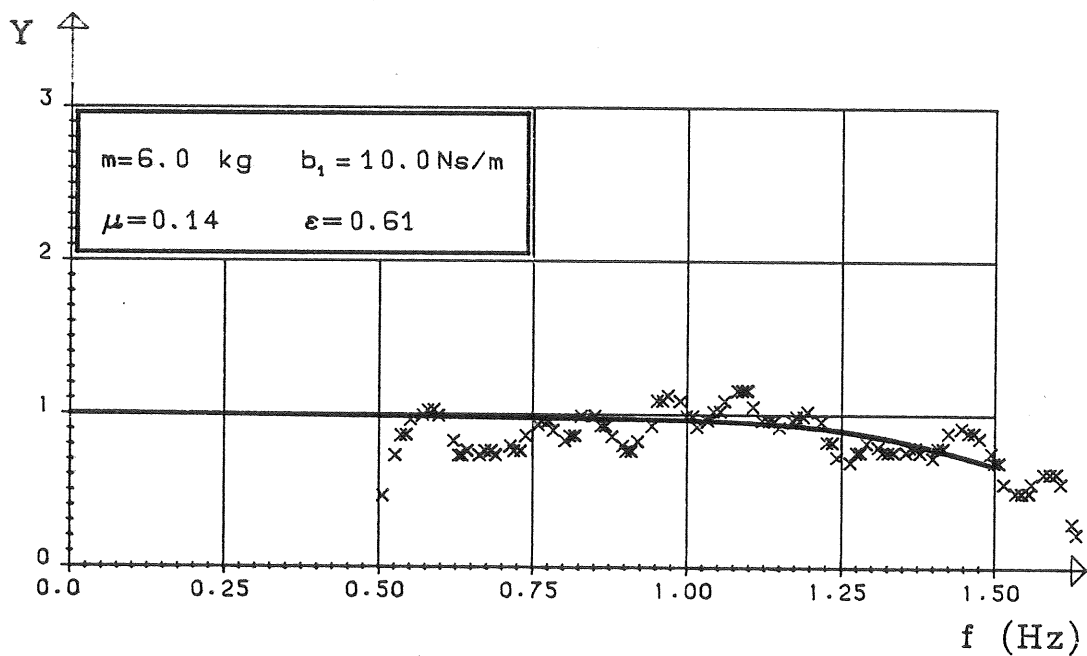
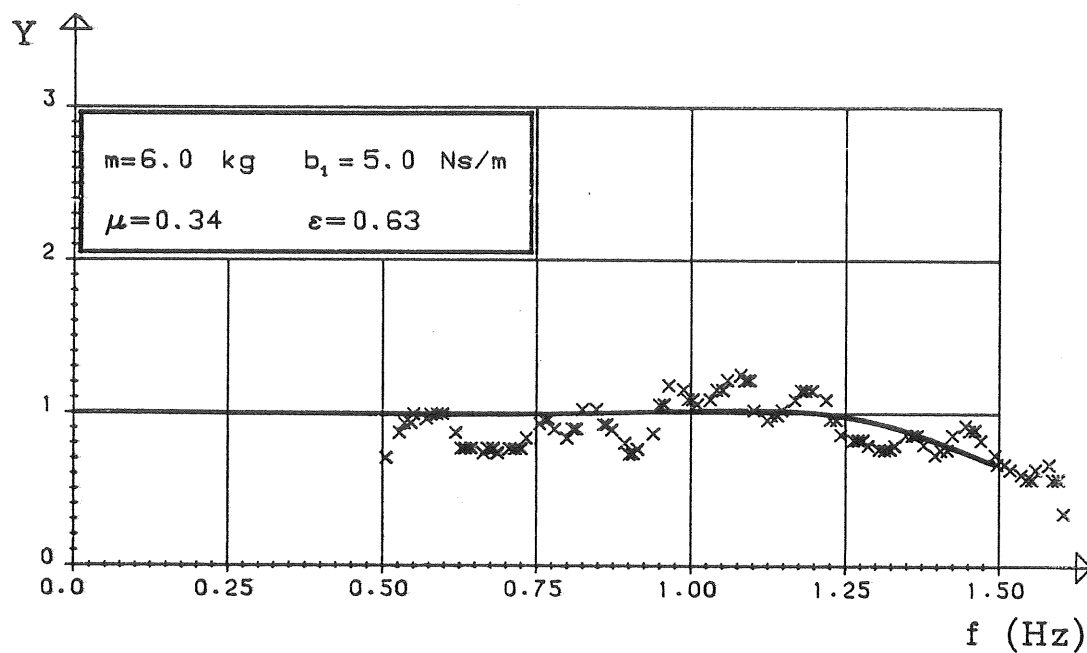
The diagrams are placed in order of increasing mass as follows

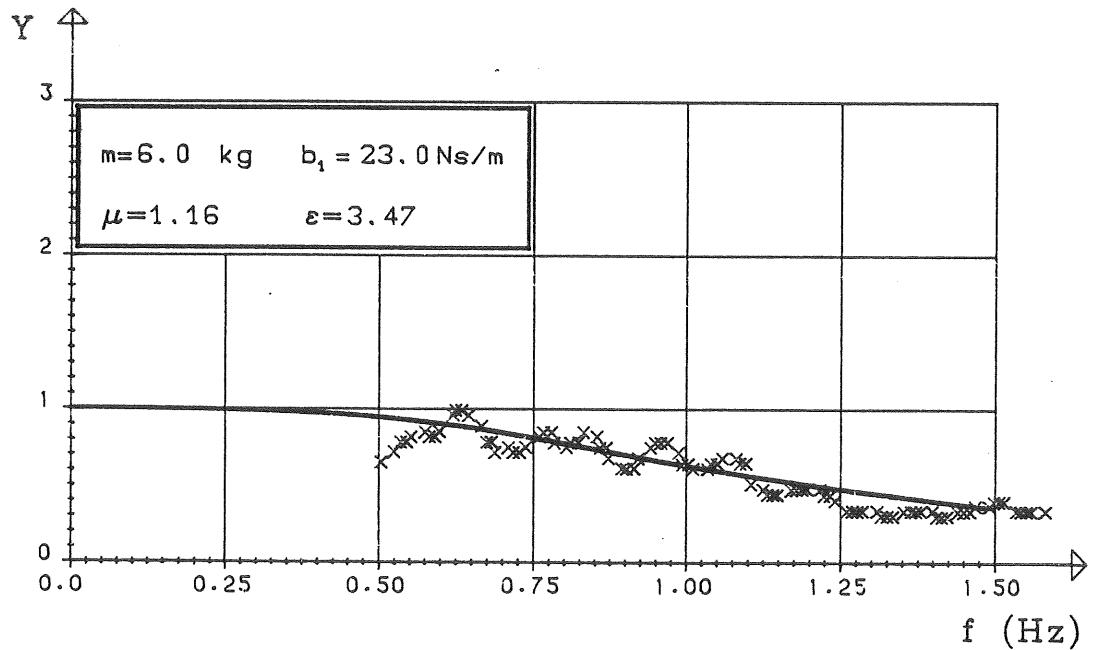
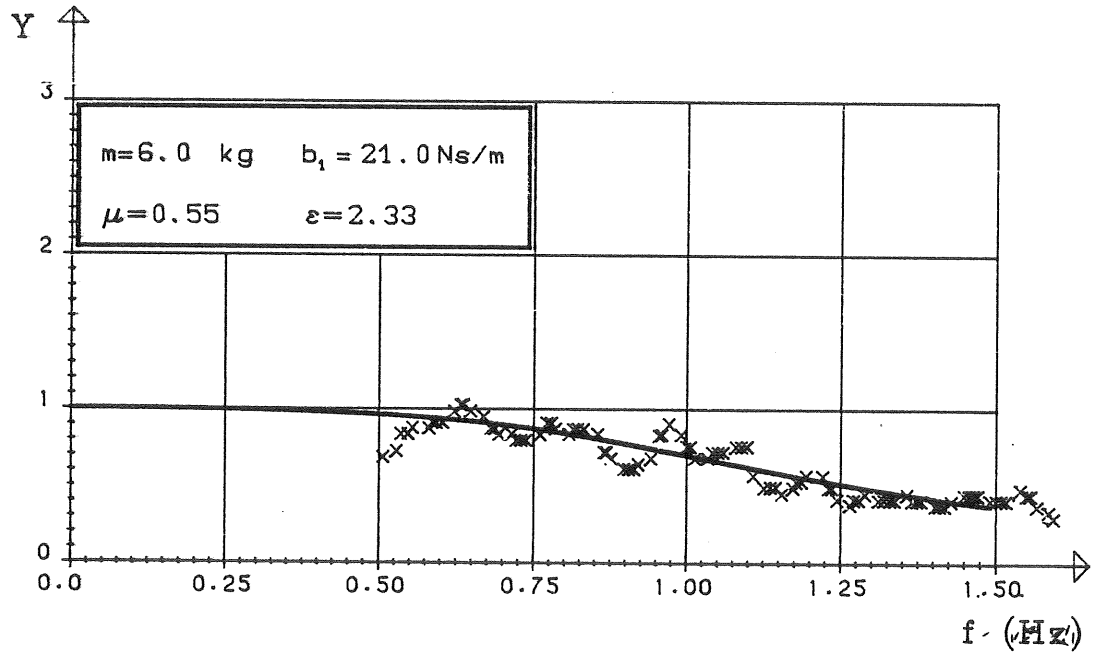
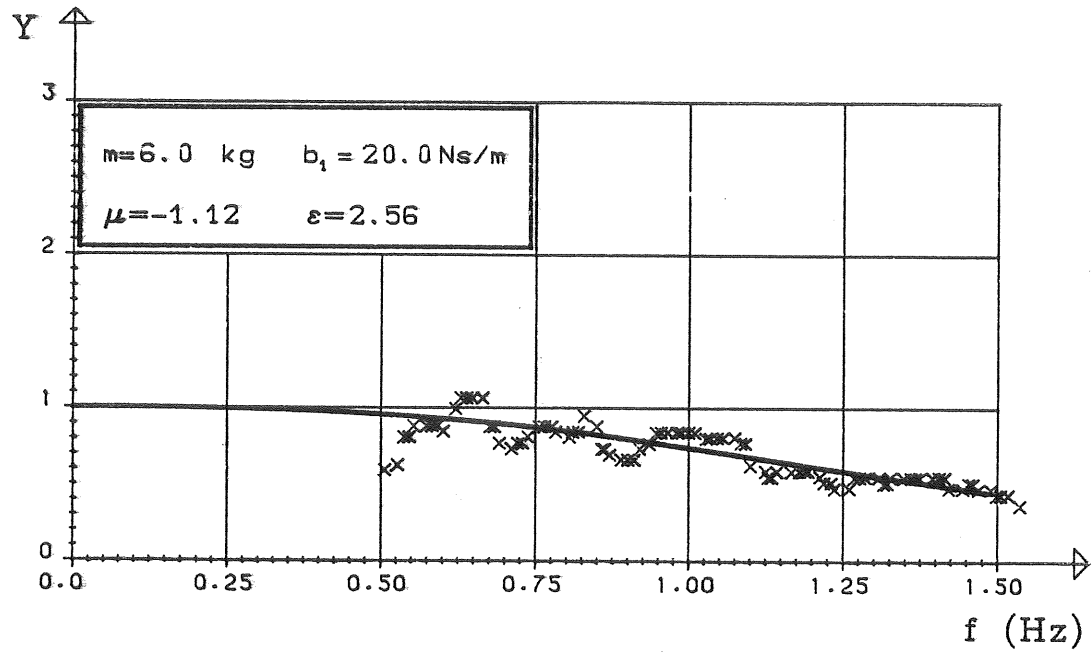
Mass kg	Page
6	A1:2
7	:6
7.5	:9
8	:12
8.5	:14
9	:18
10	:21
11	:28
11.5	:32
12	:37
13	:43
13.5	:49
14	:53
15	:60
16	:64

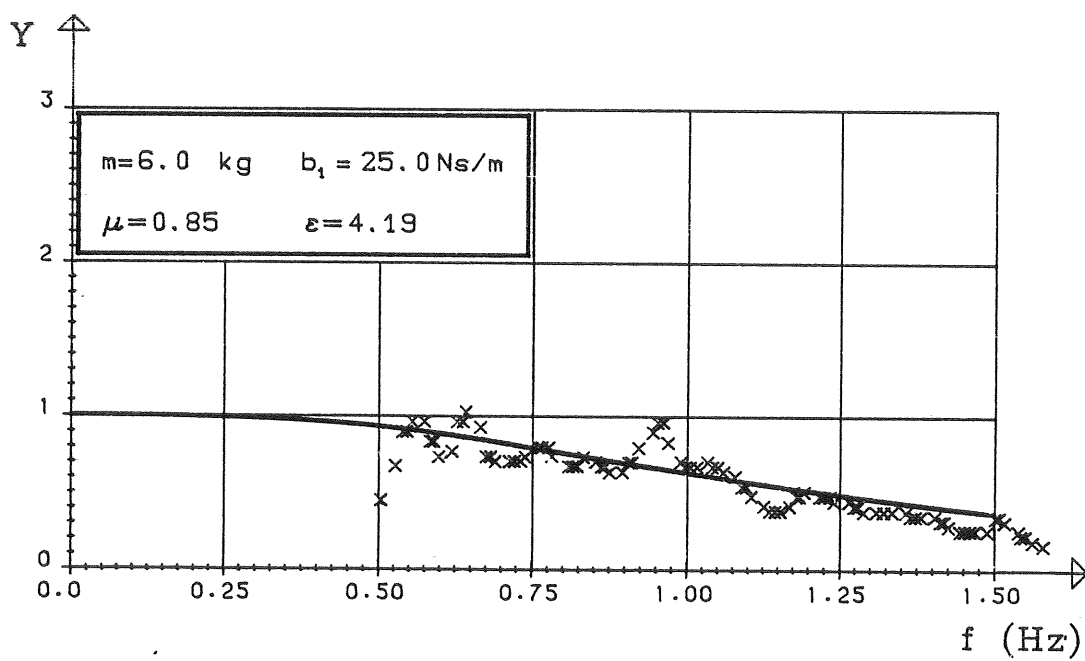
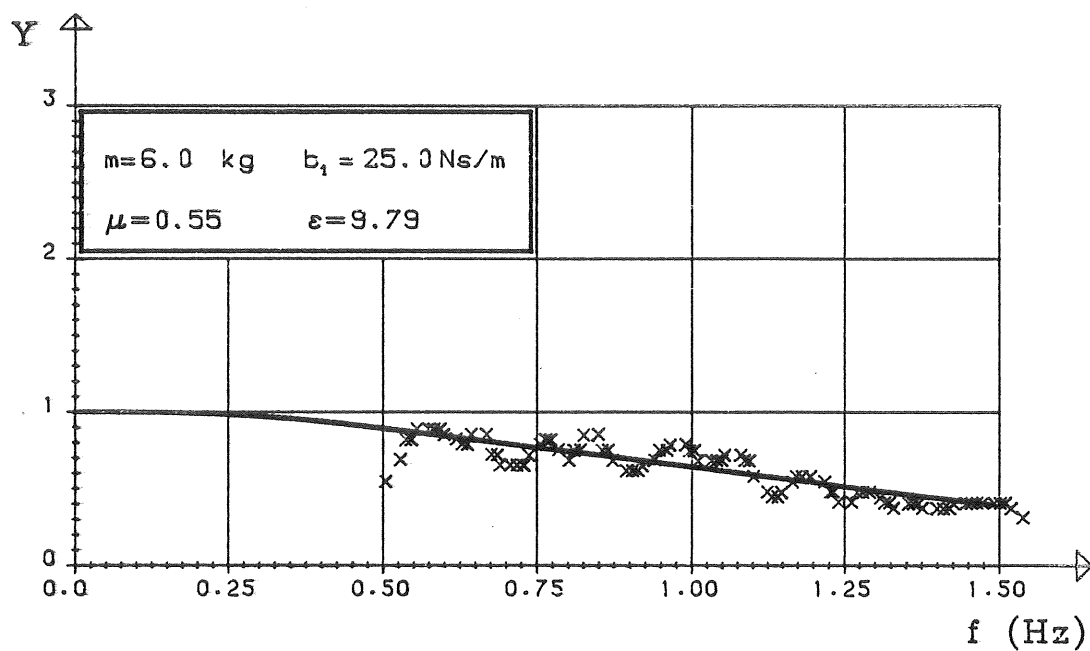
For each mass the diagrams are placed in order of increasing damping.

A1.2 BOJMASSA= 6 KG

YTTRE DÄMPNING= 5 - 25 Ns/m

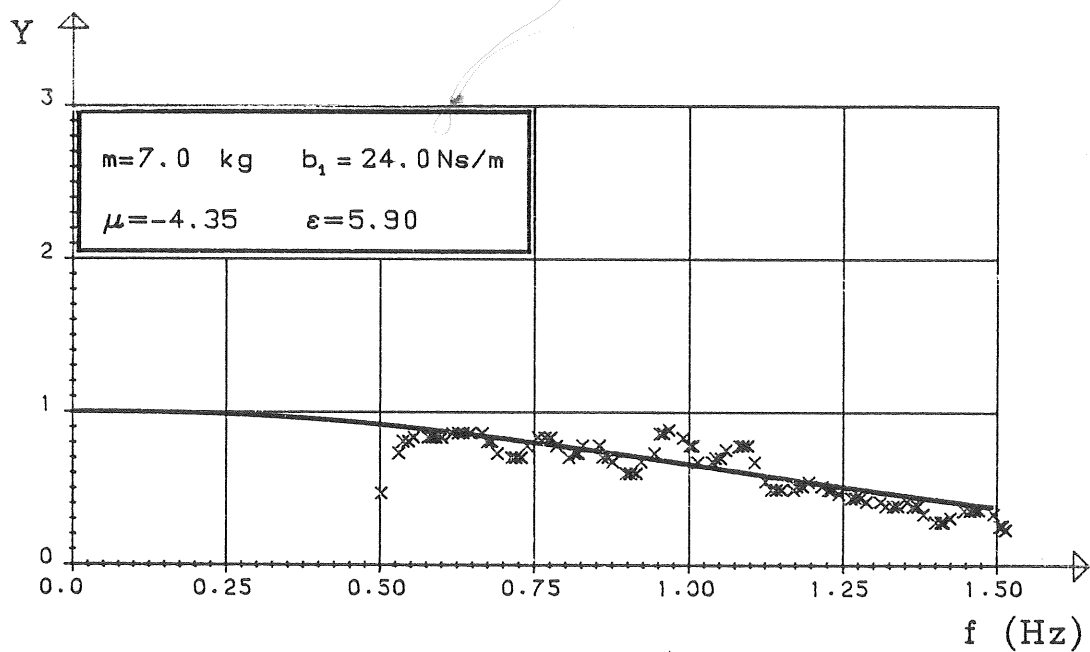
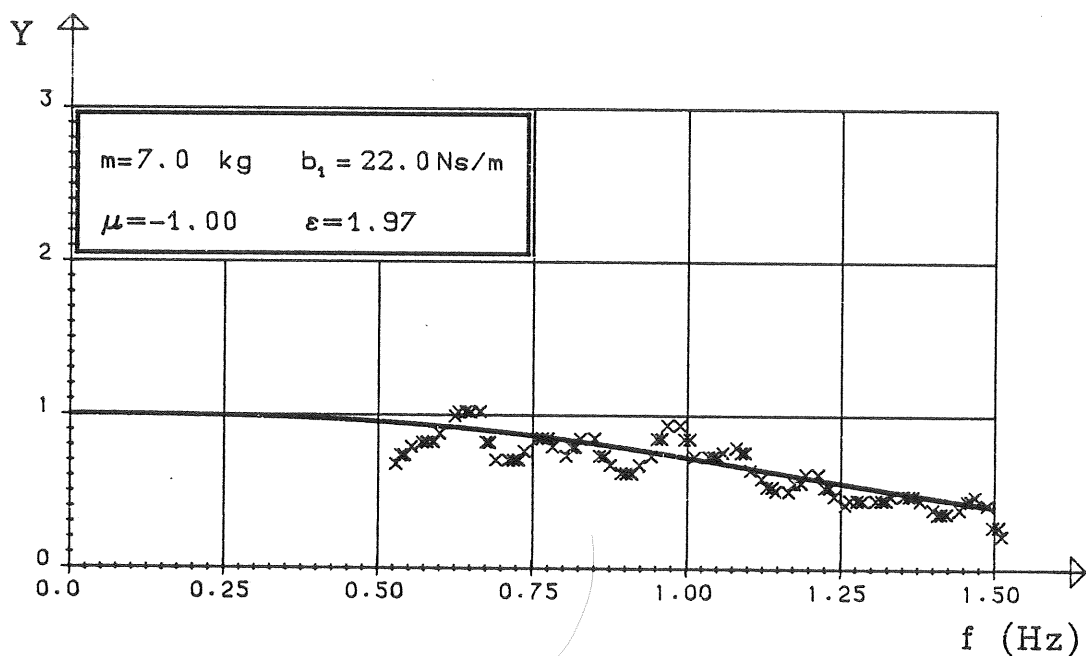
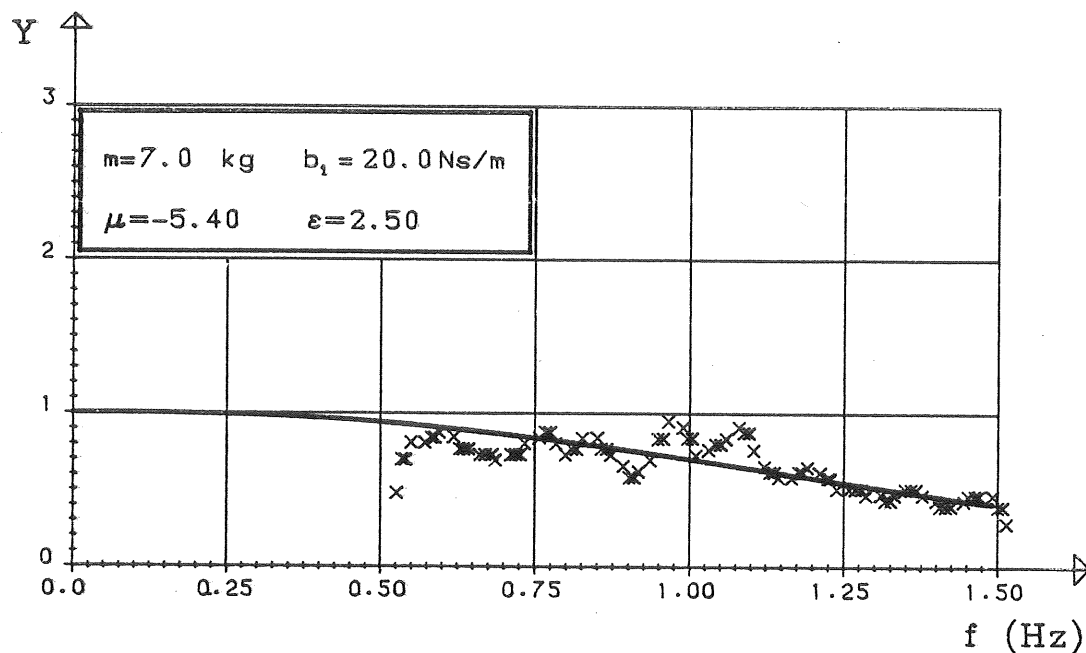


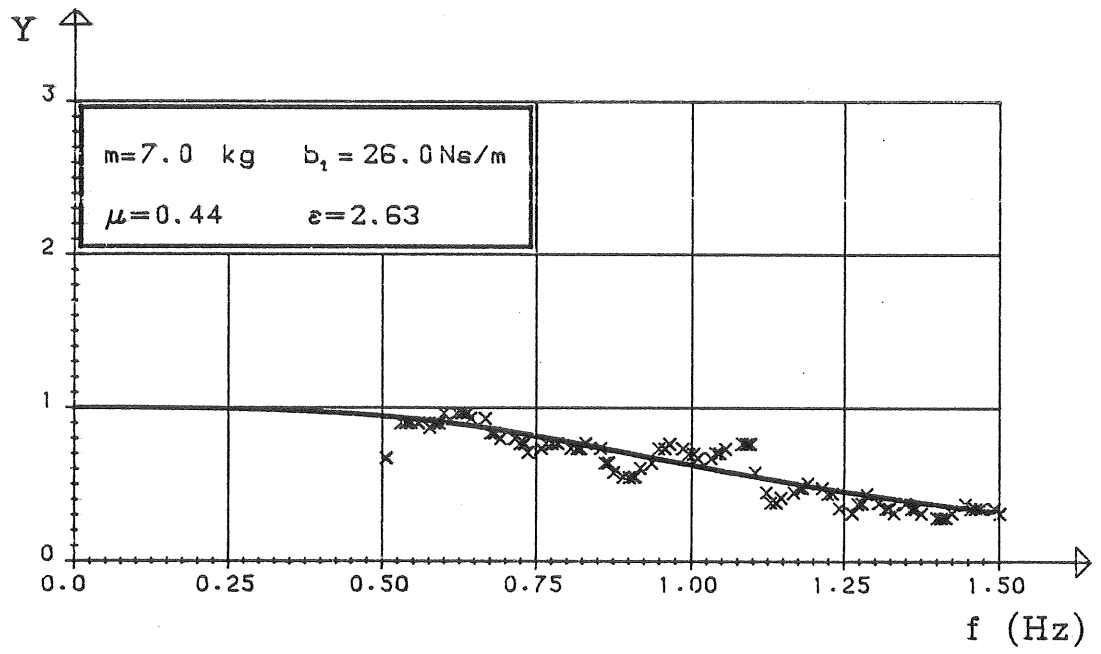




A1.3 BOJMASSA= 7 KG

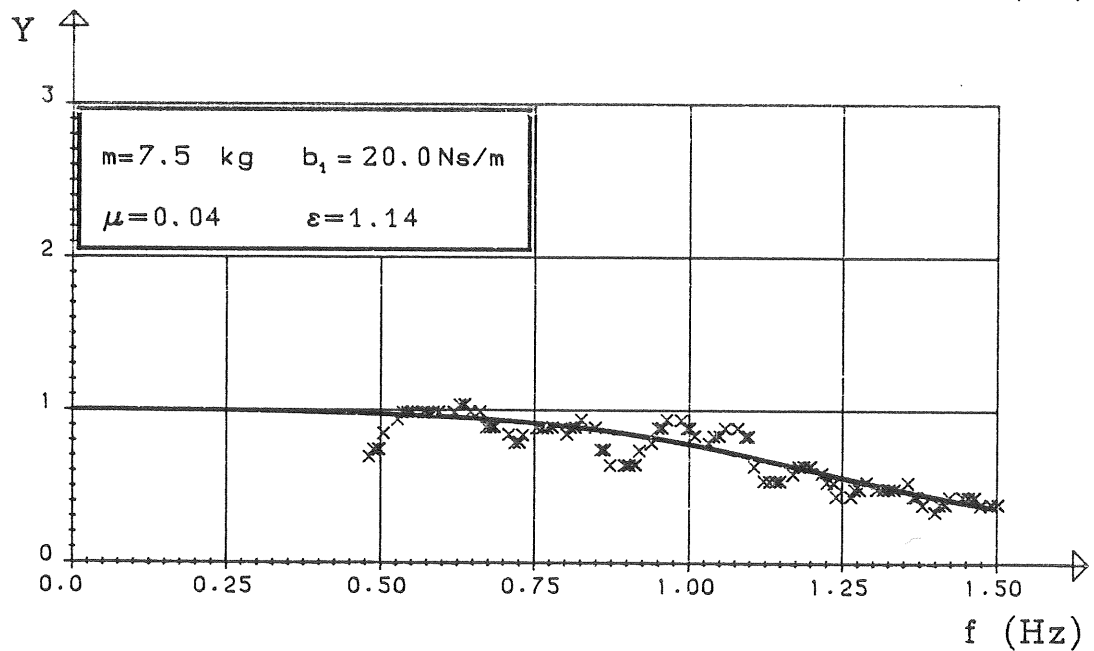
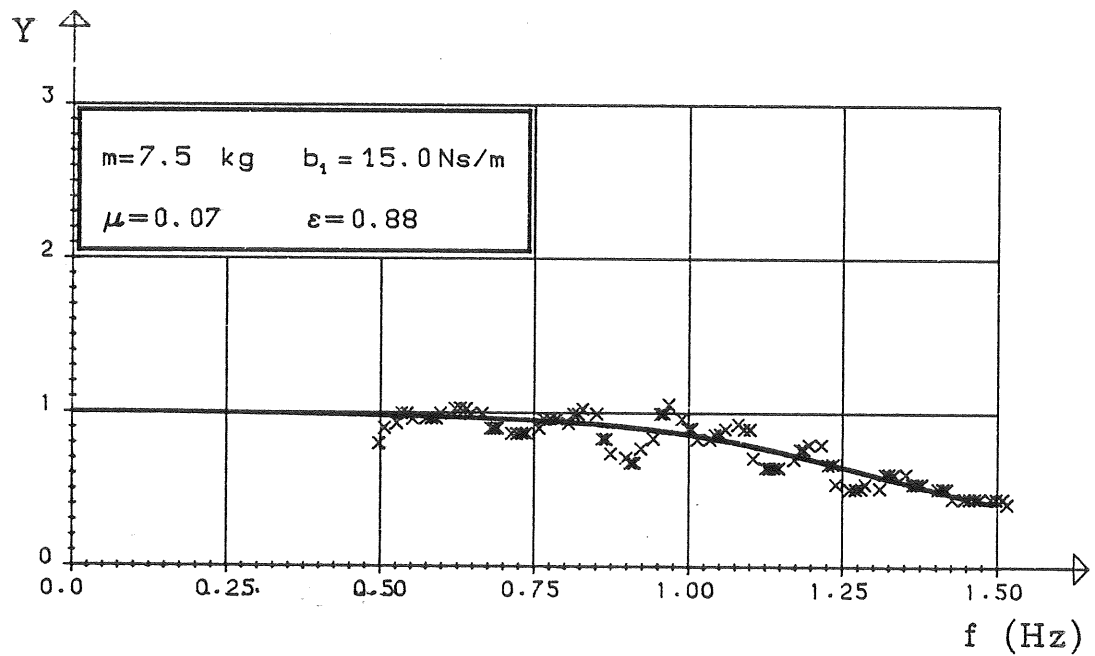
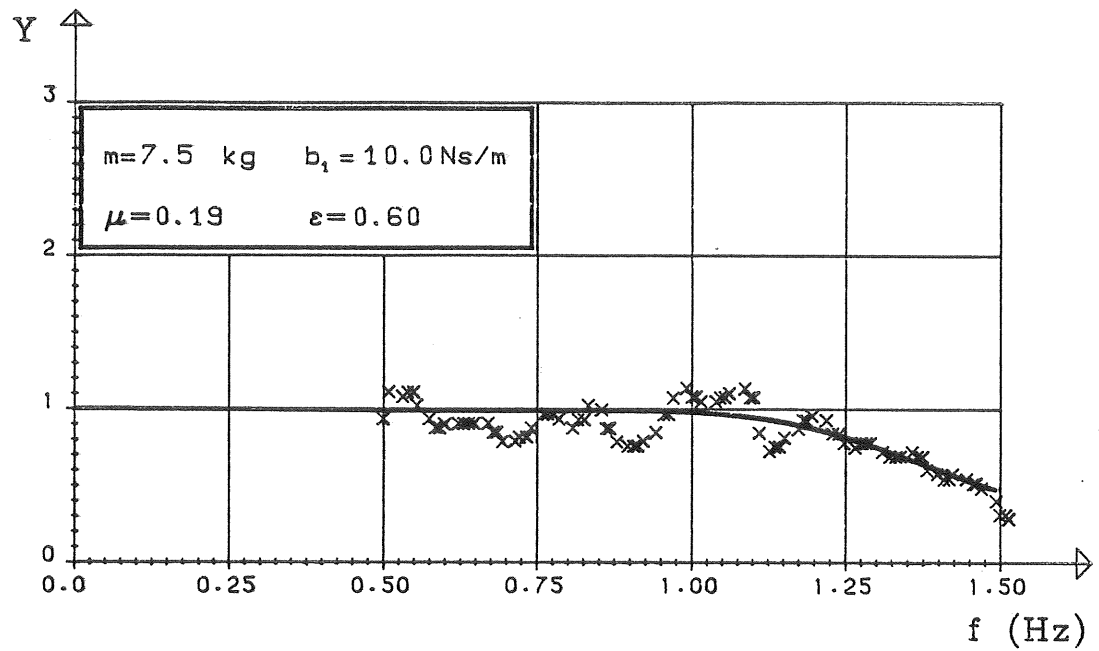
YTTRE DÄMPNING= 20 - 26 Ns/m

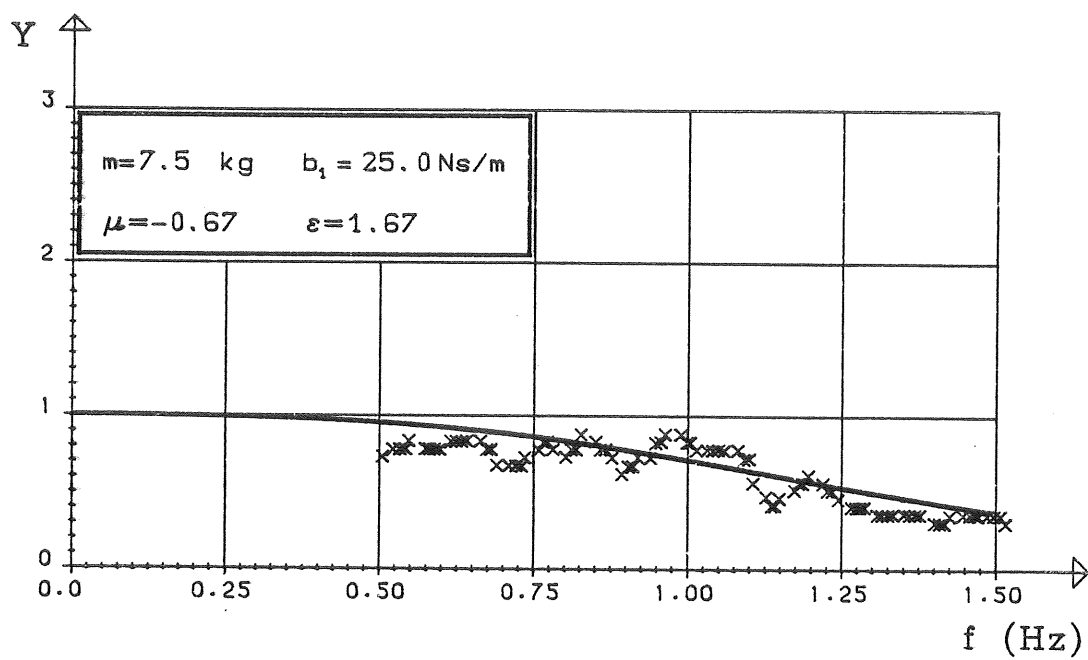




A1.4 BOJMASSA: 7,5 KG

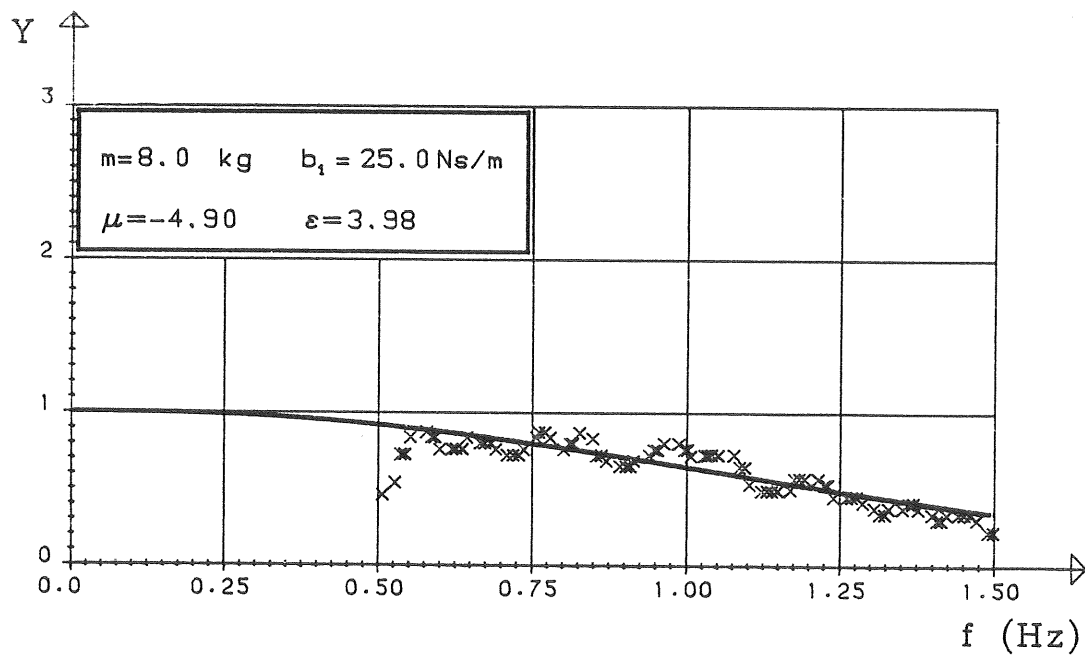
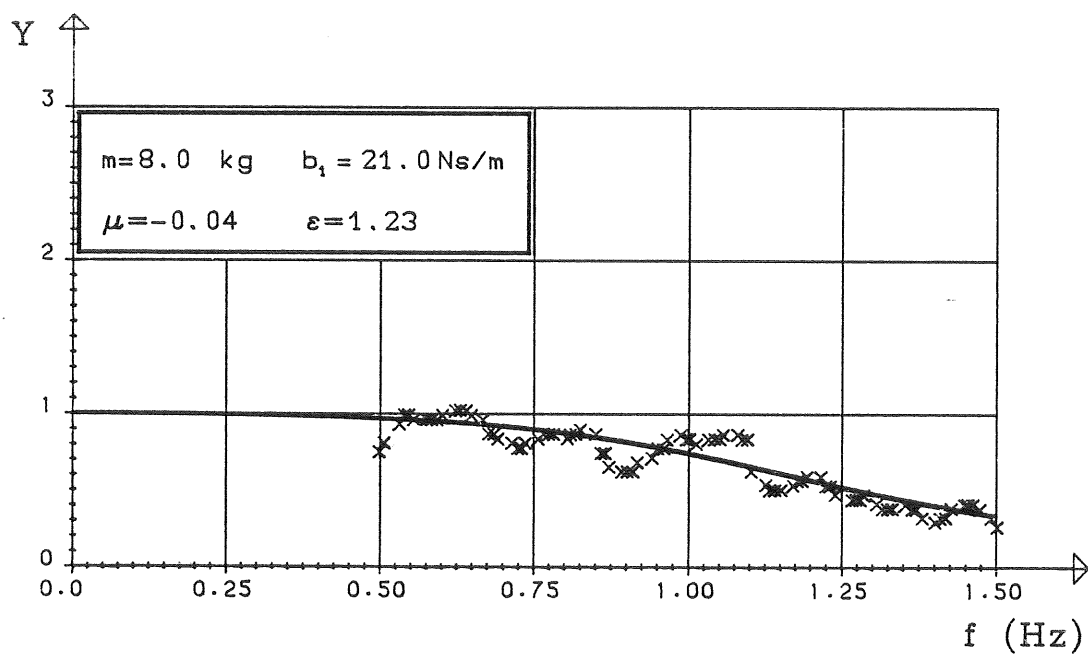
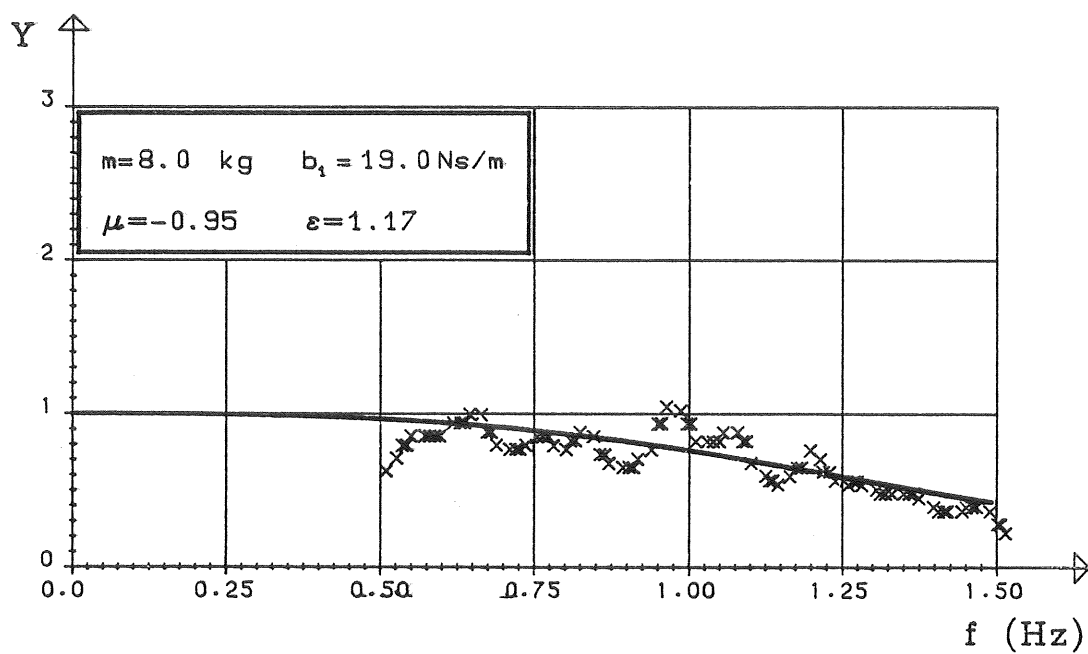
YTTRE DÄMPNING: 10 - 25 Ns/M





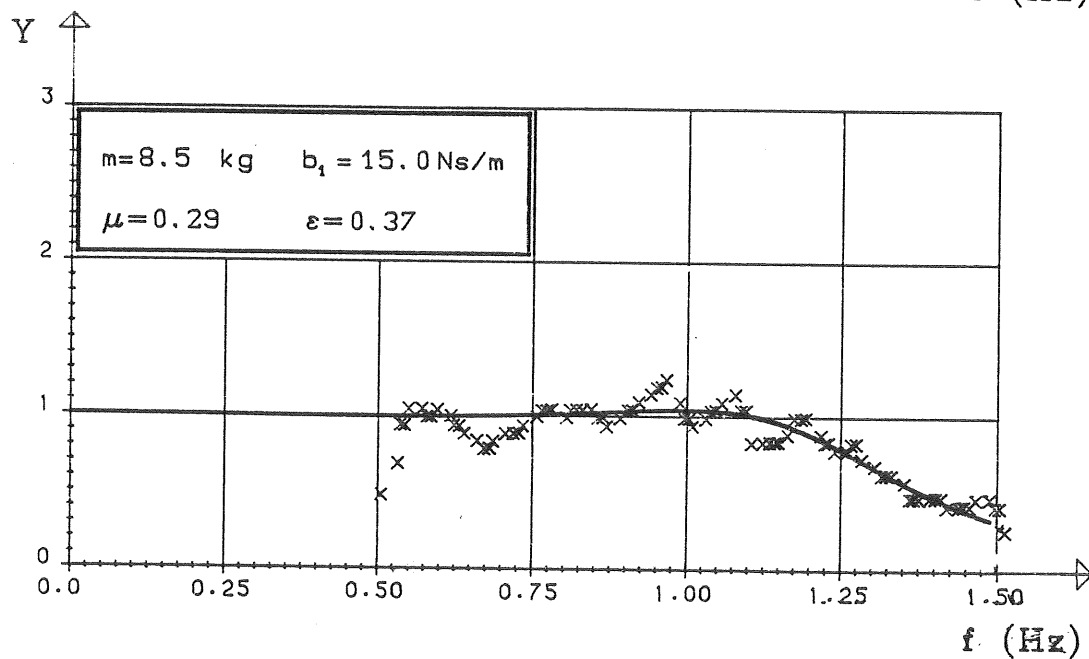
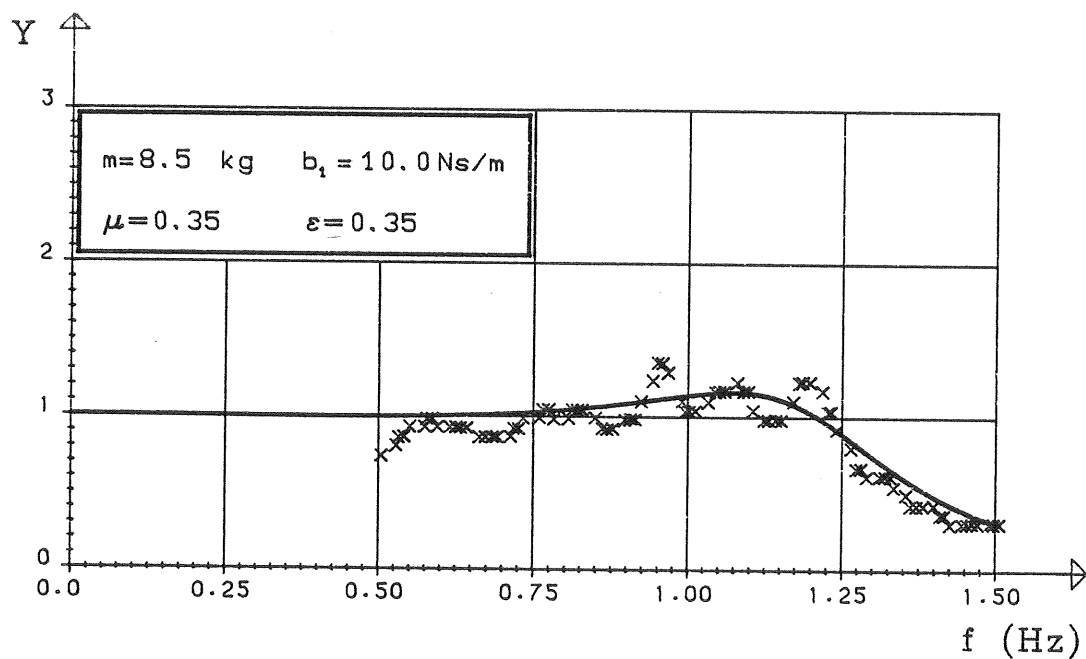
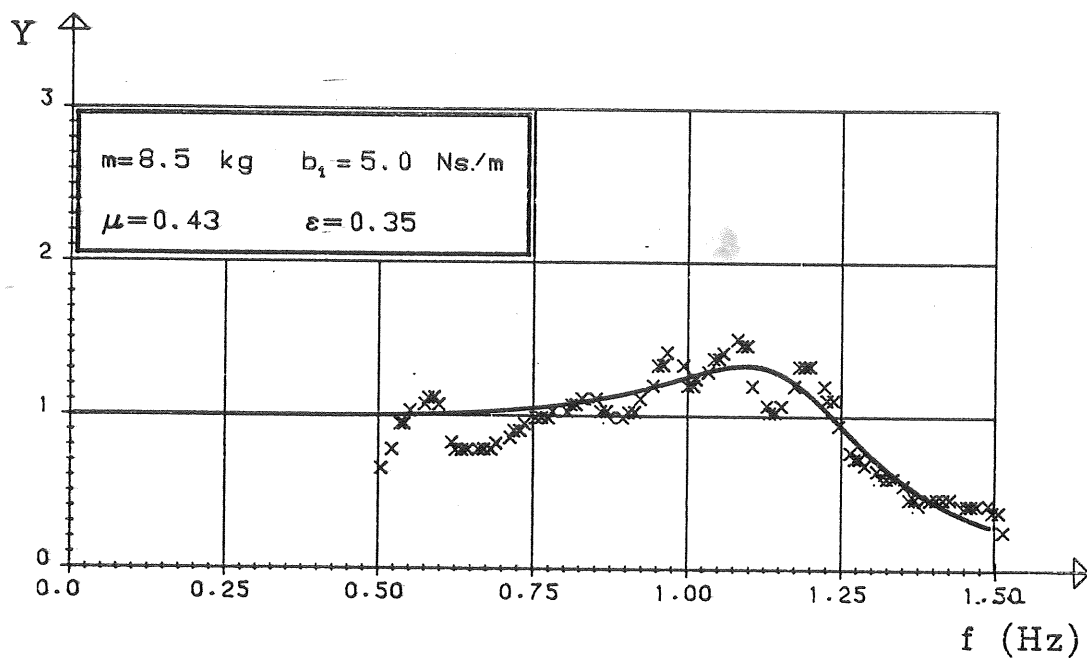
A1.5 BOJMASSA: 8. KG

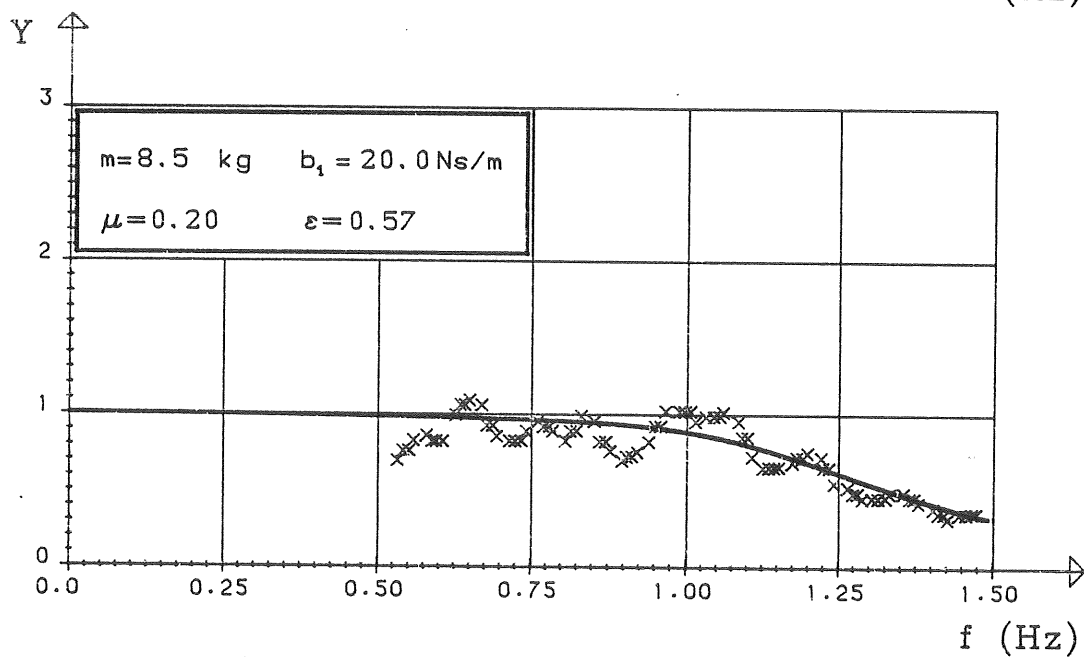
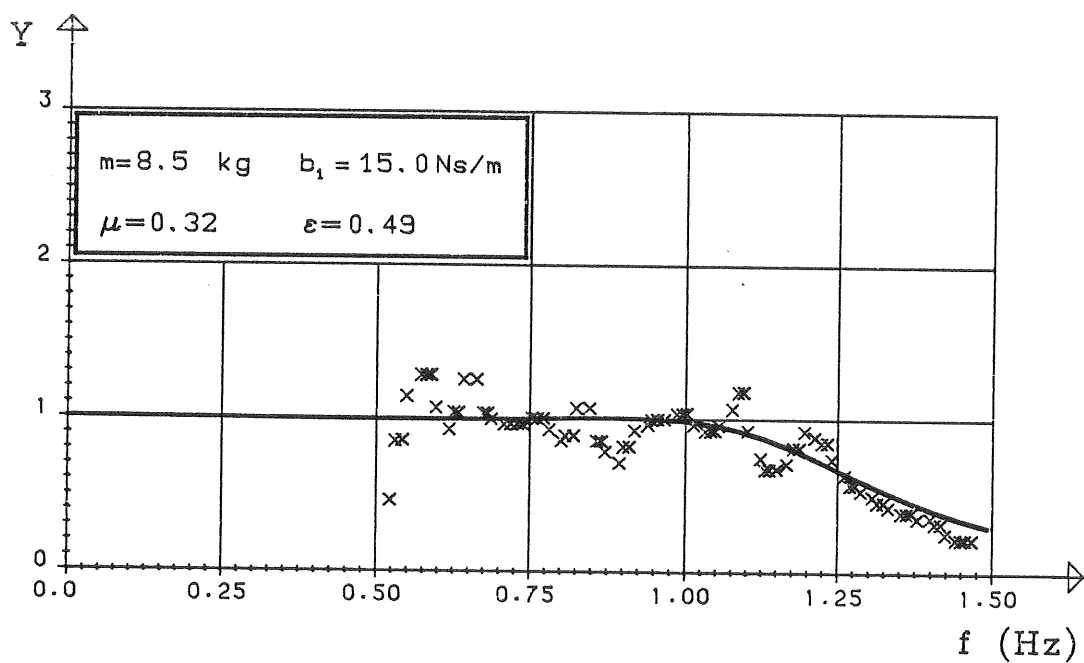
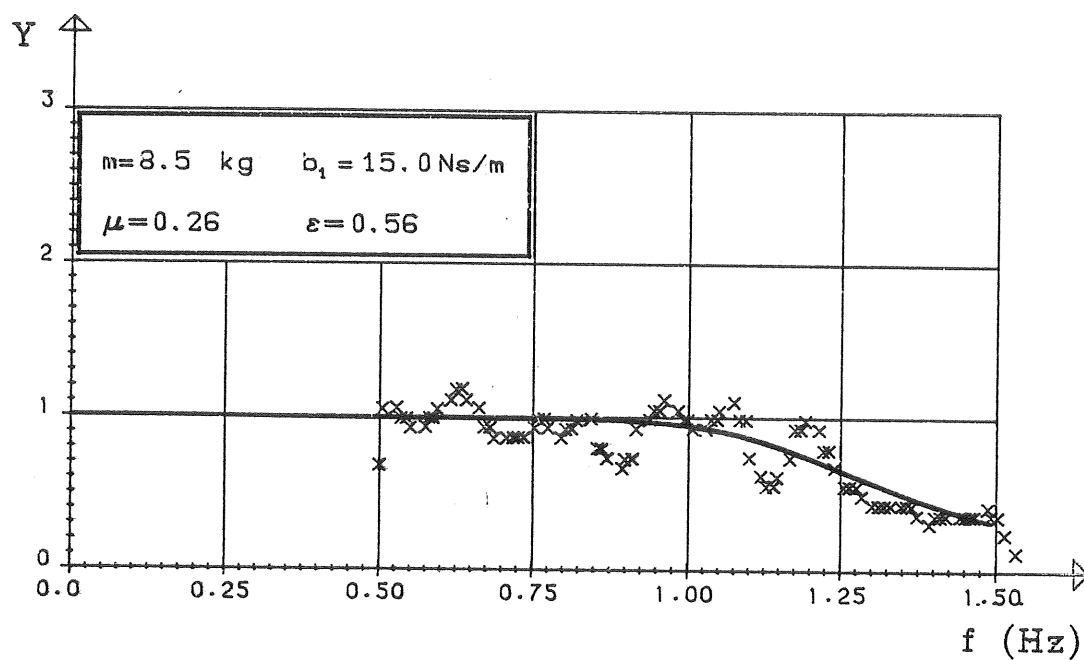
YTTRE DÄPNING: 19 - 25 NS/M

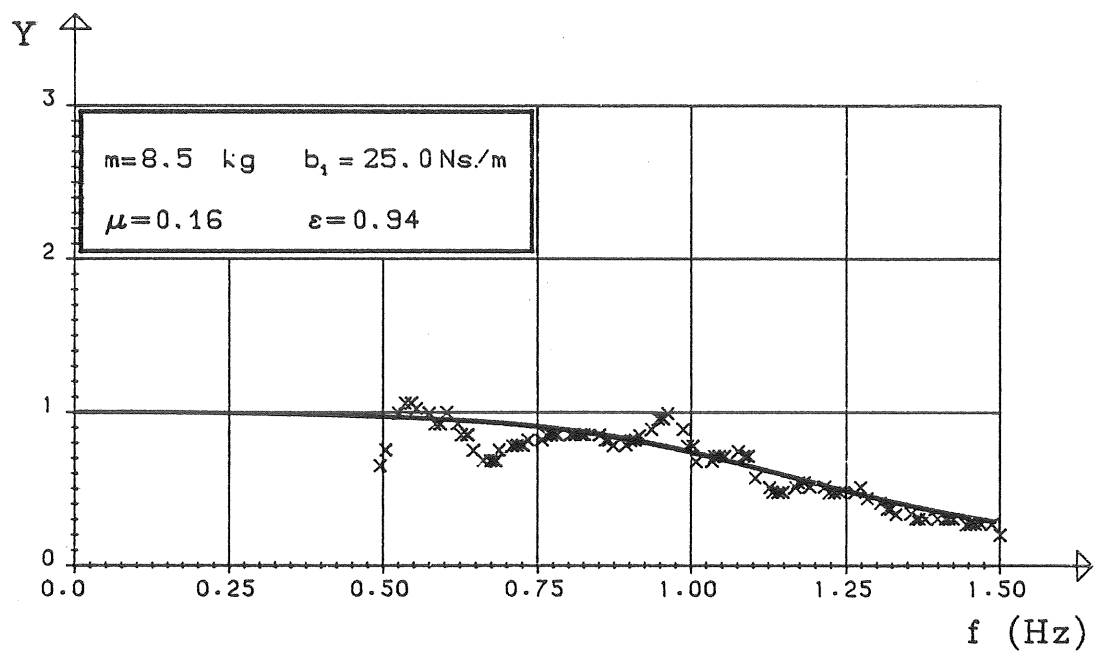


A1.6 BOJMASSA: 8.5 KG

YTTRE DÄMPNING: 5 - 25 Ns/m

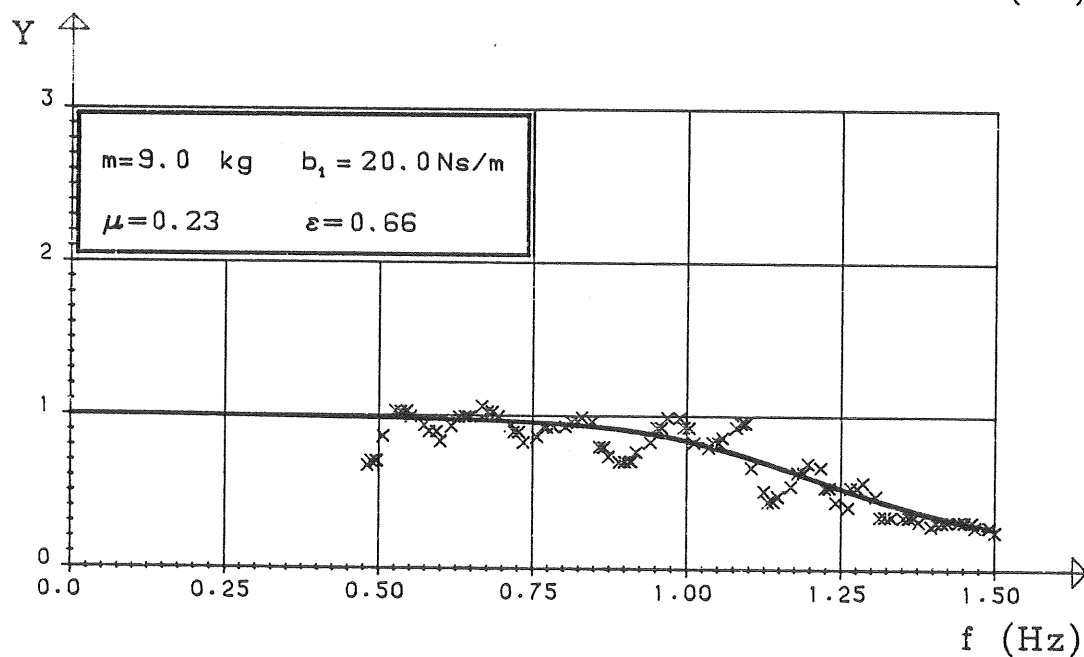
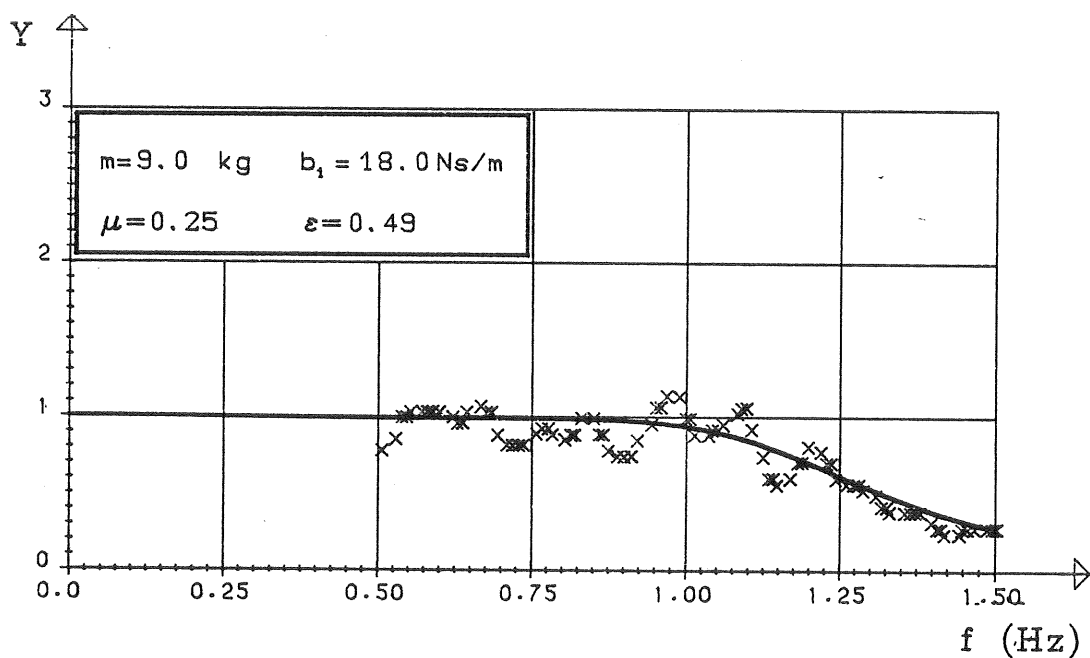
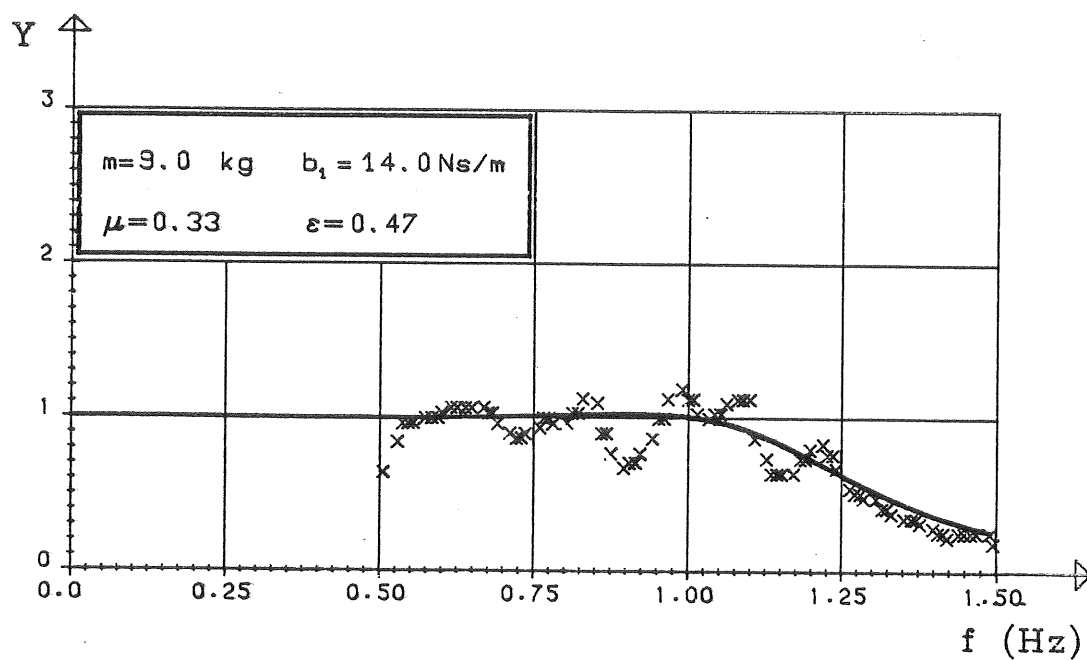


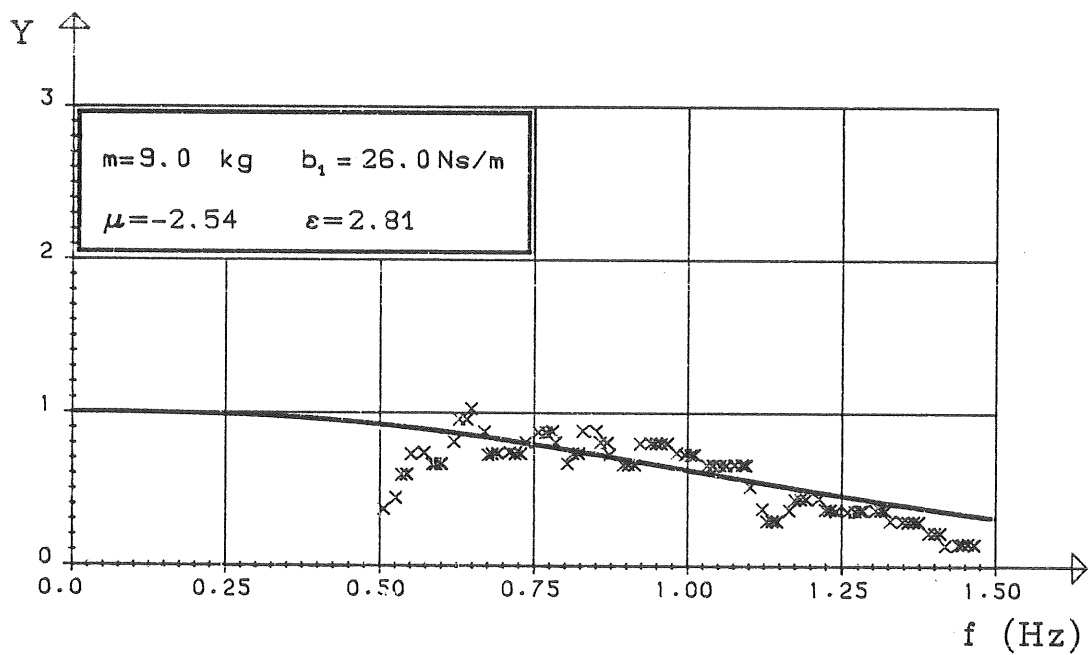
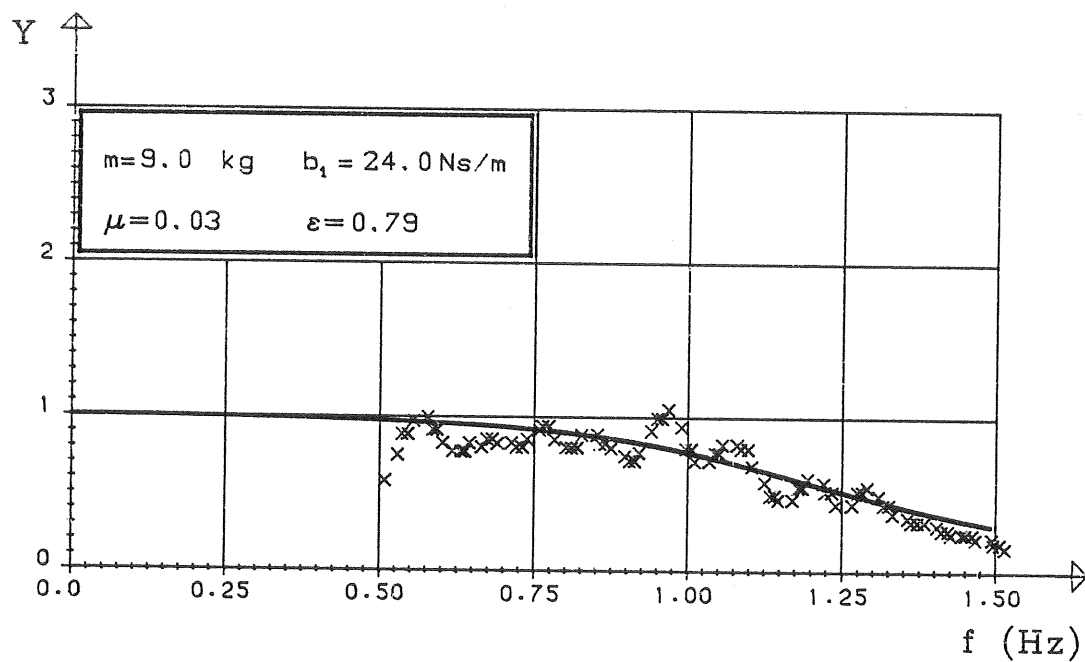
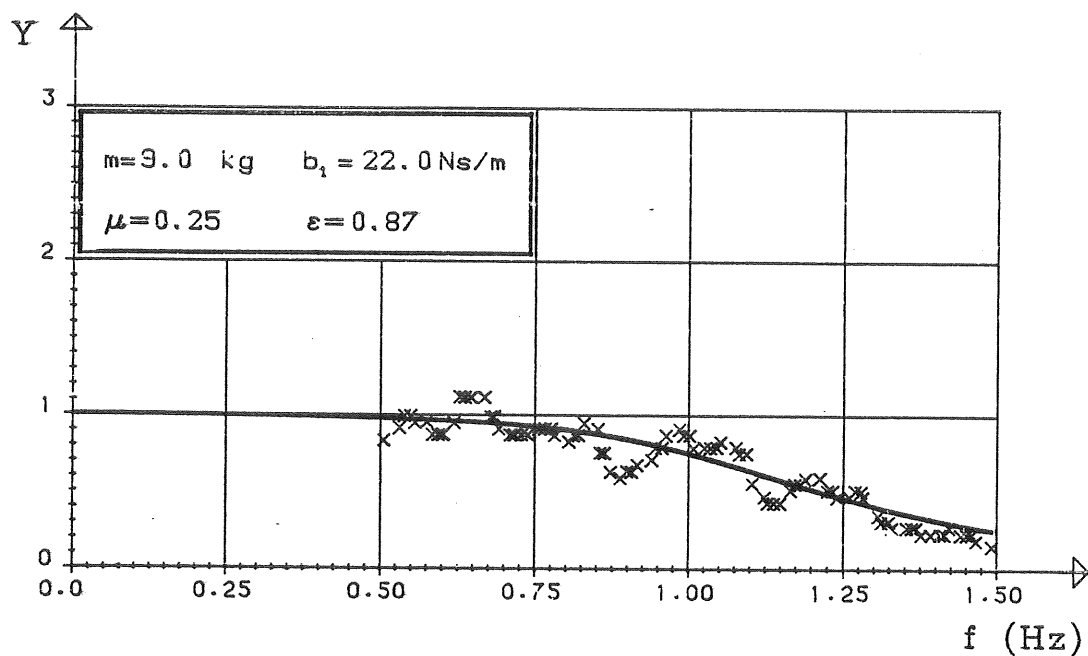




A1.7 BOJMASSA: 9, KG

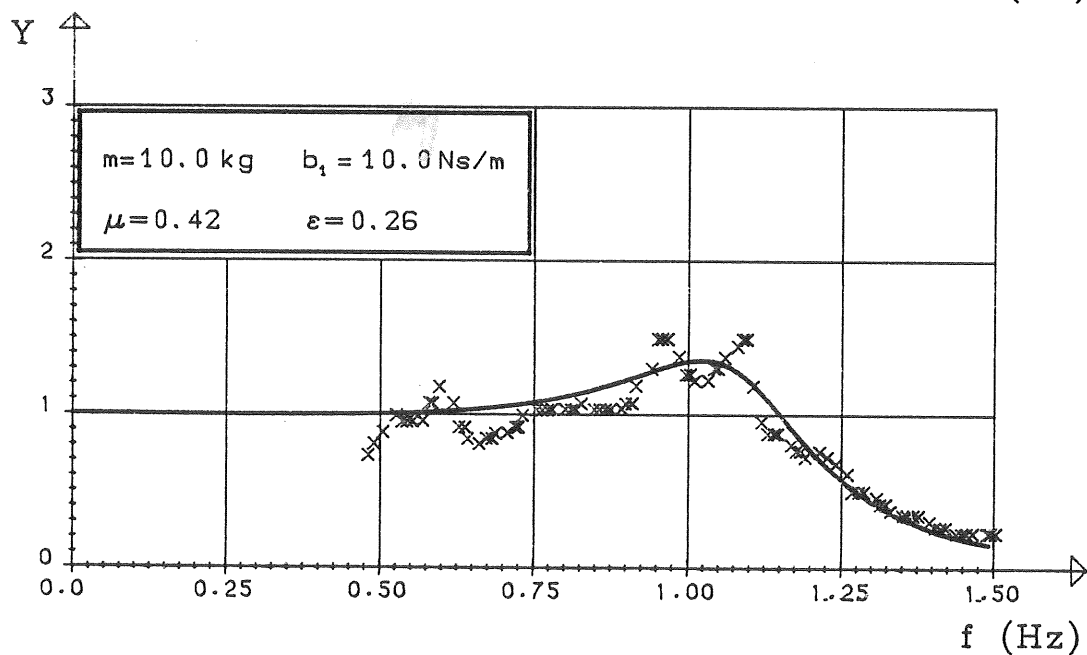
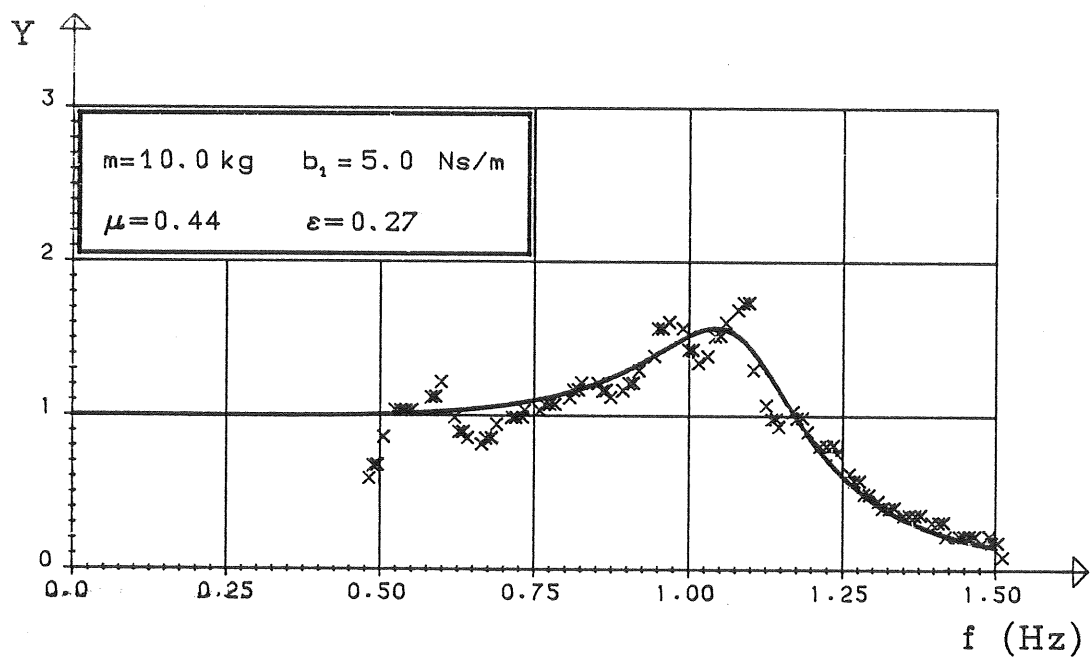
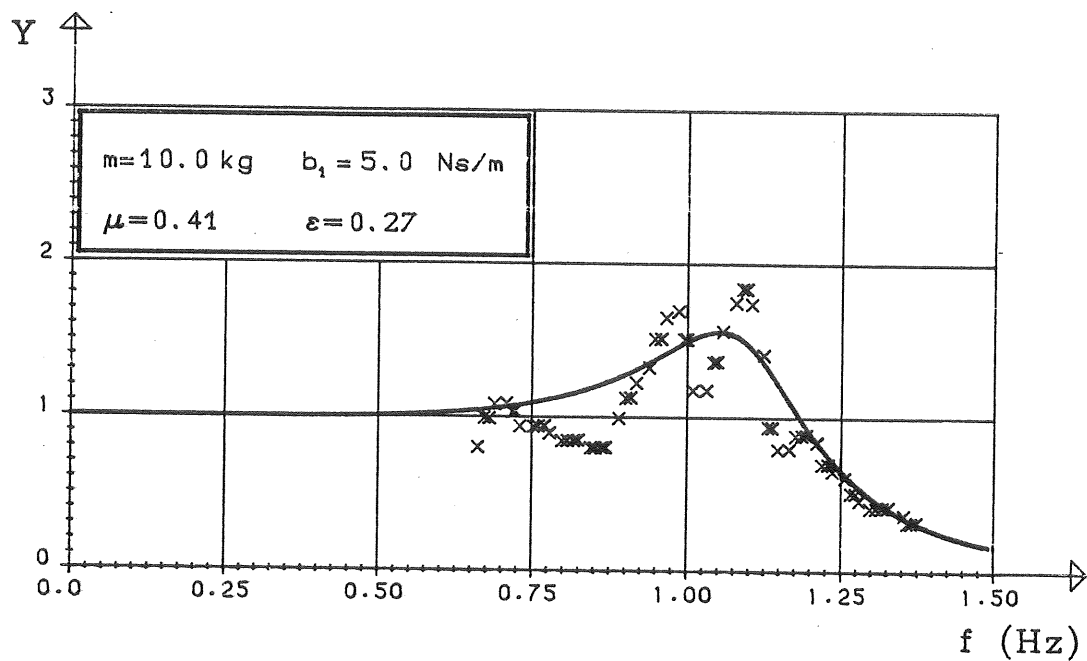
YTTRE DÄMPNING: 14 - 26 Ns/M

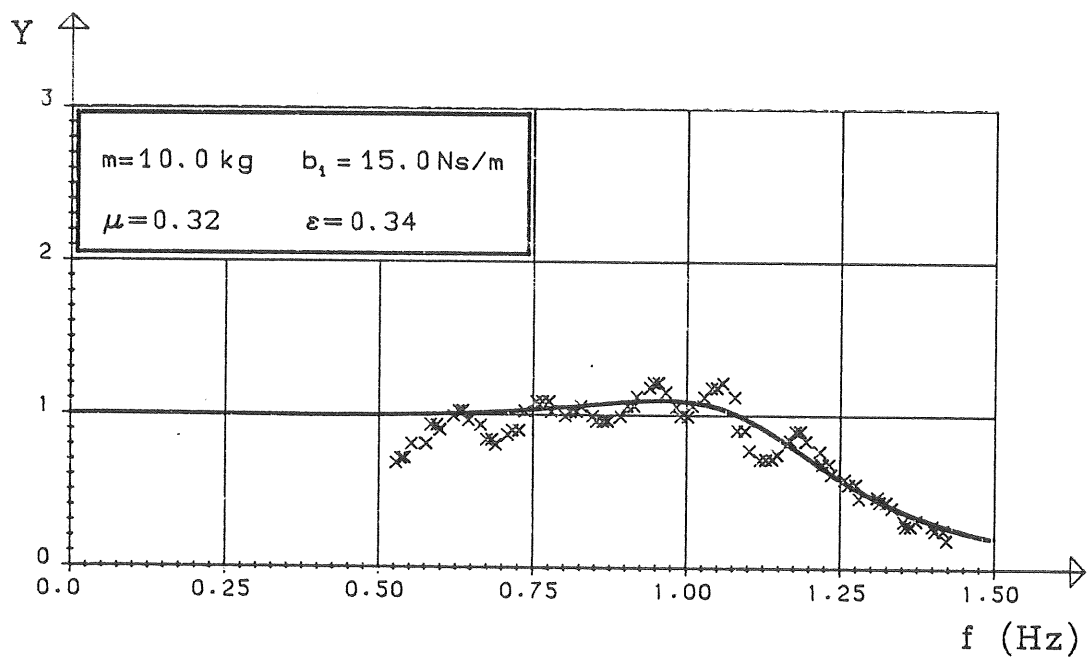
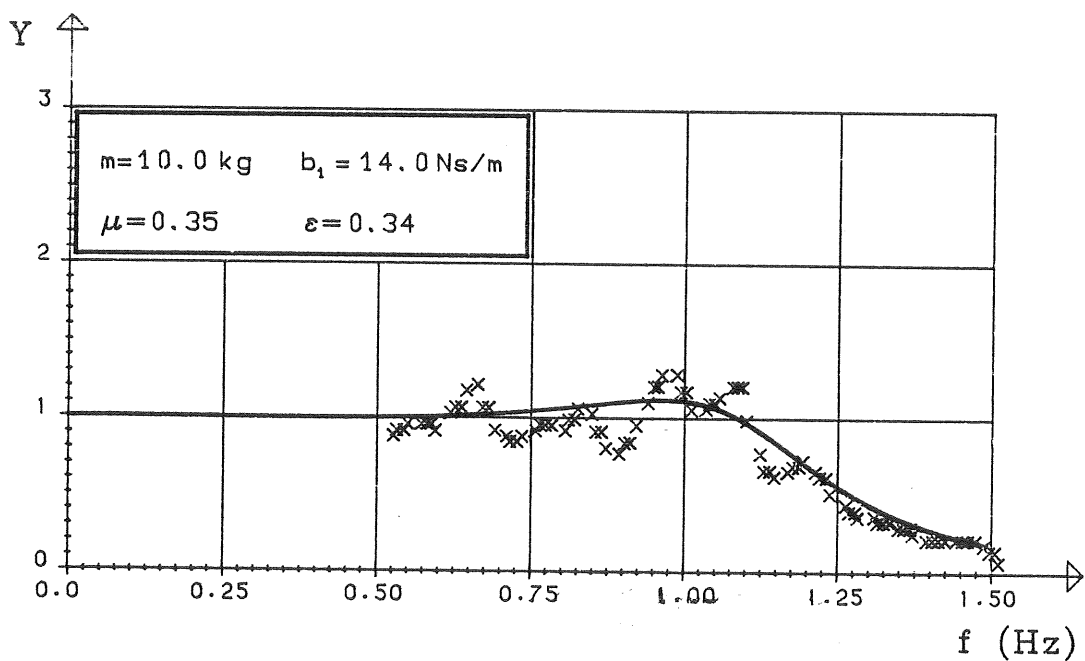
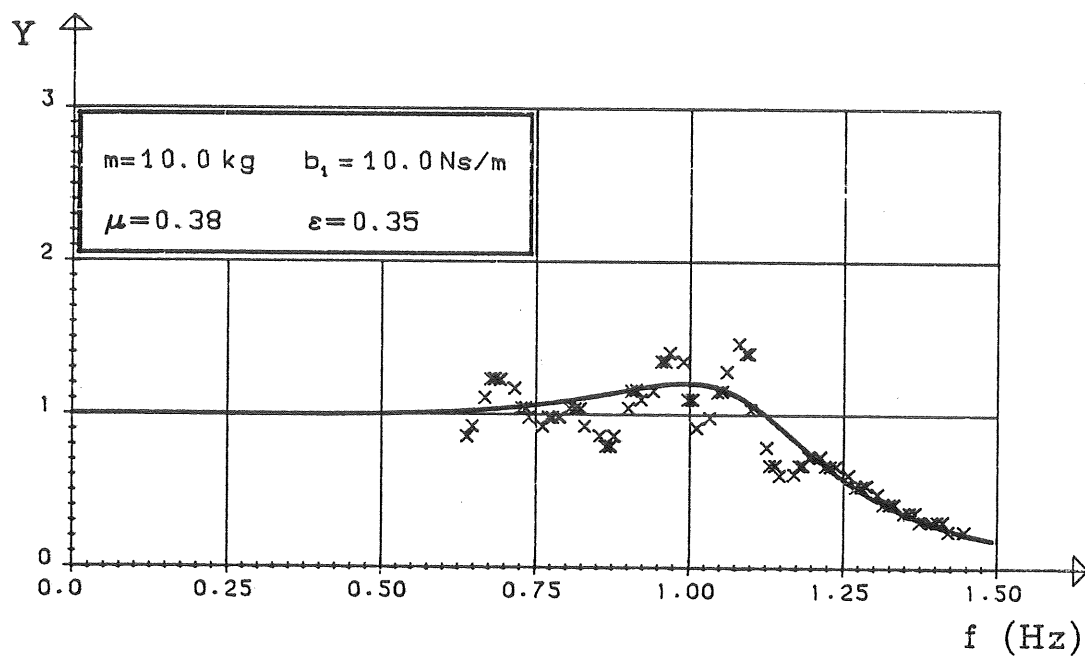


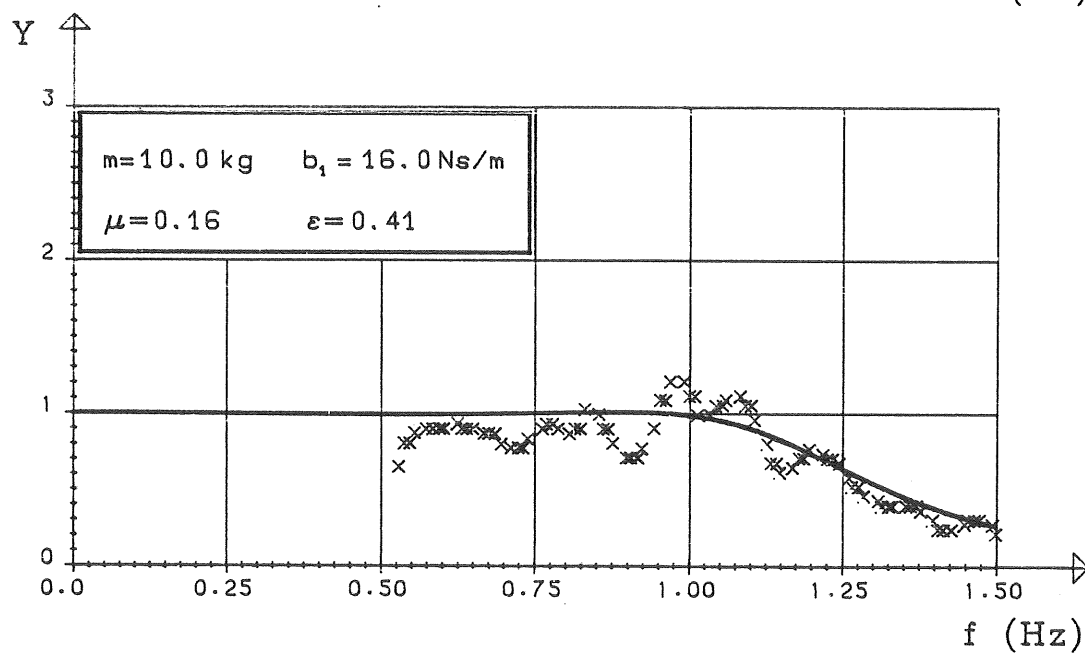
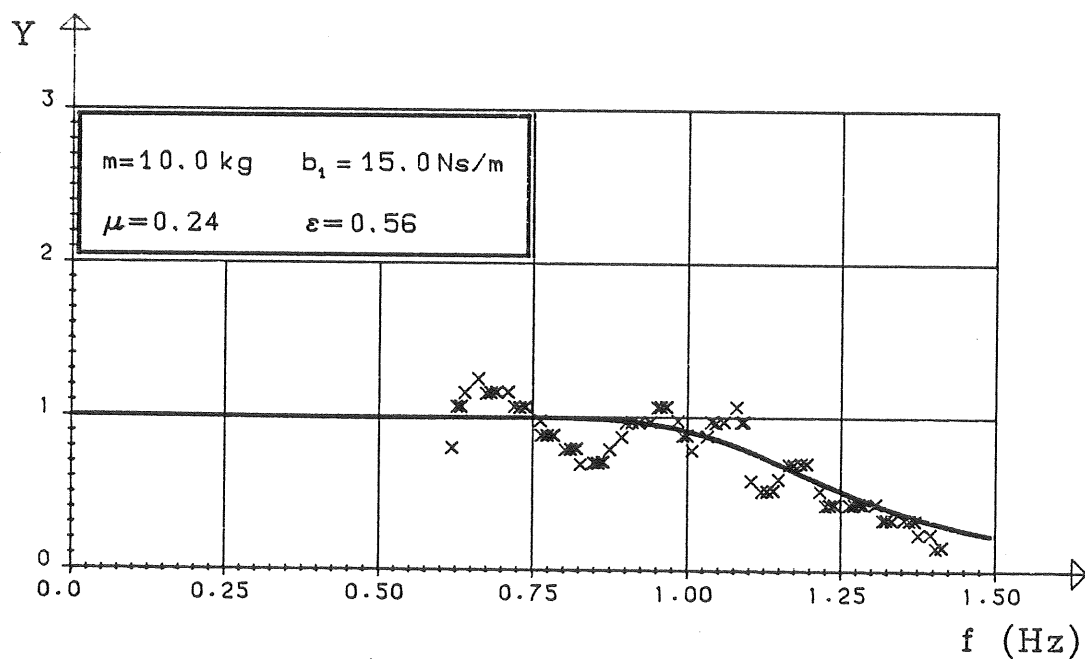
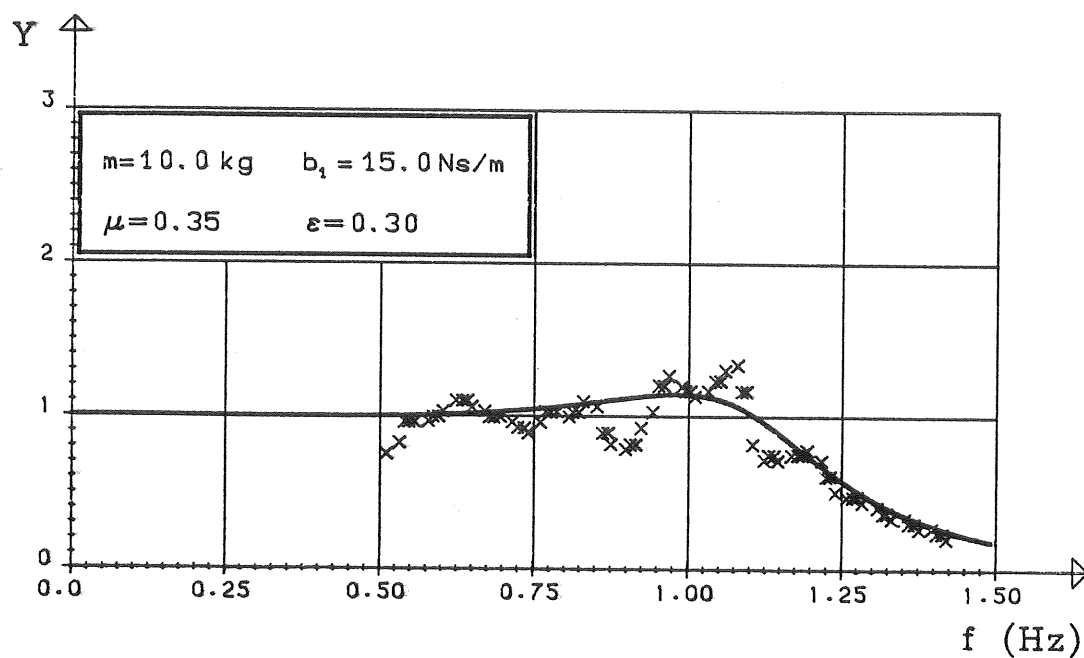


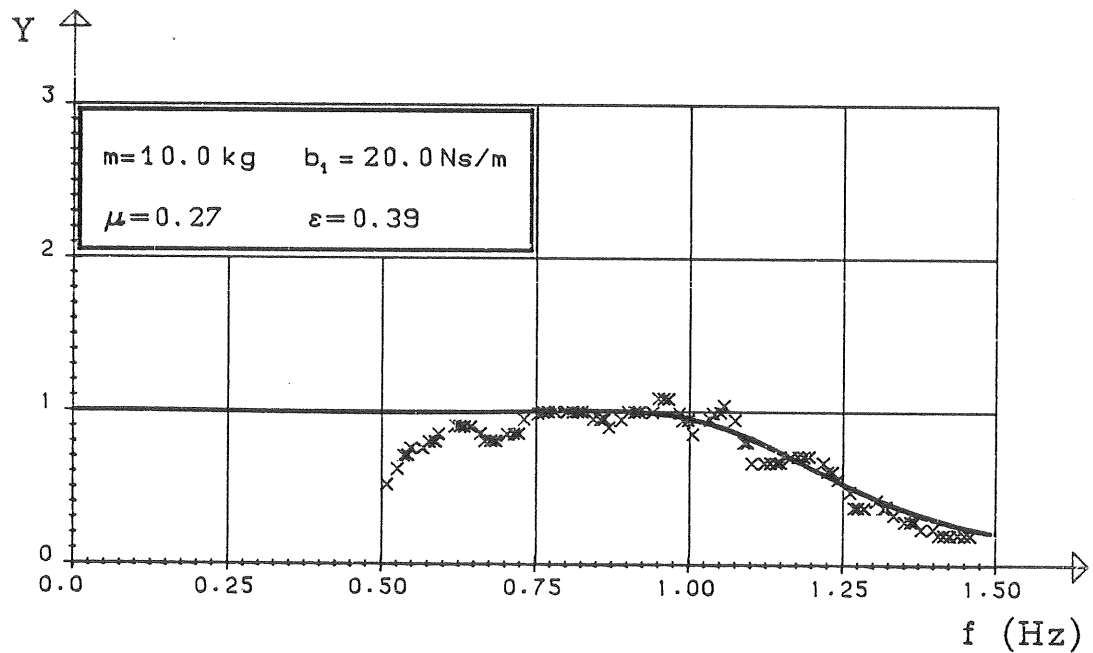
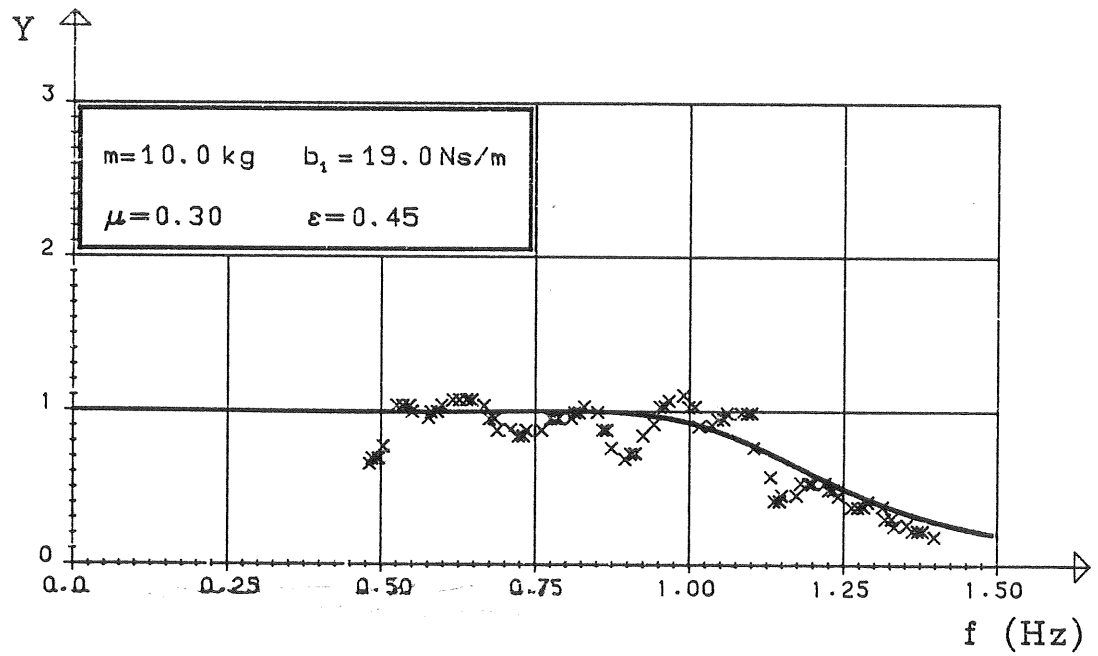
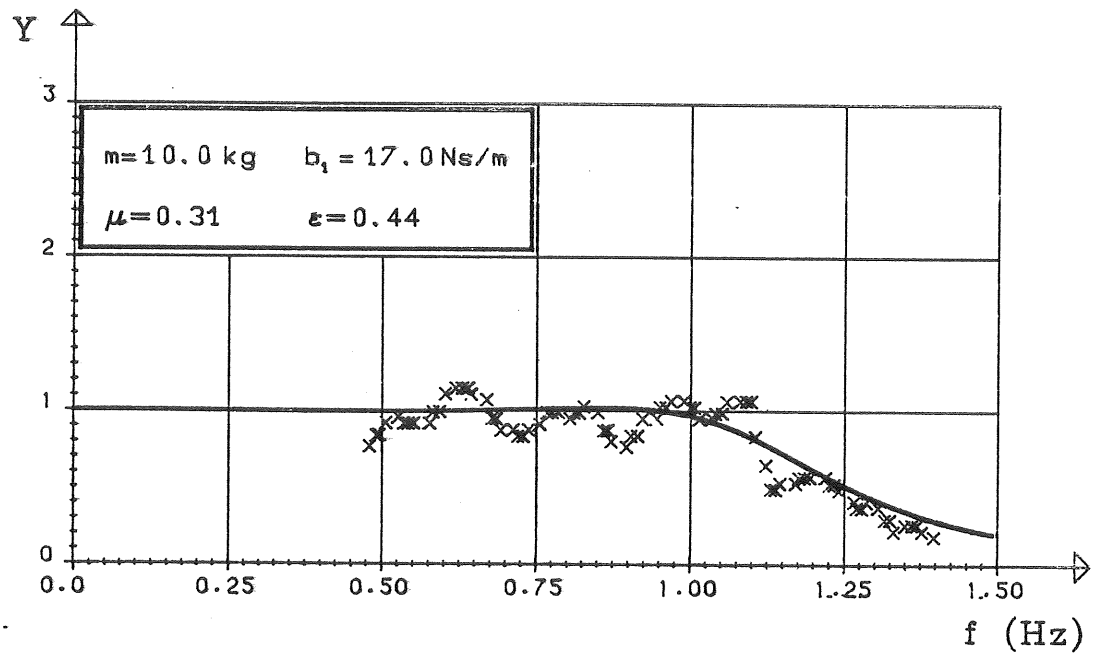
A1.8 BOJMASSA: 10. KG

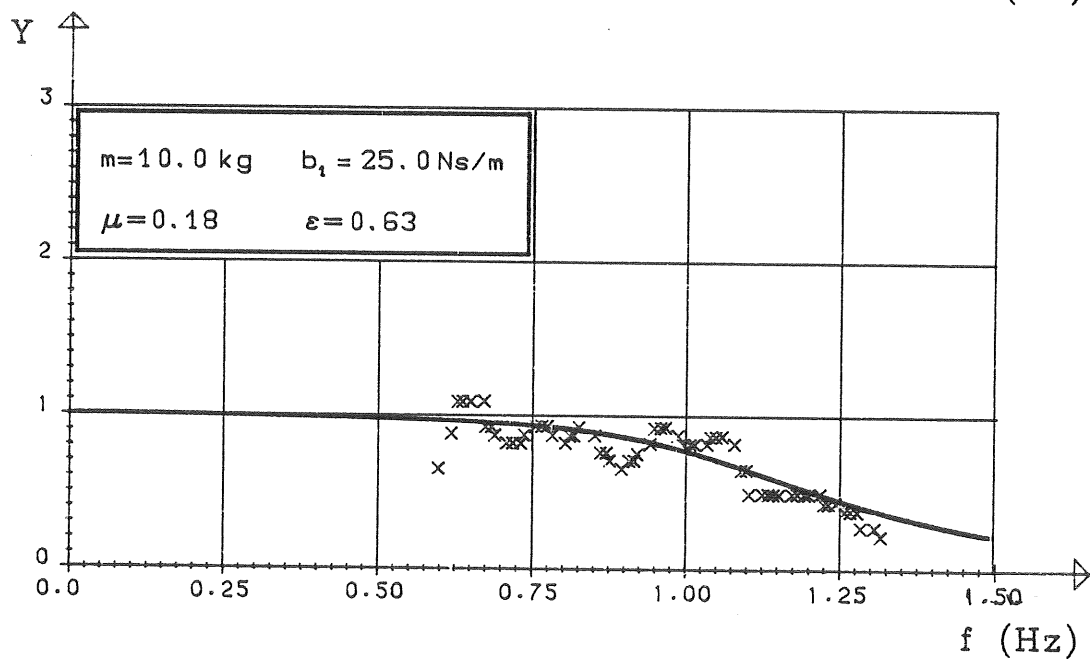
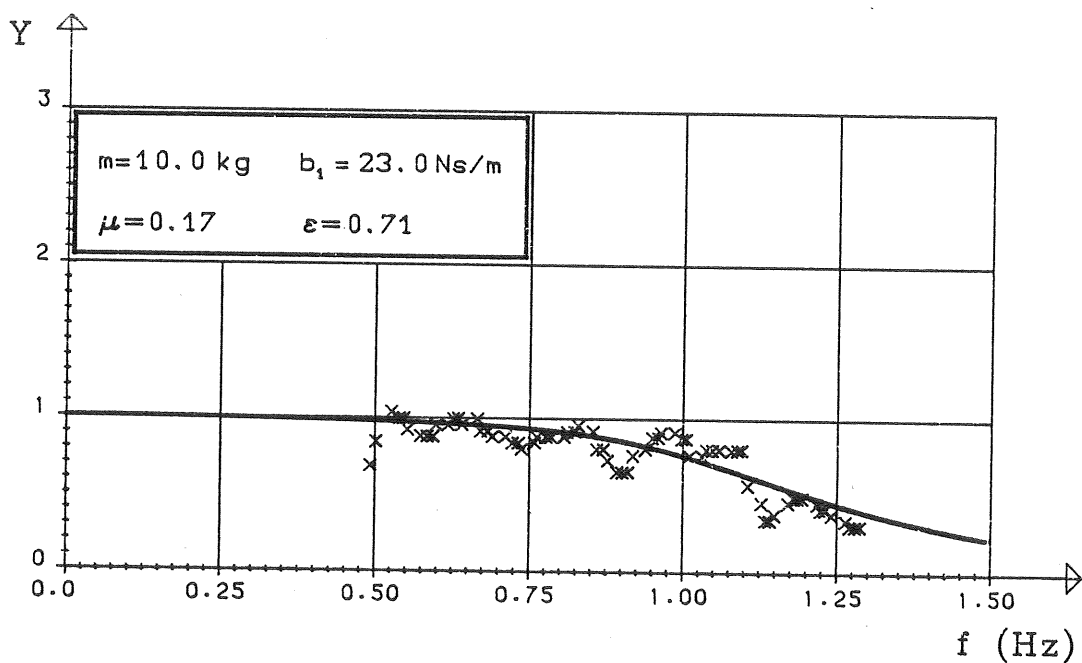
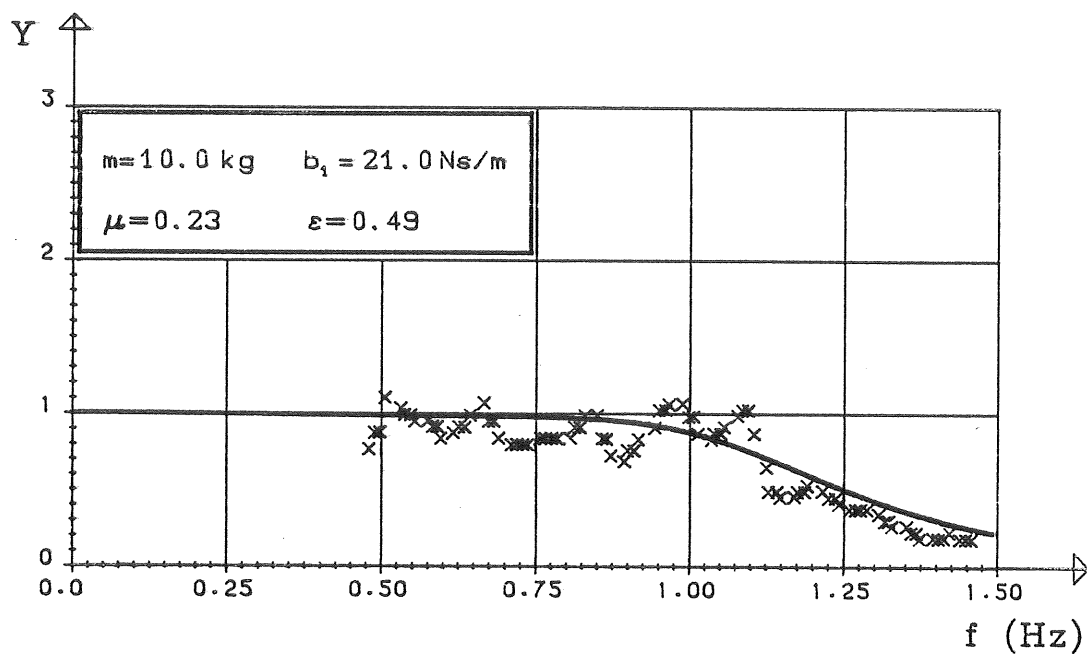
YTTRE DÄMPNING: 5 - 30 Ns/m

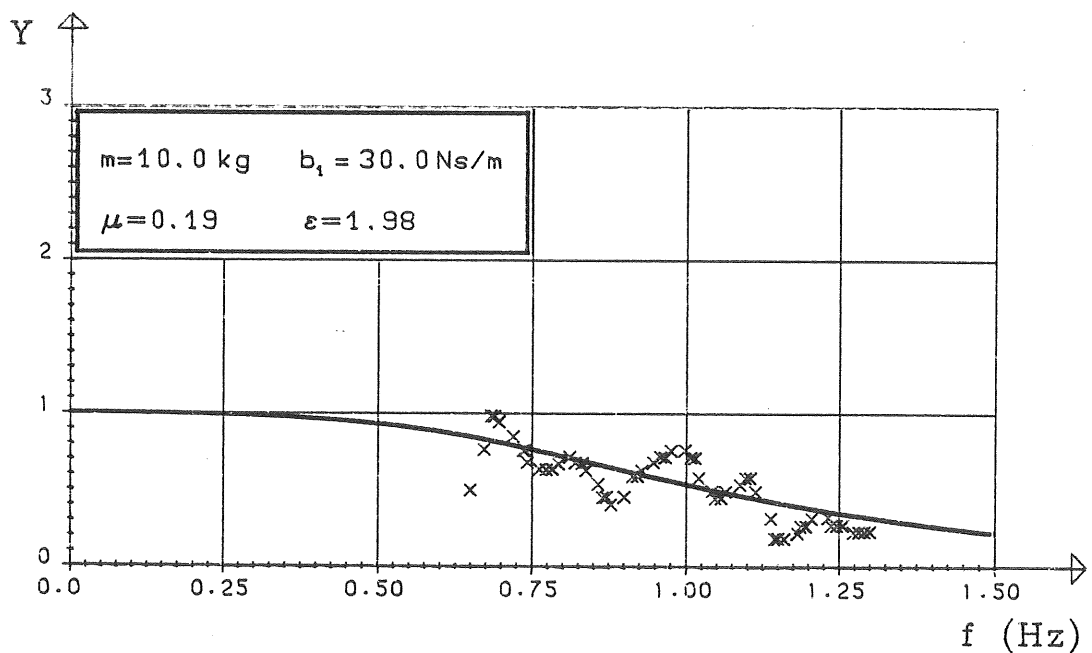
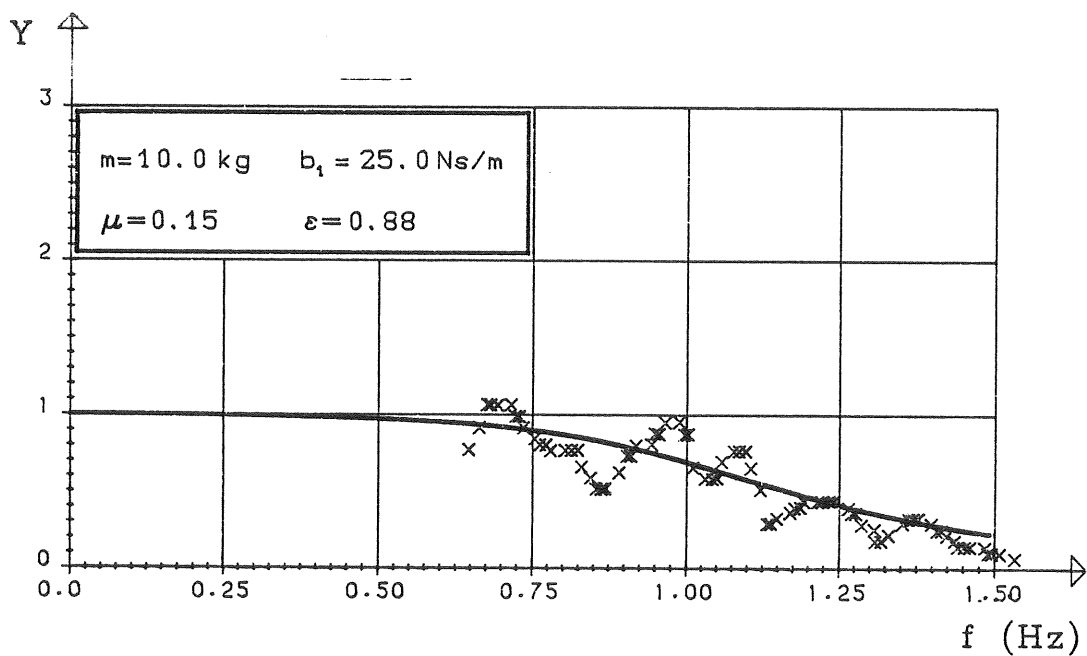
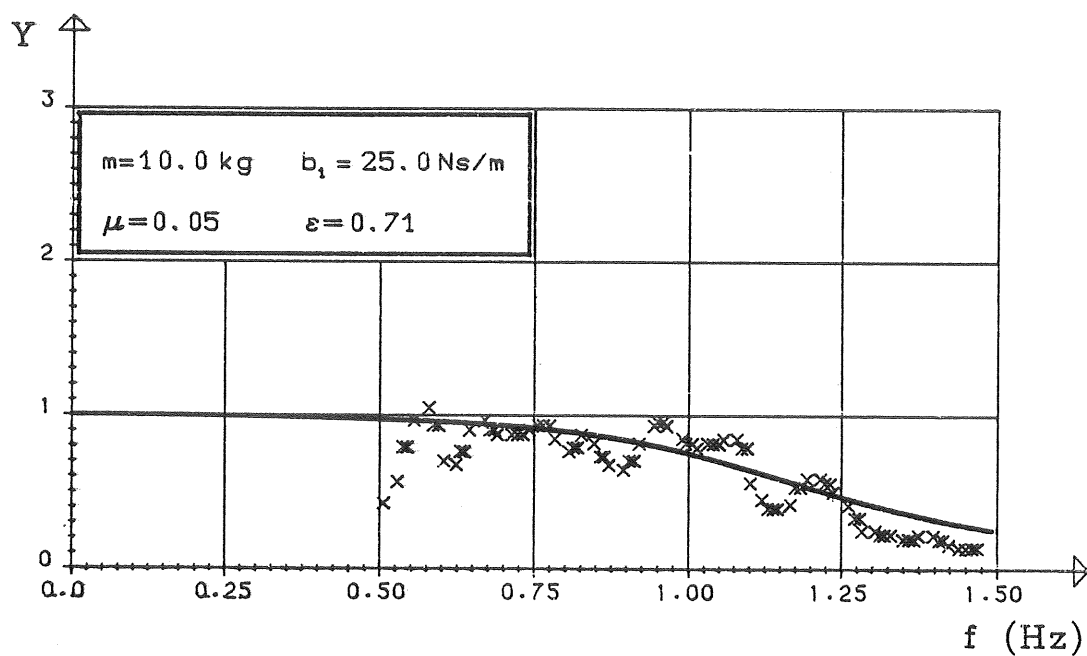






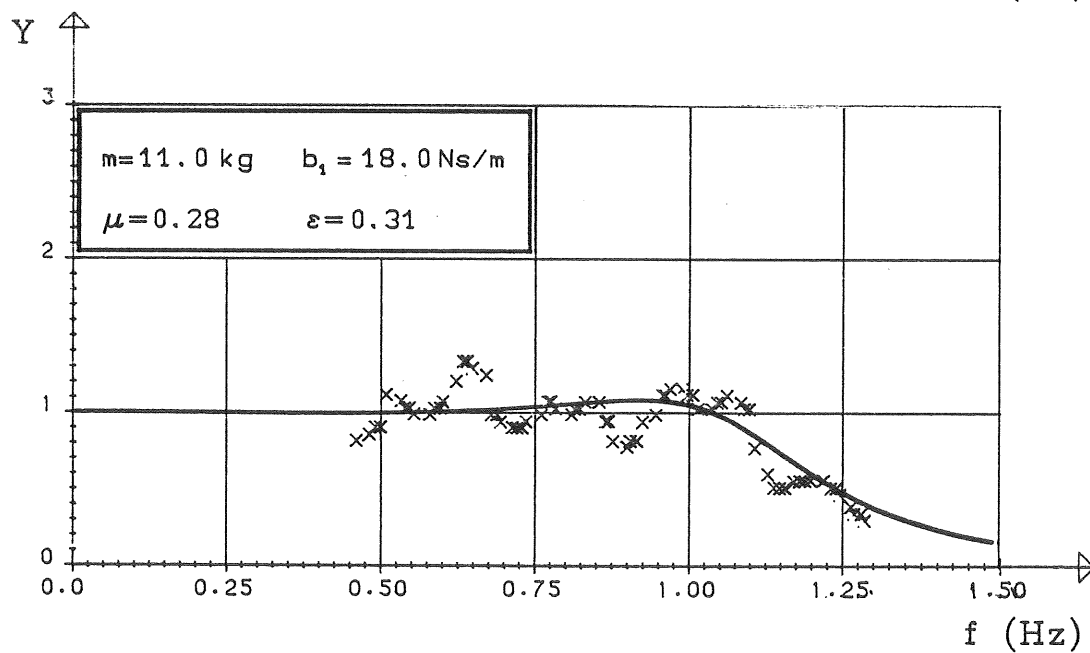
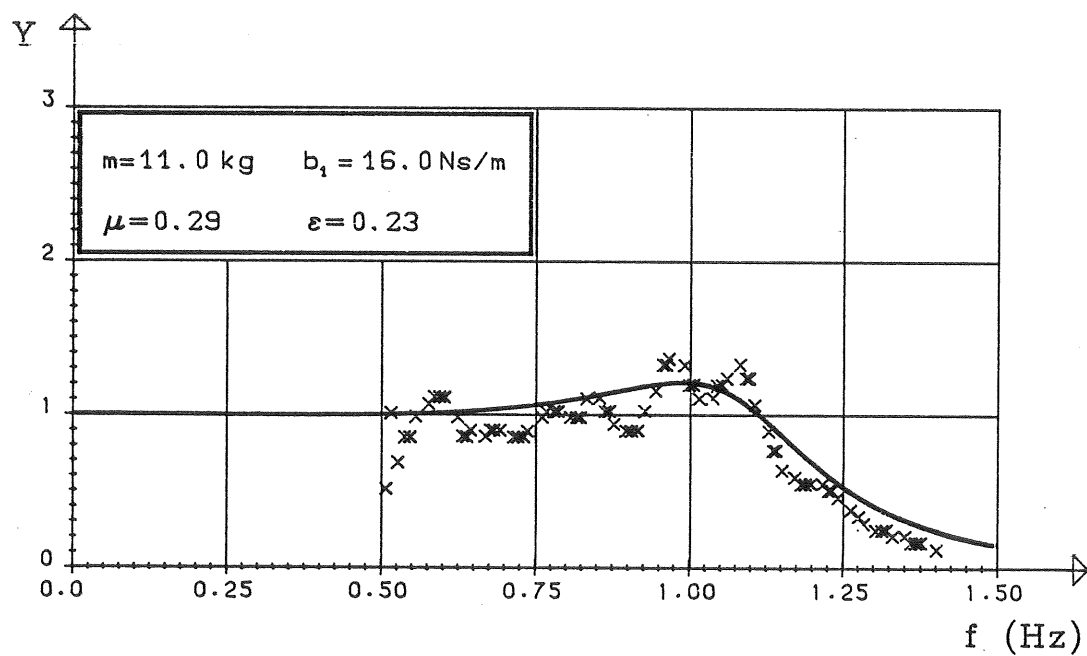
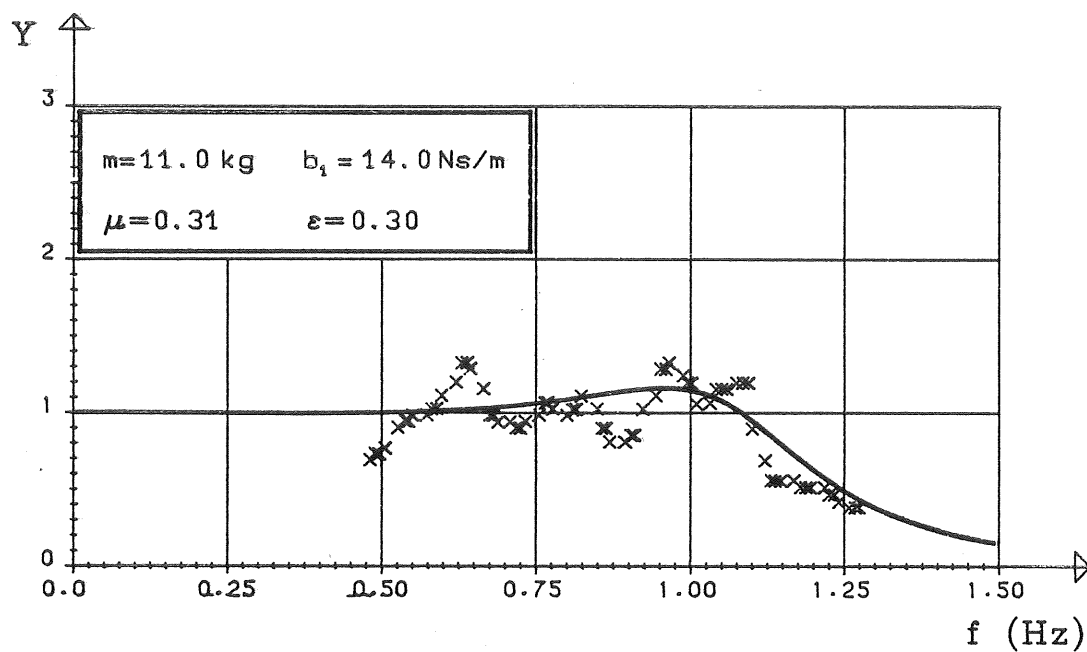


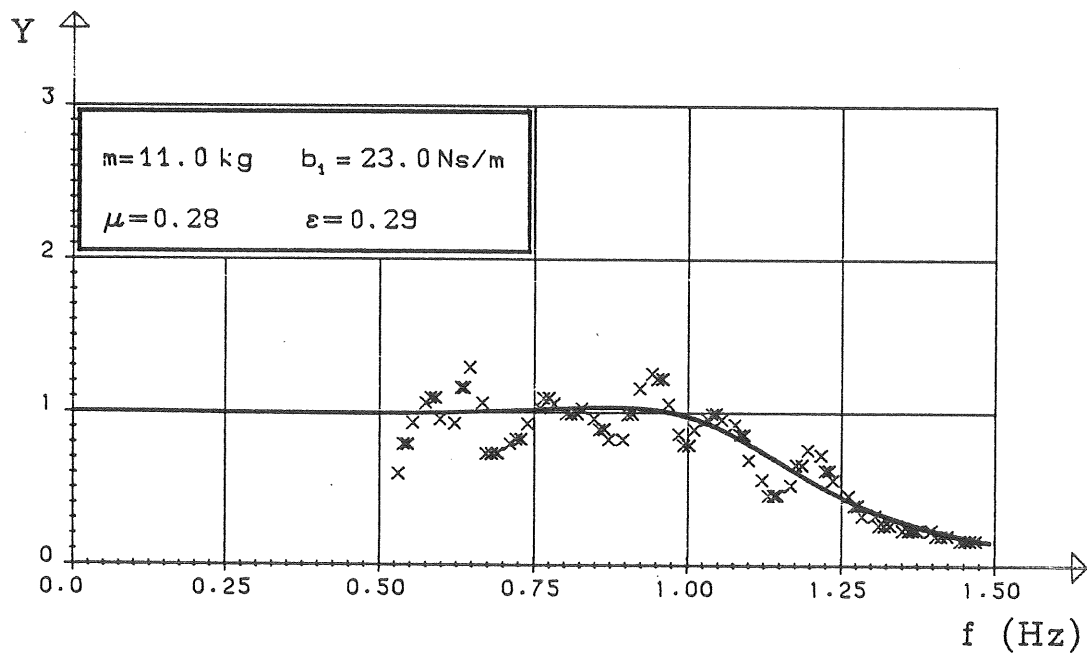
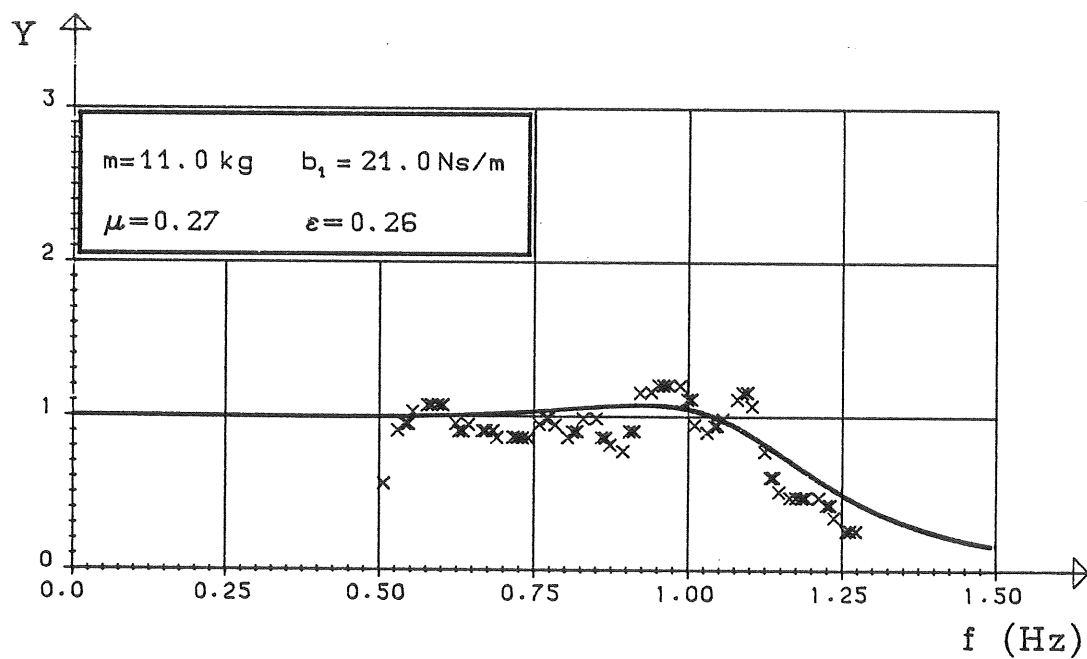
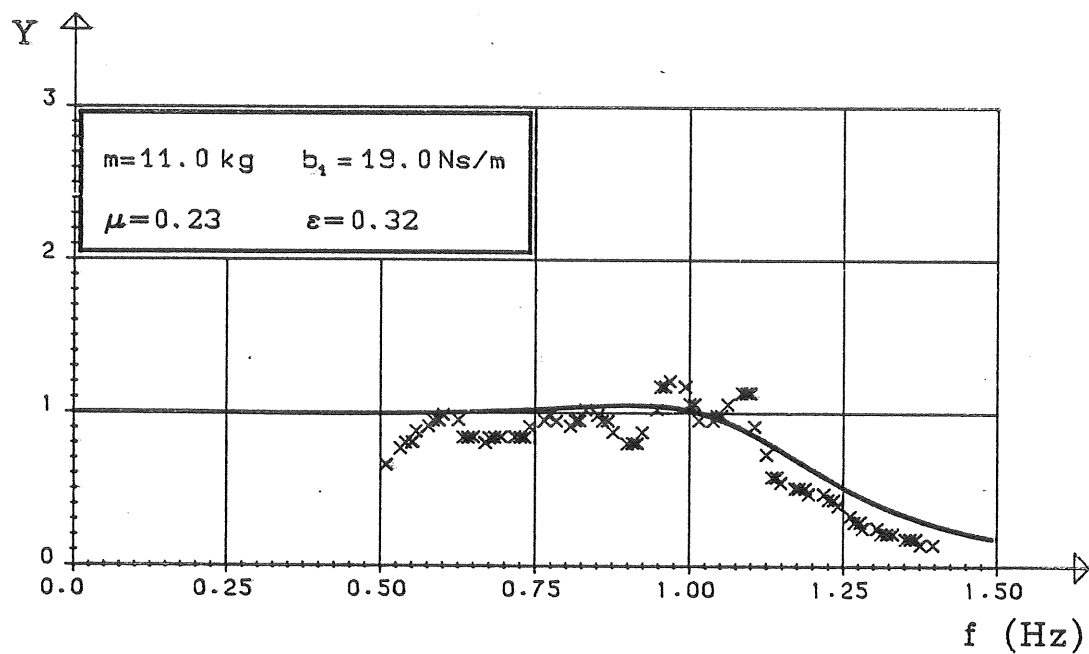


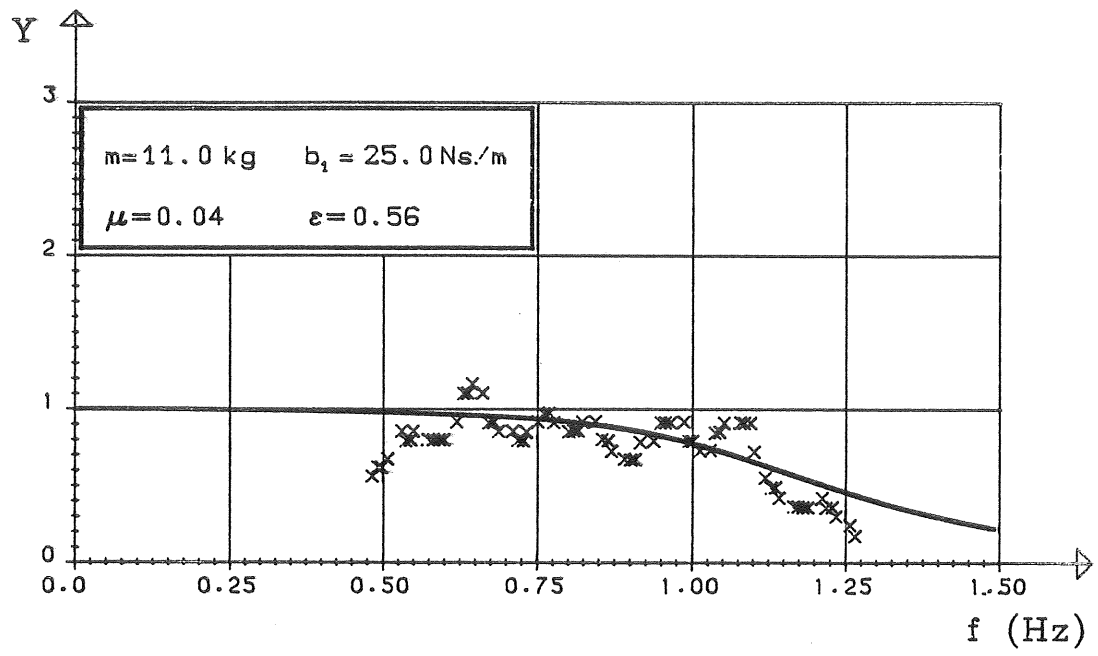


A1.9 BOJMASSA: 11. KG

YTTRE DÄMPNING: 14 - 25 Ns/m

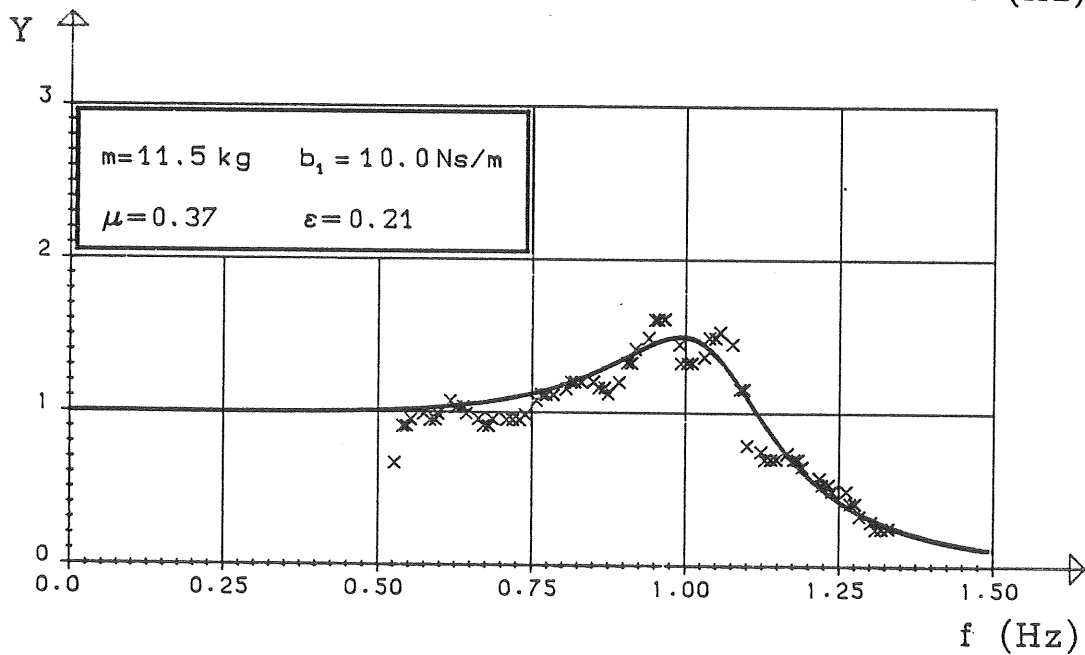
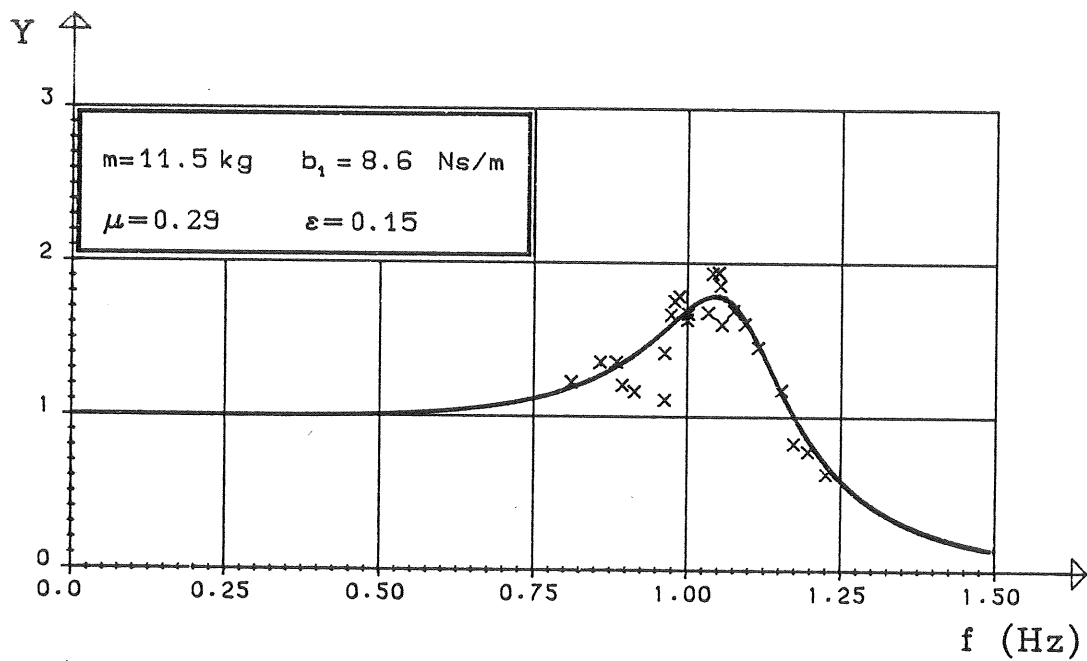
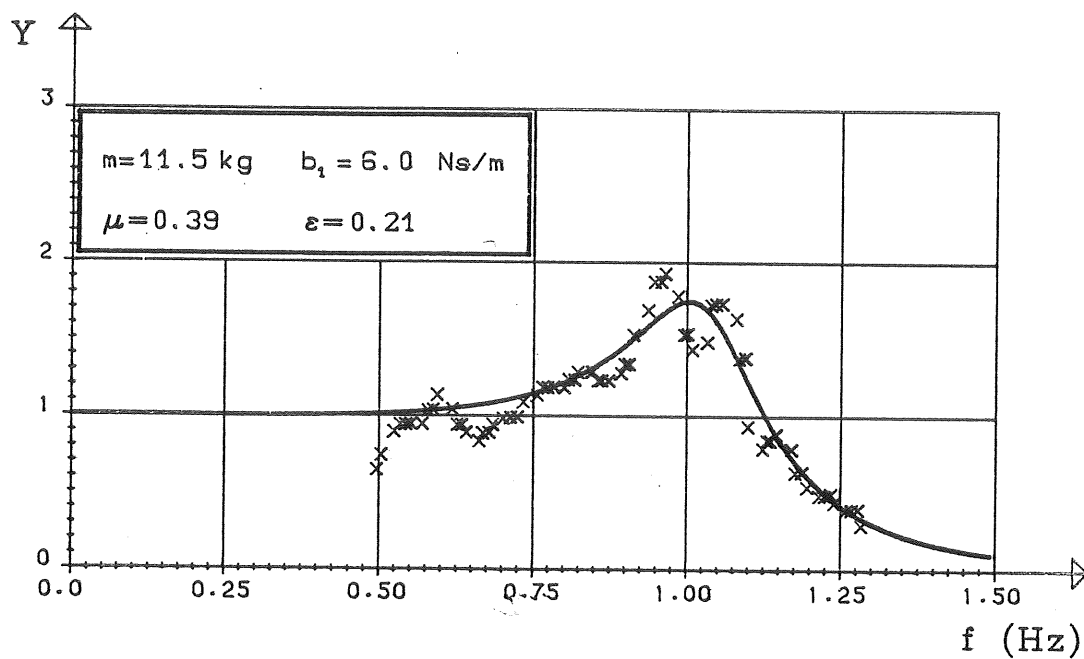


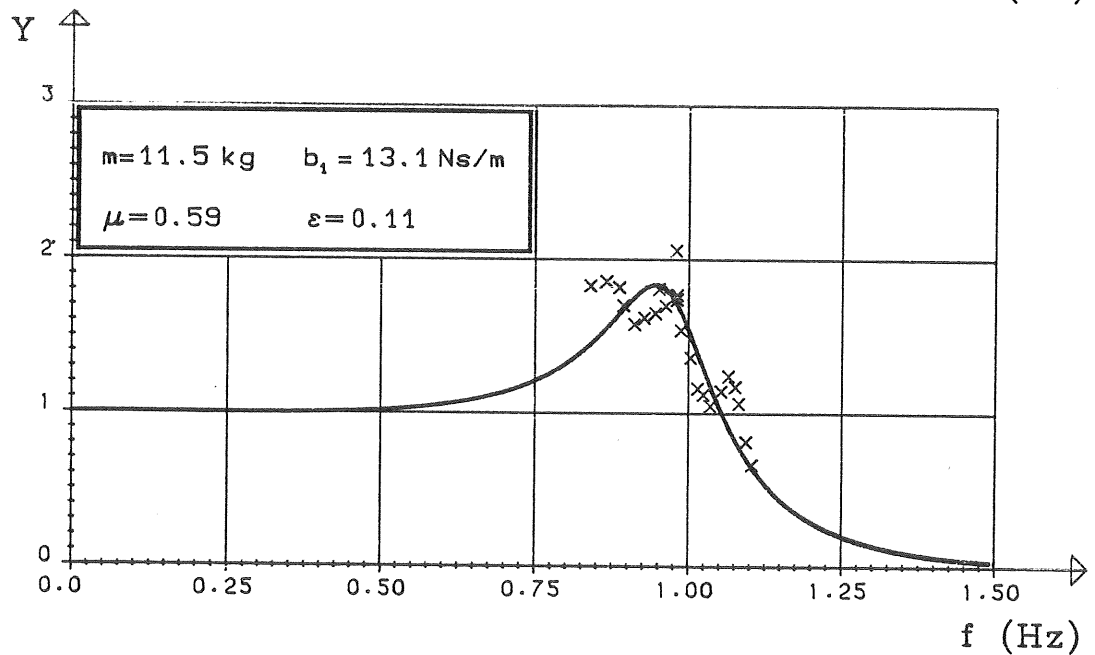
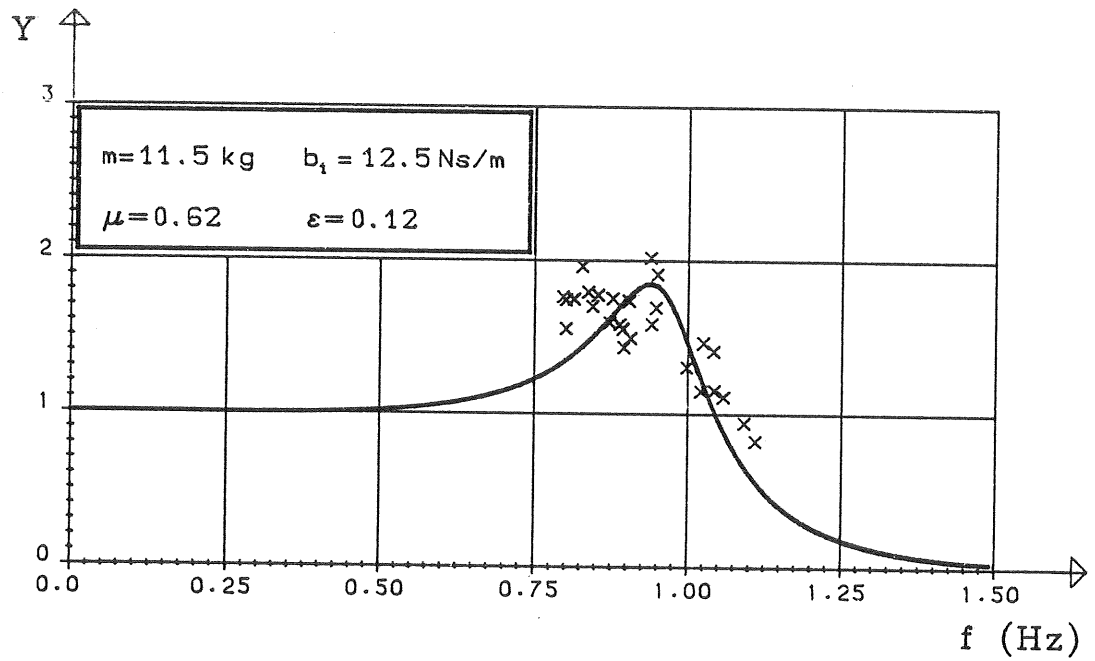
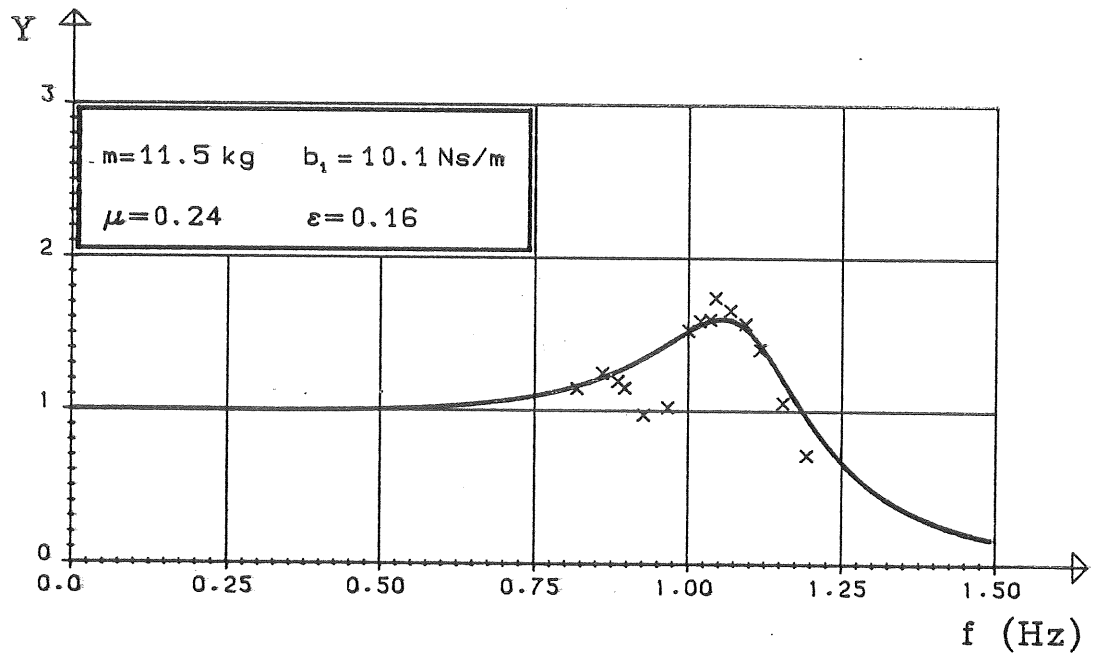


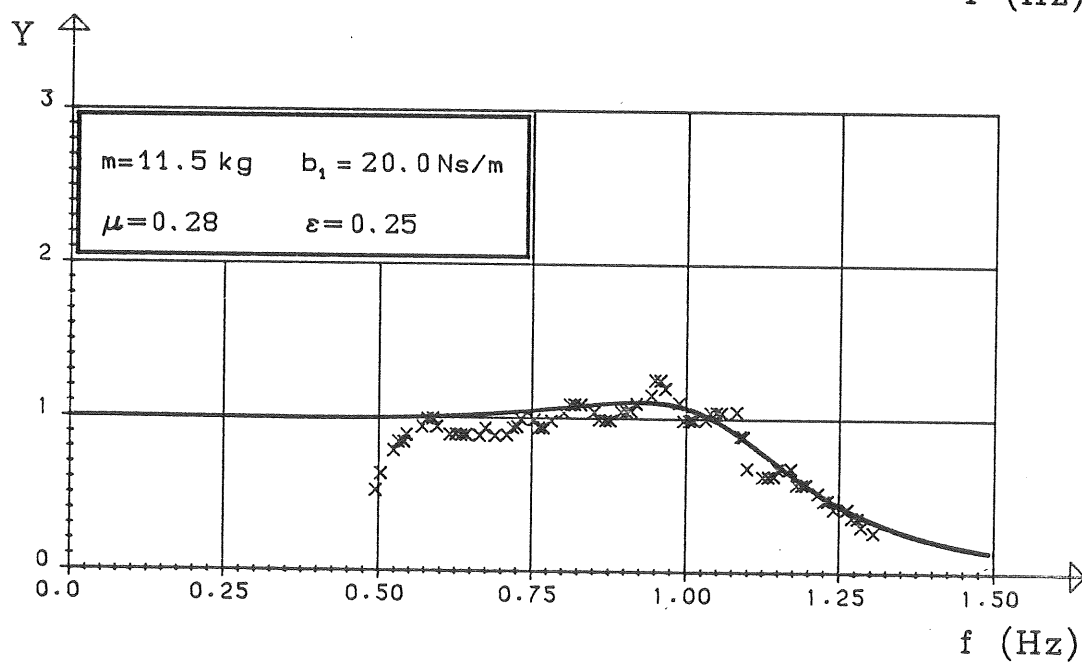
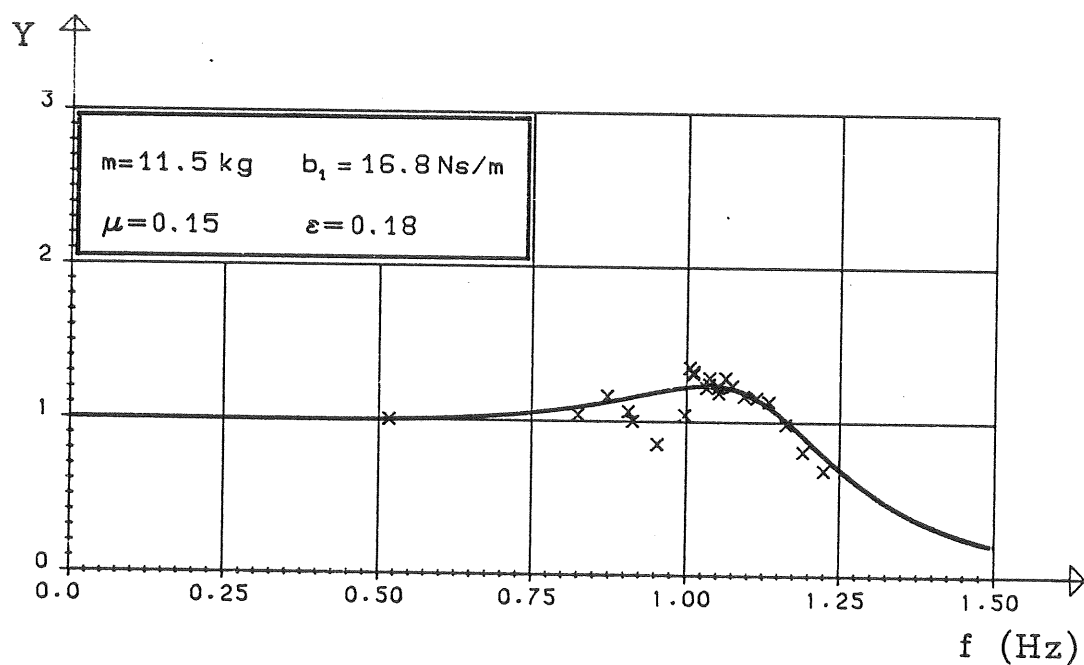
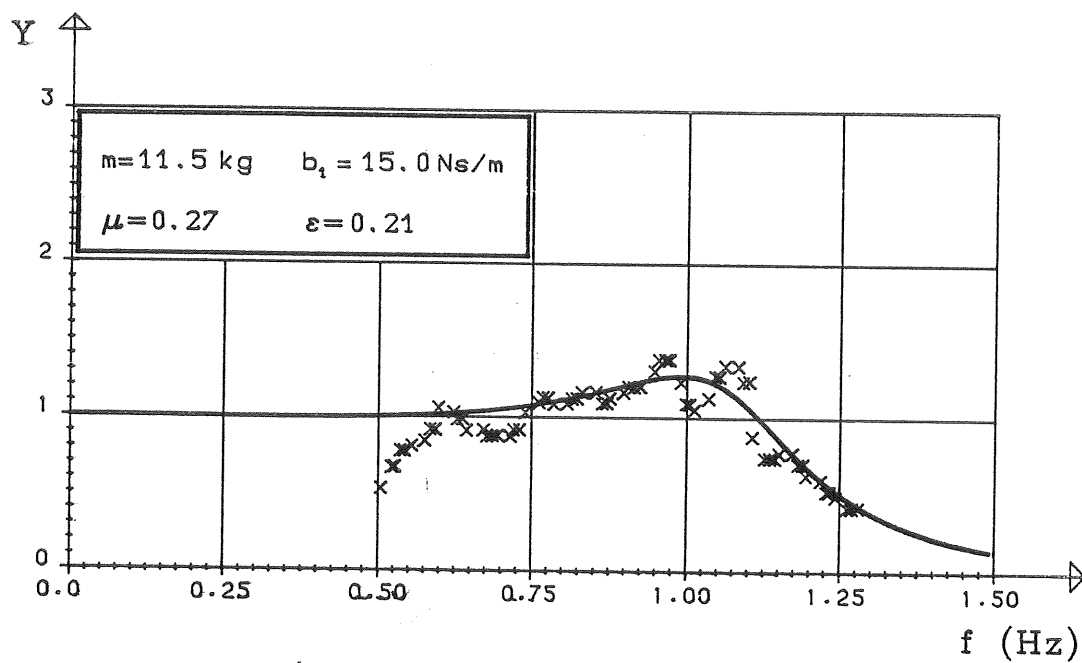


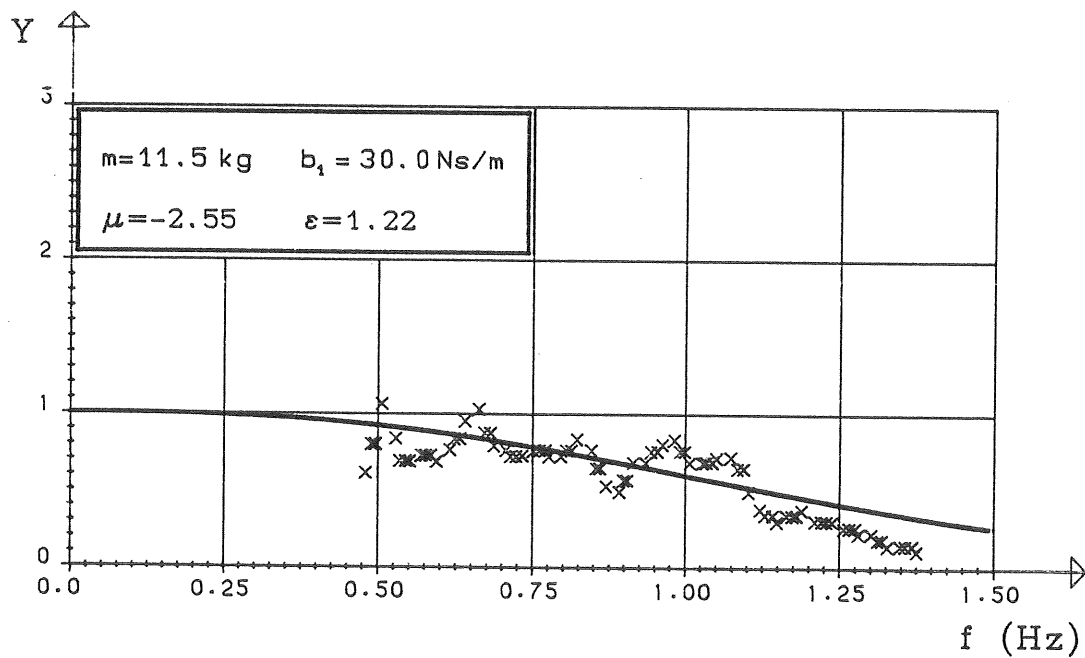
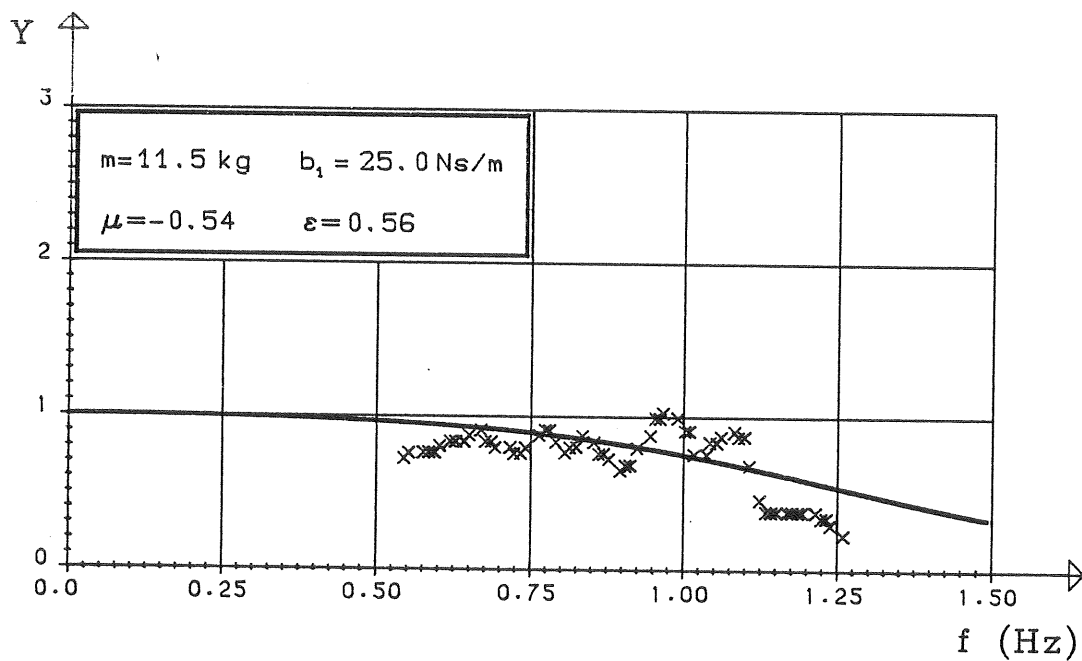
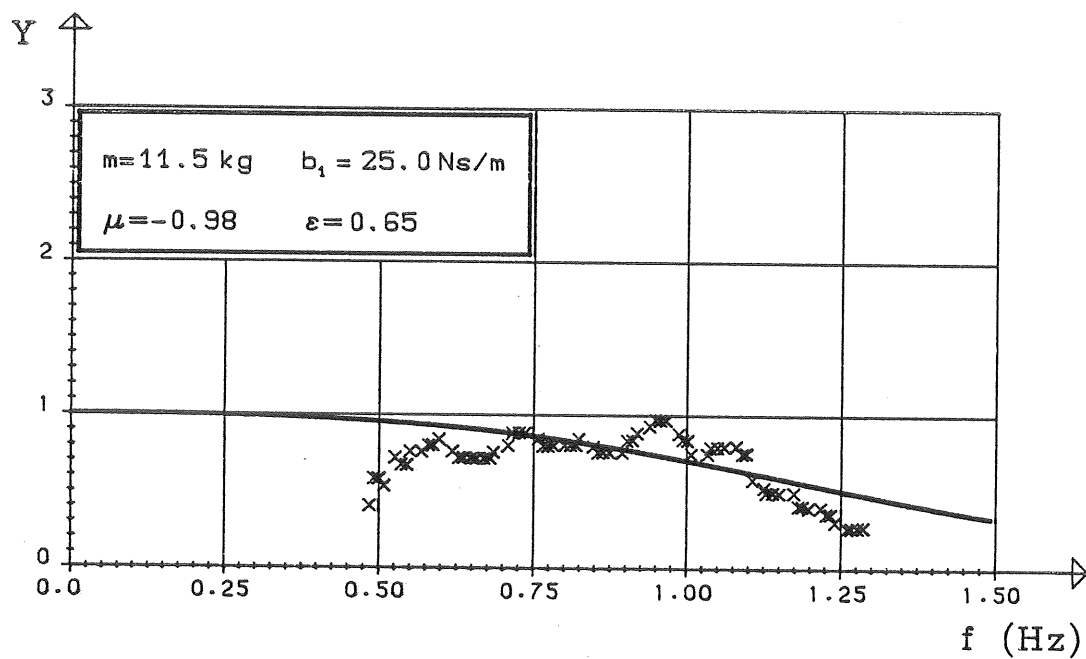
A1.10 BOJMASSA: 11.5 KG

YTTRE DÄMPNING: 6 - 30 Ns/M



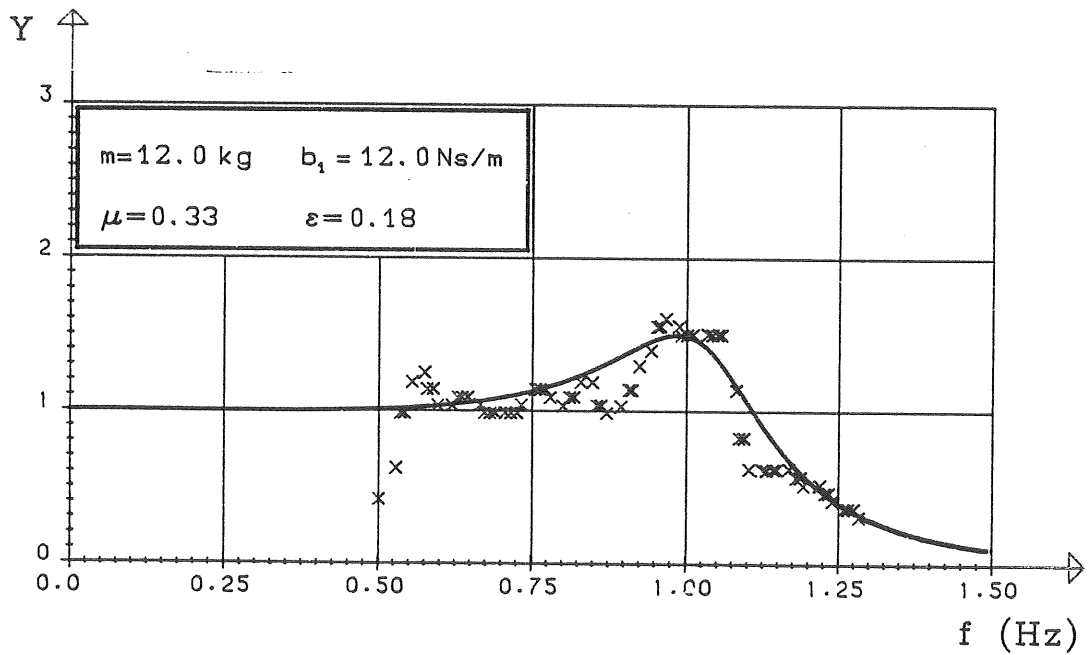
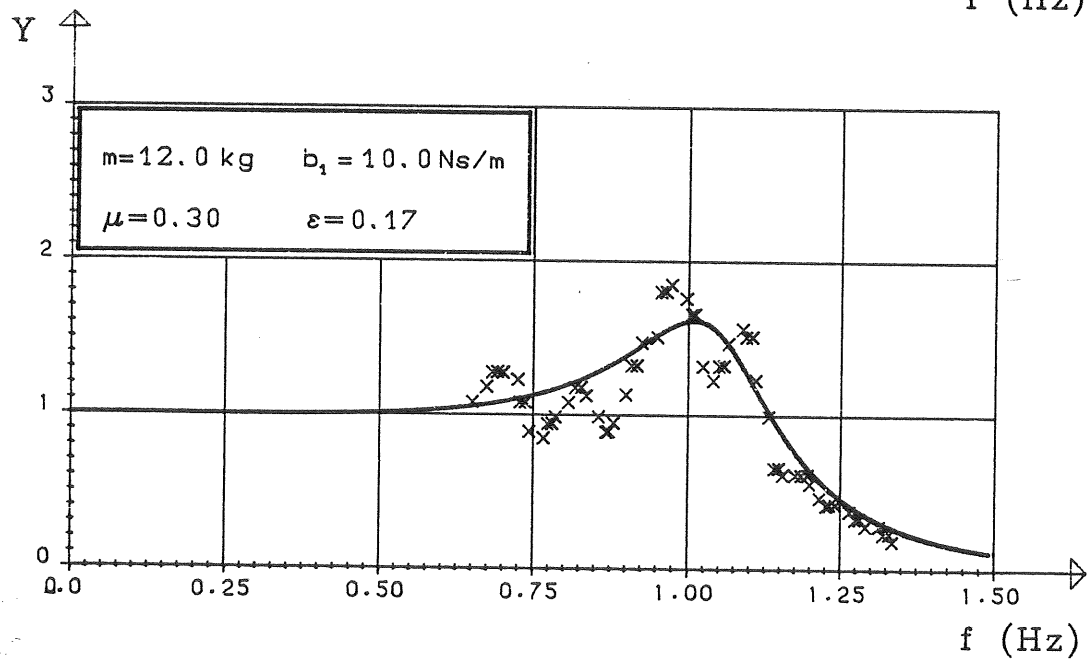
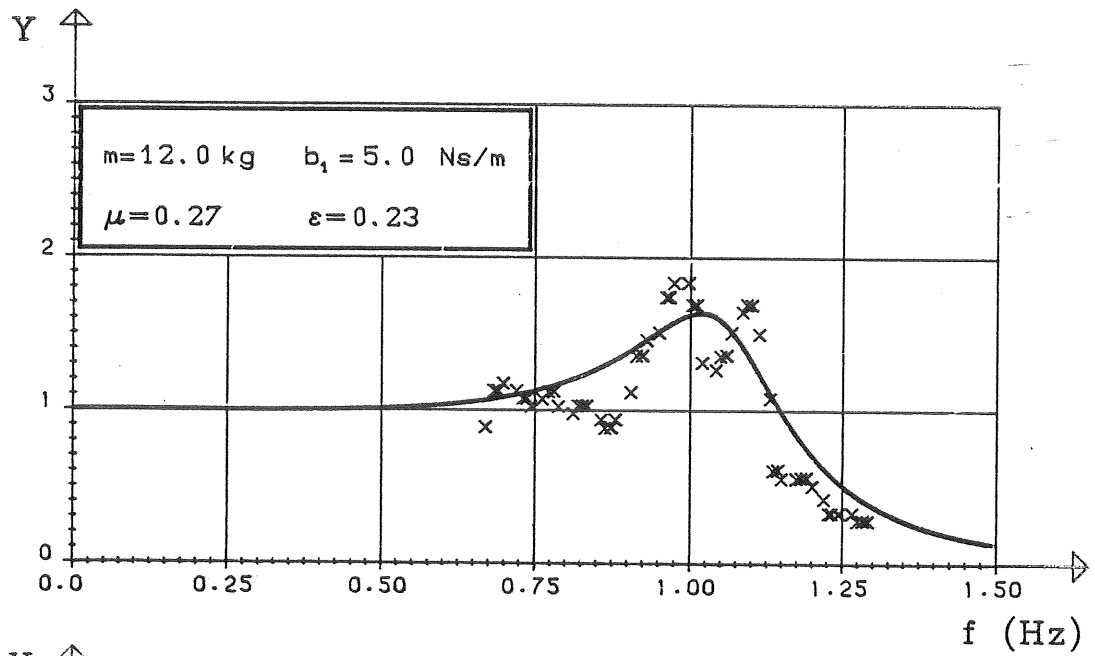


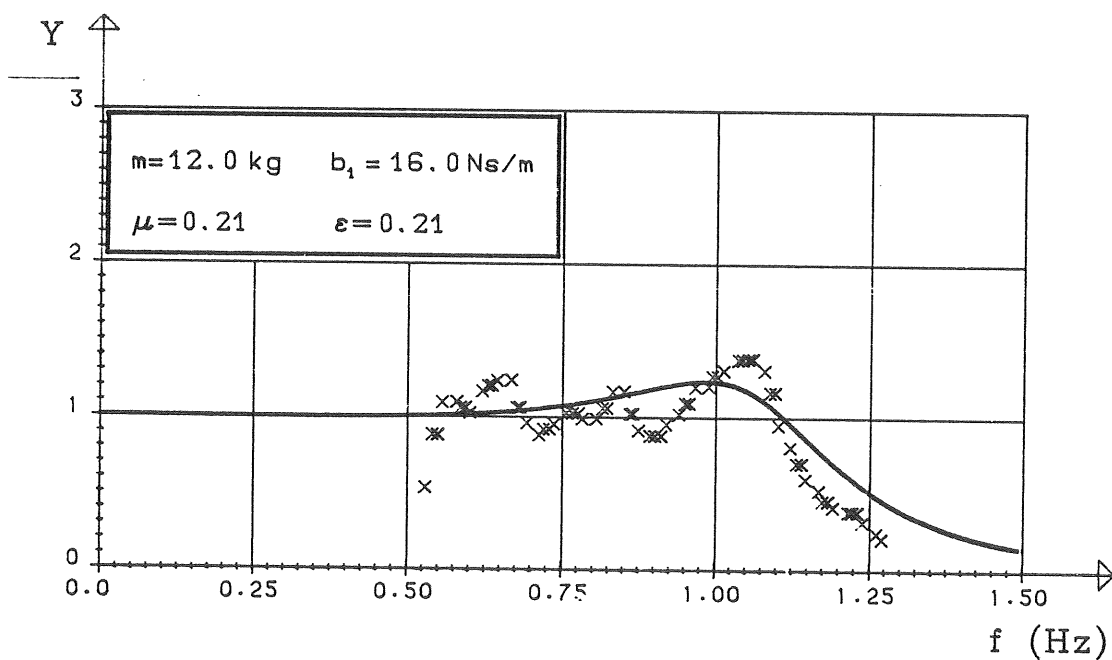
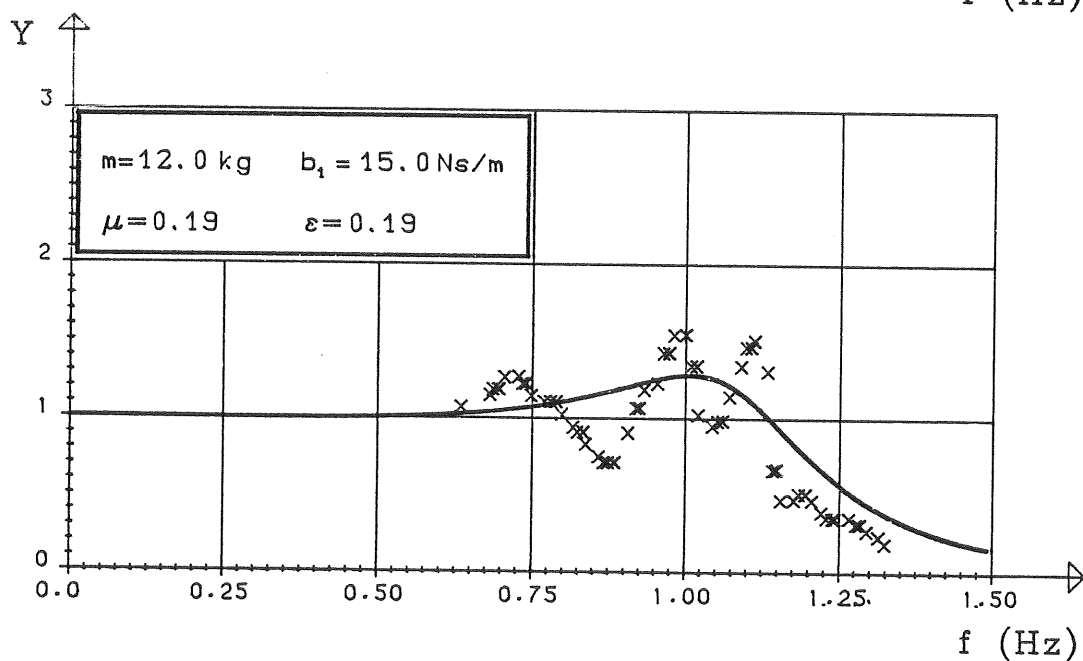
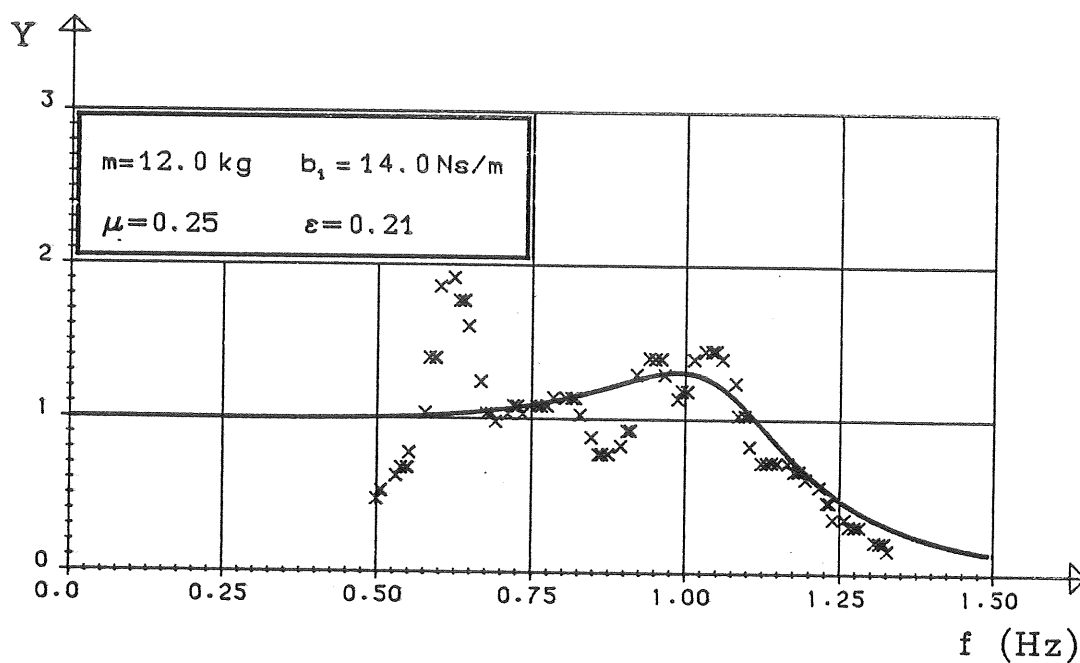


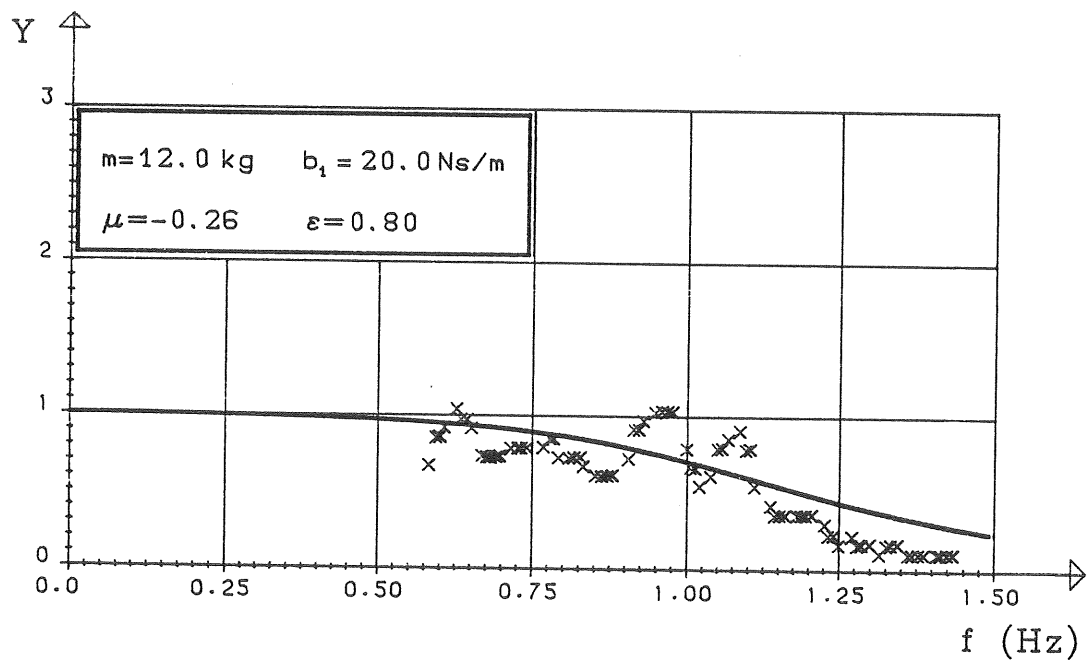
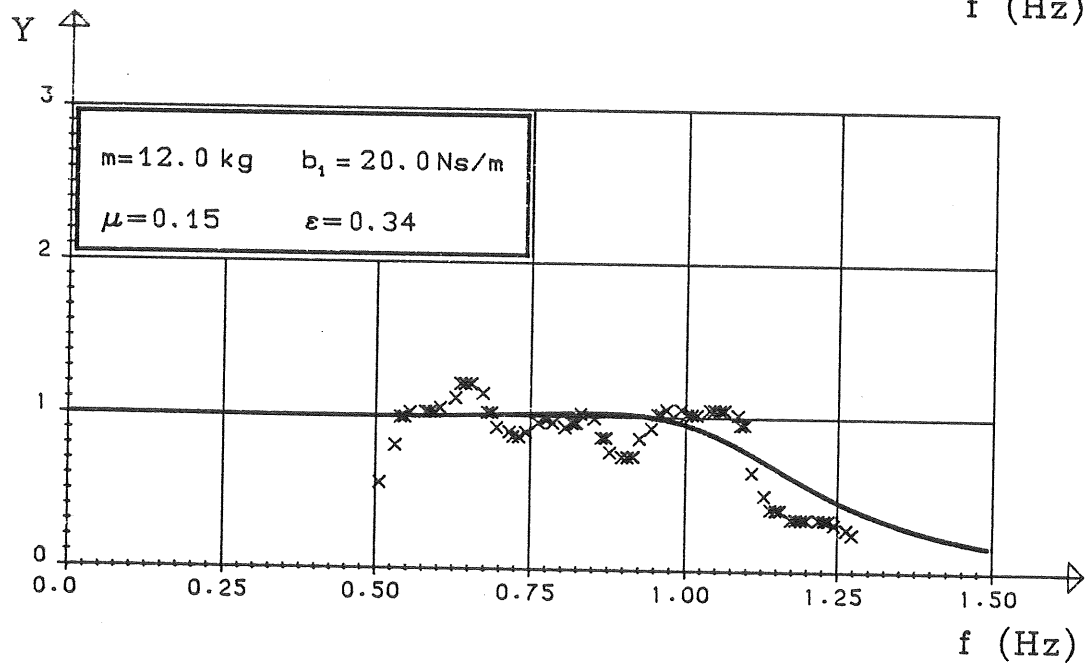
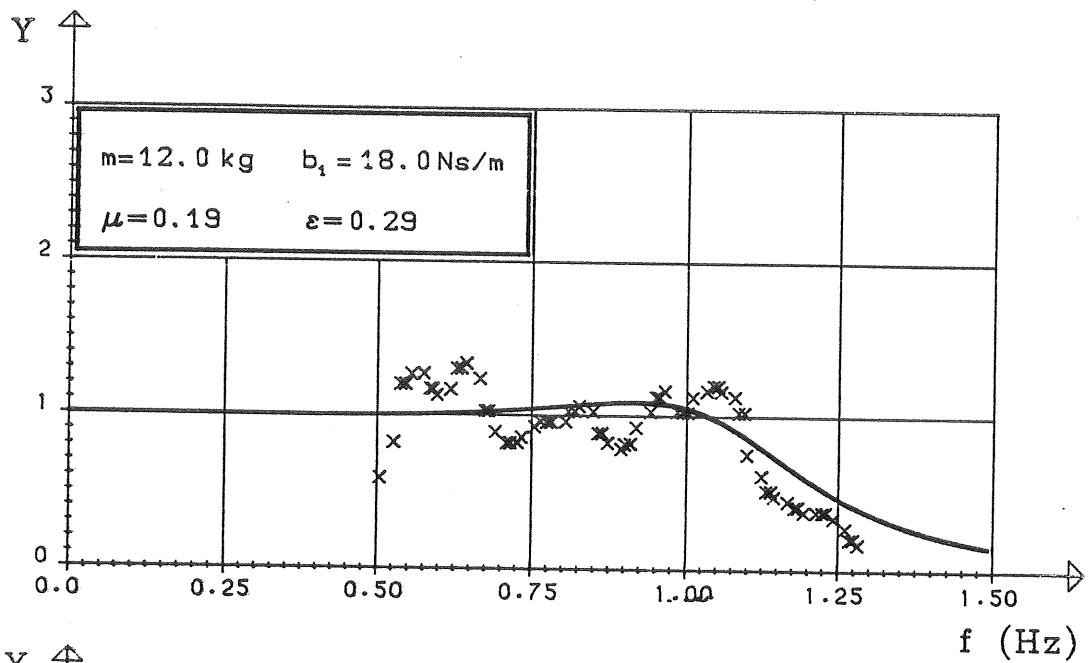


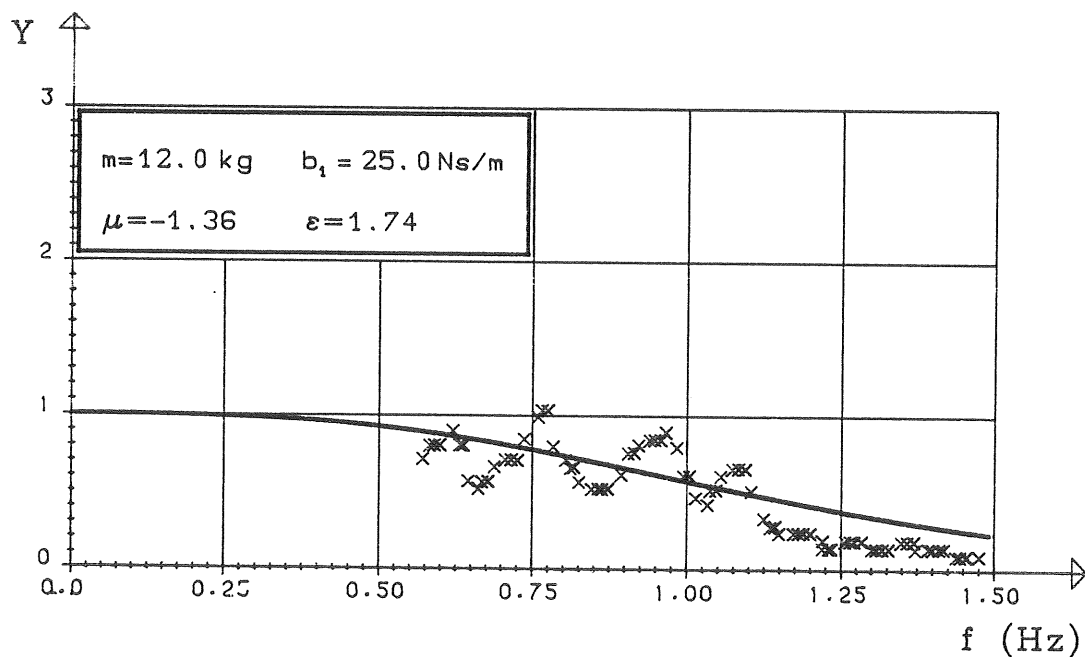
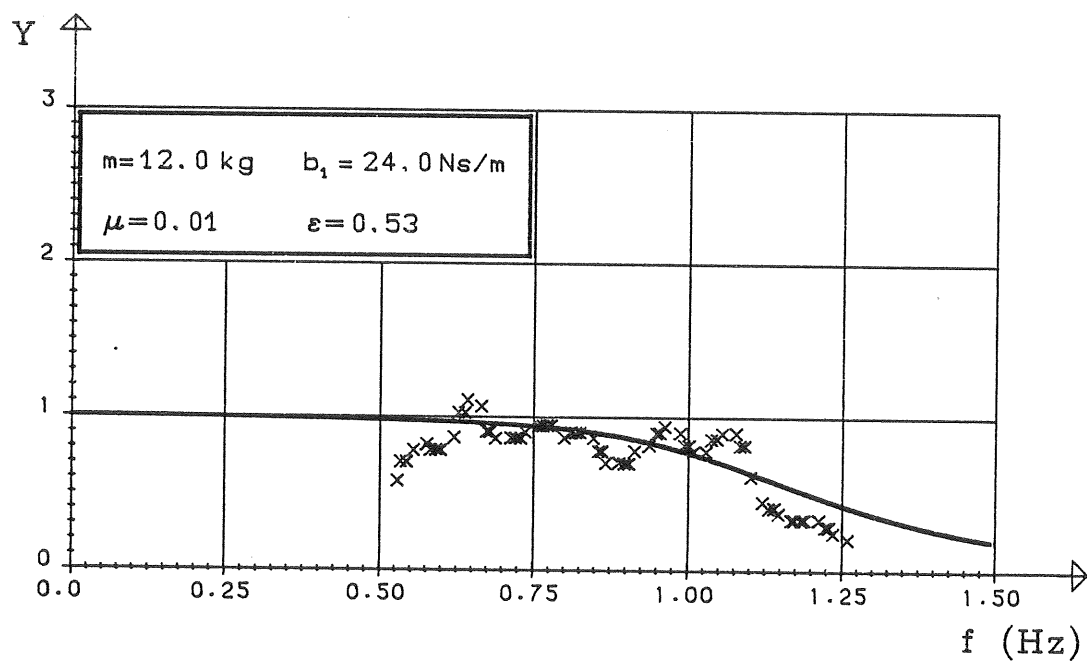
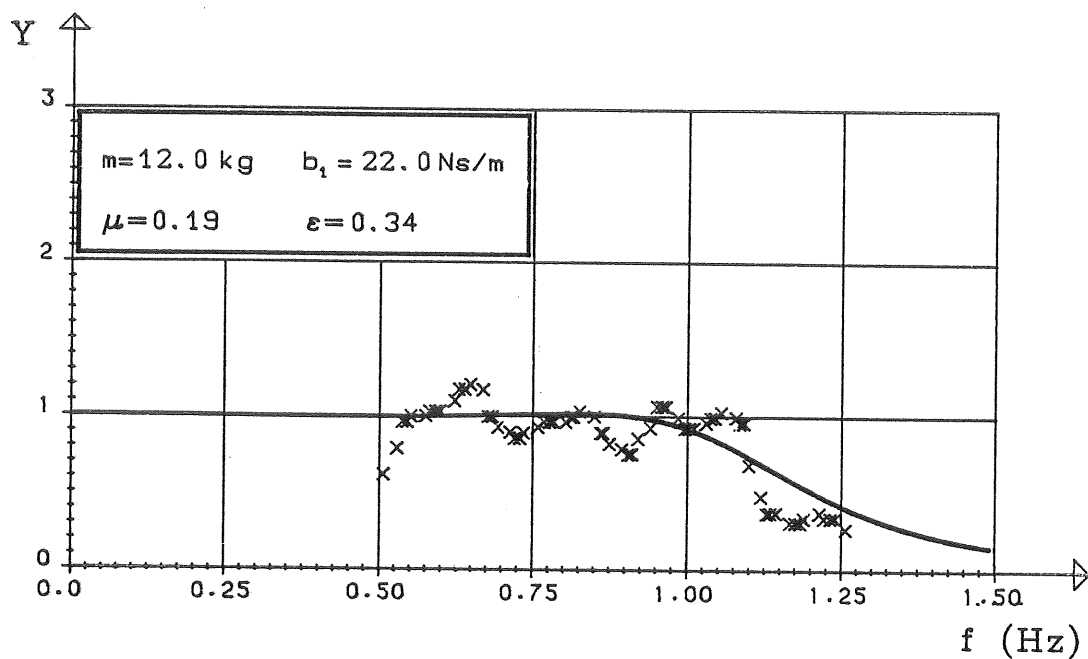
A1.11 BOJMASSA: 12. KG

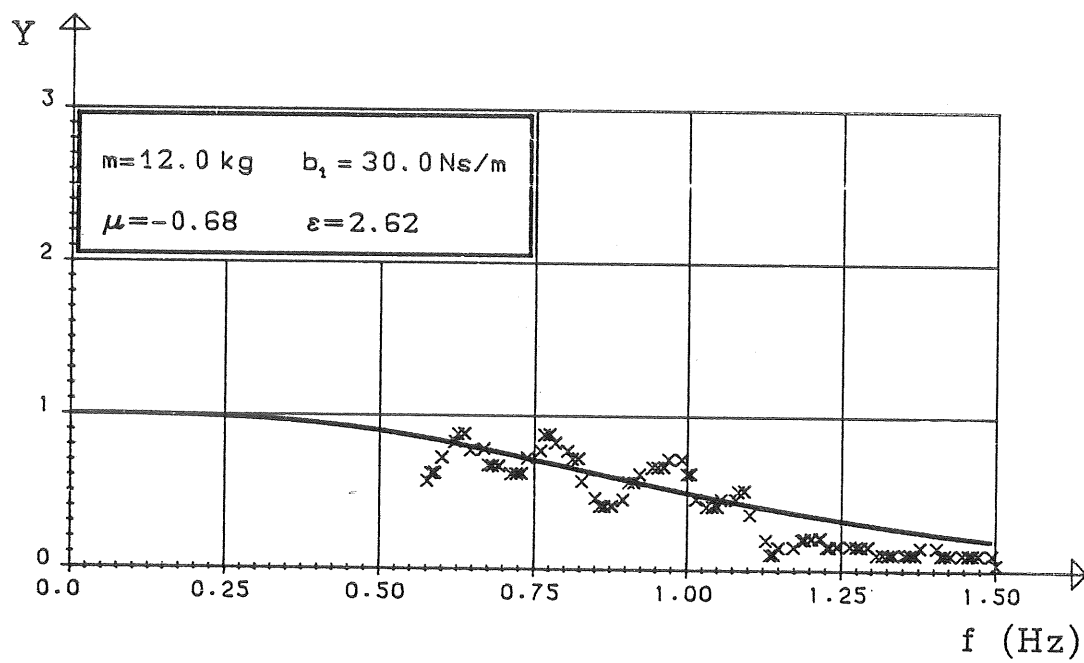
YTTRE DÄMPNING: 5 - 30 Ns/m





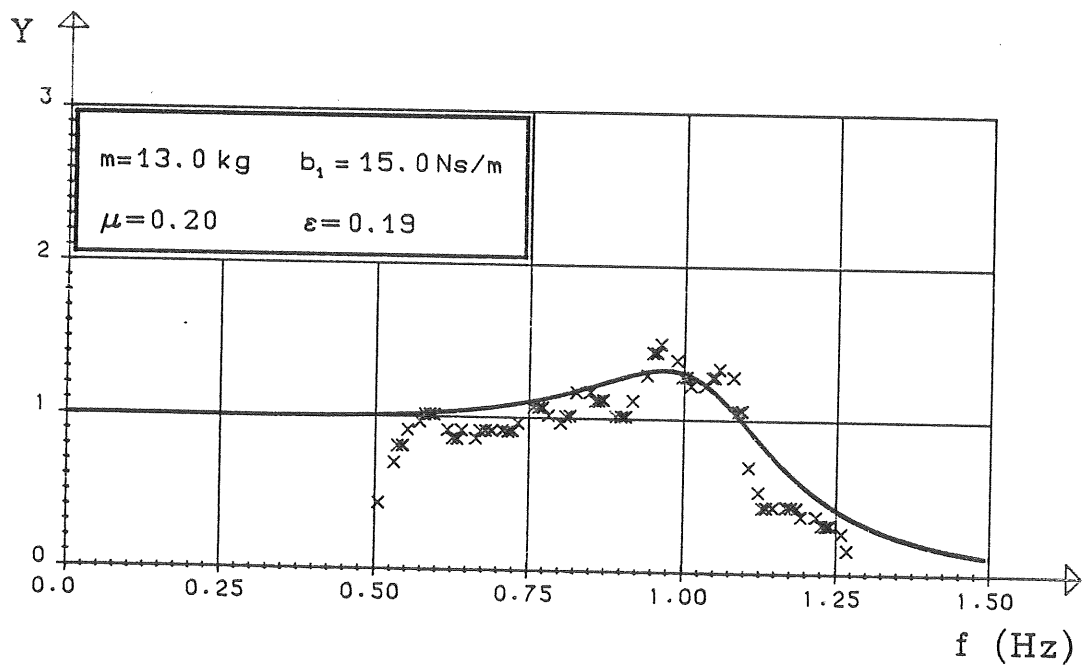
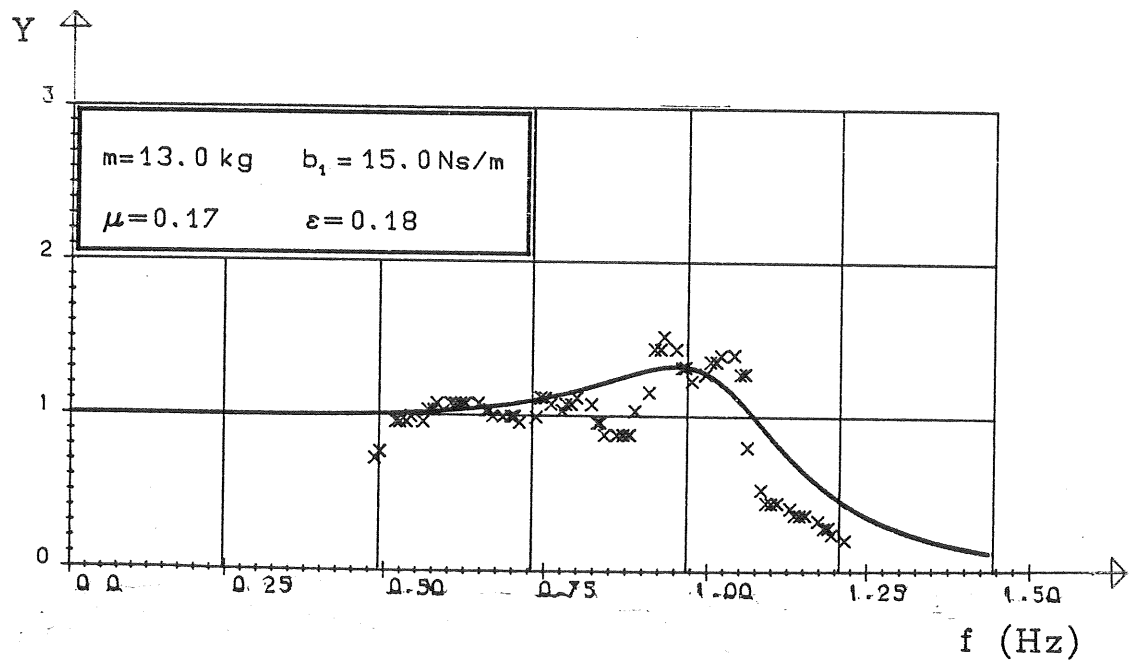
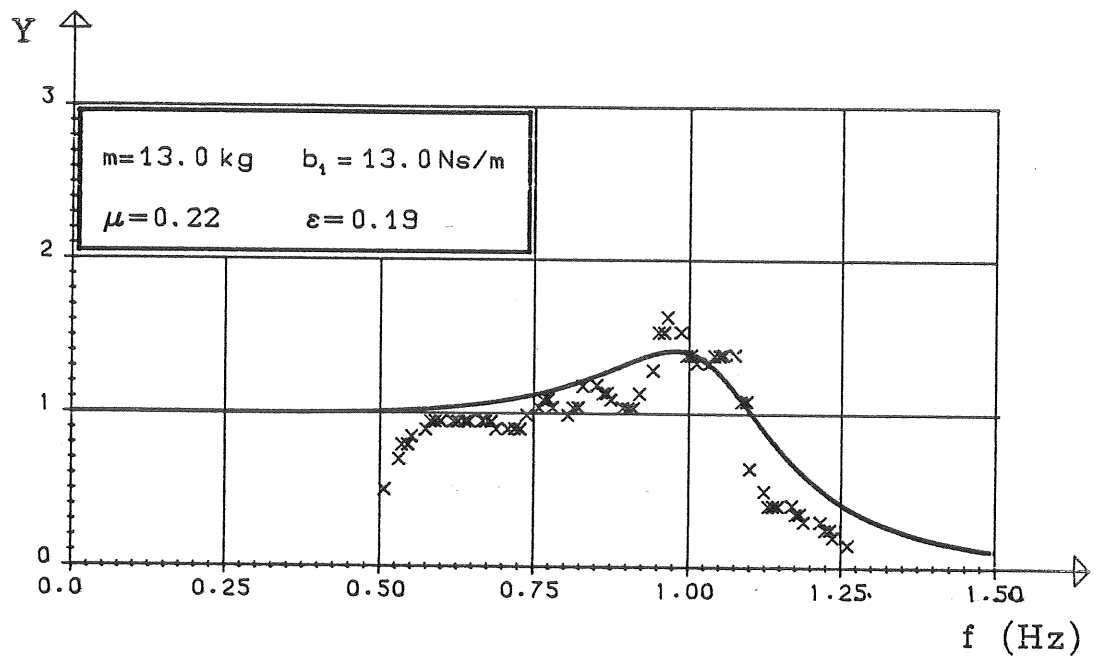


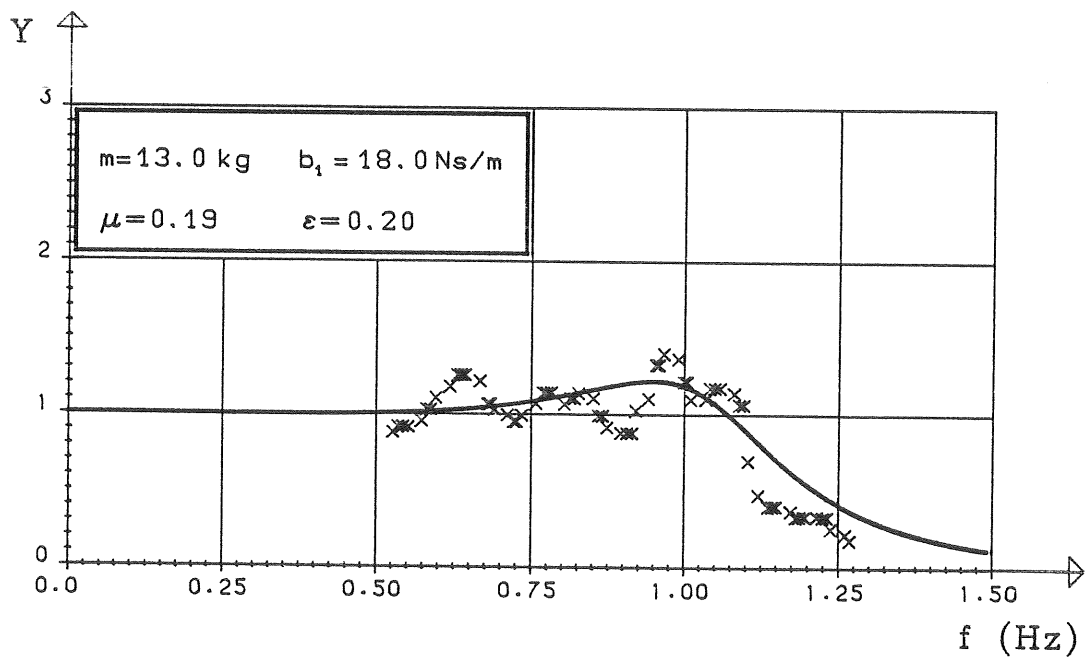
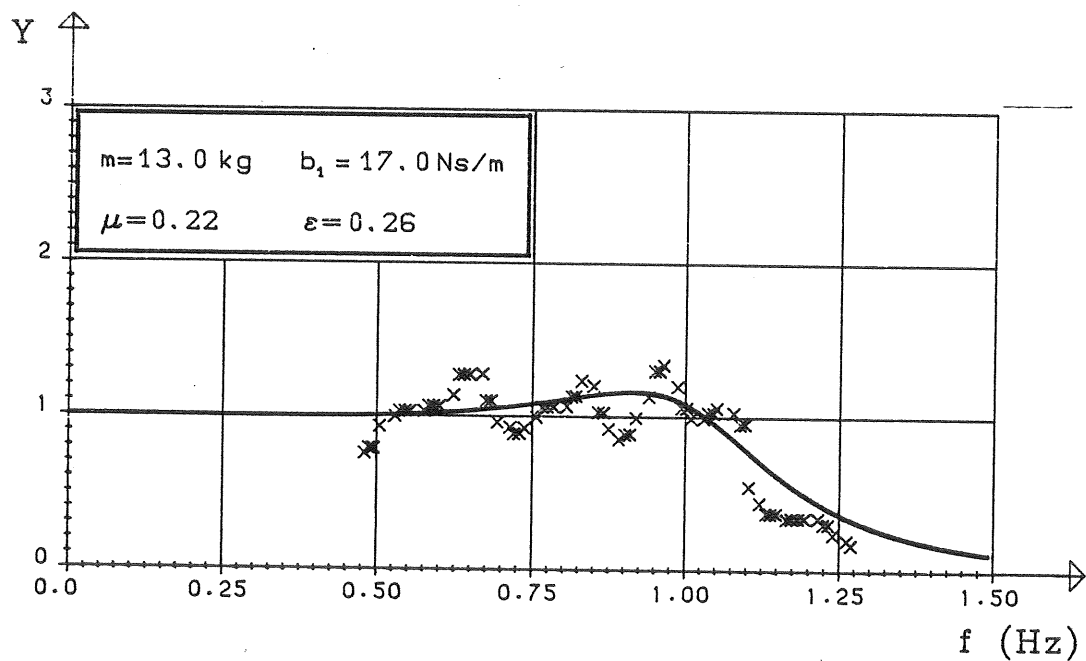
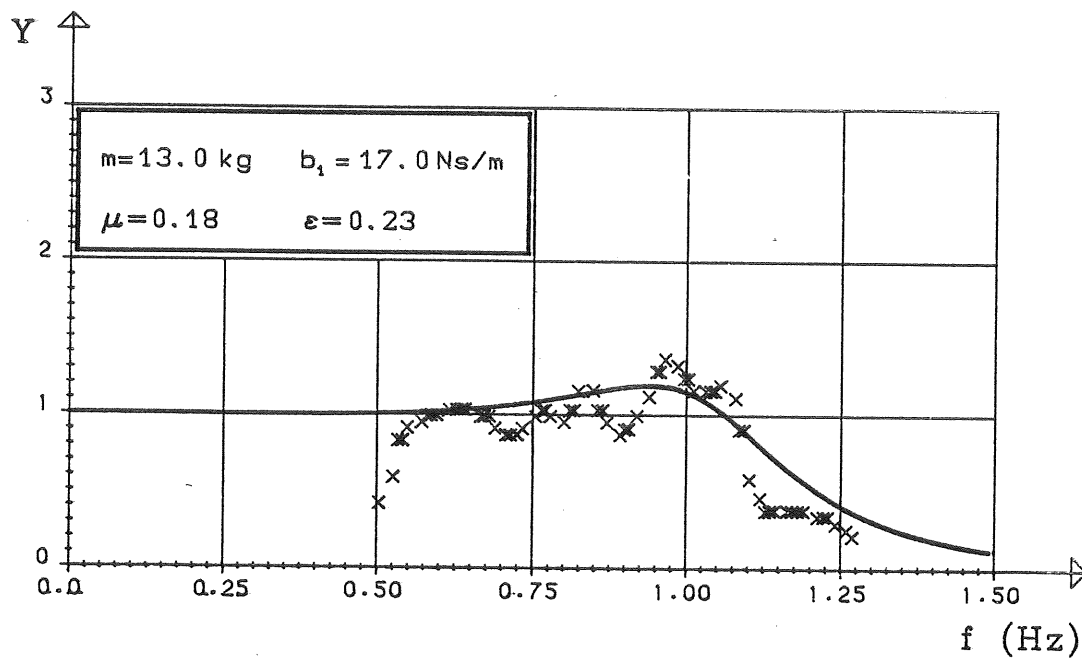


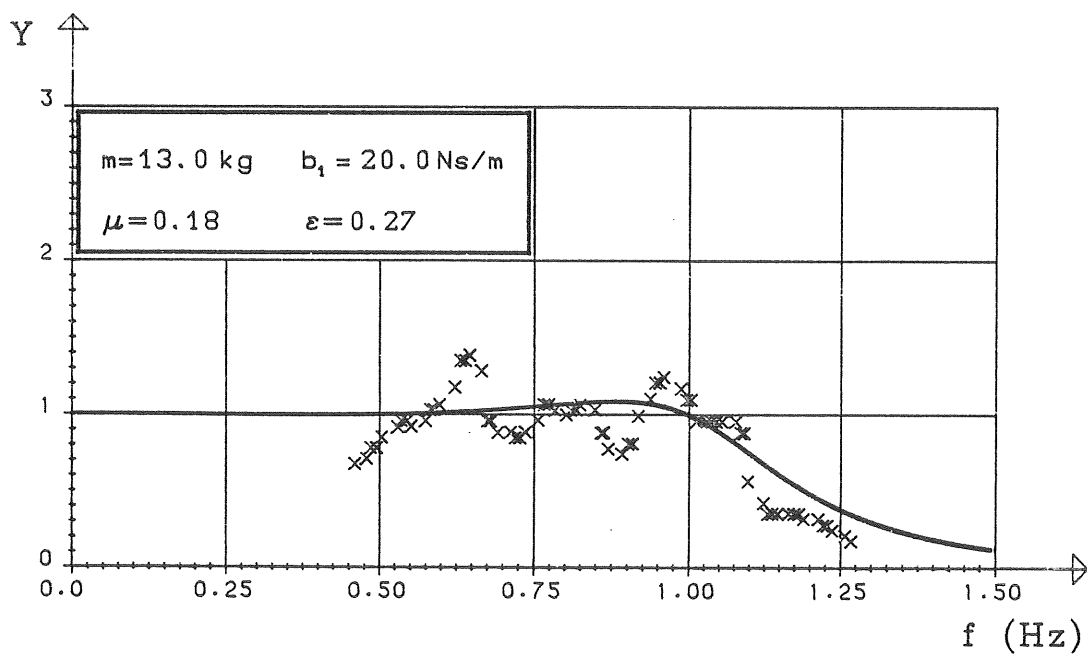
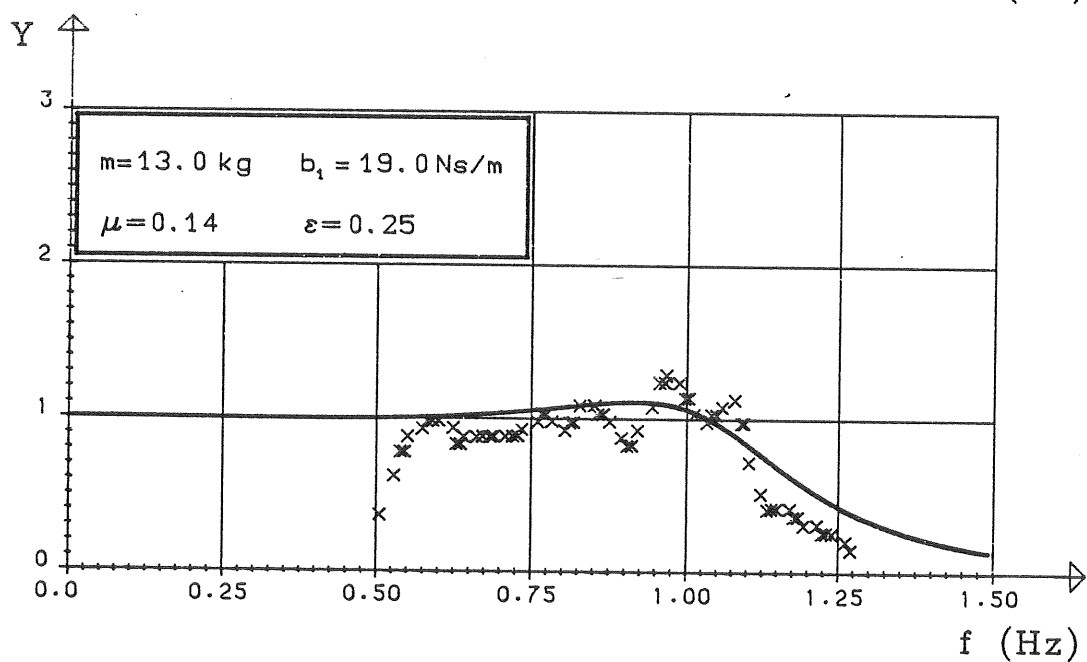
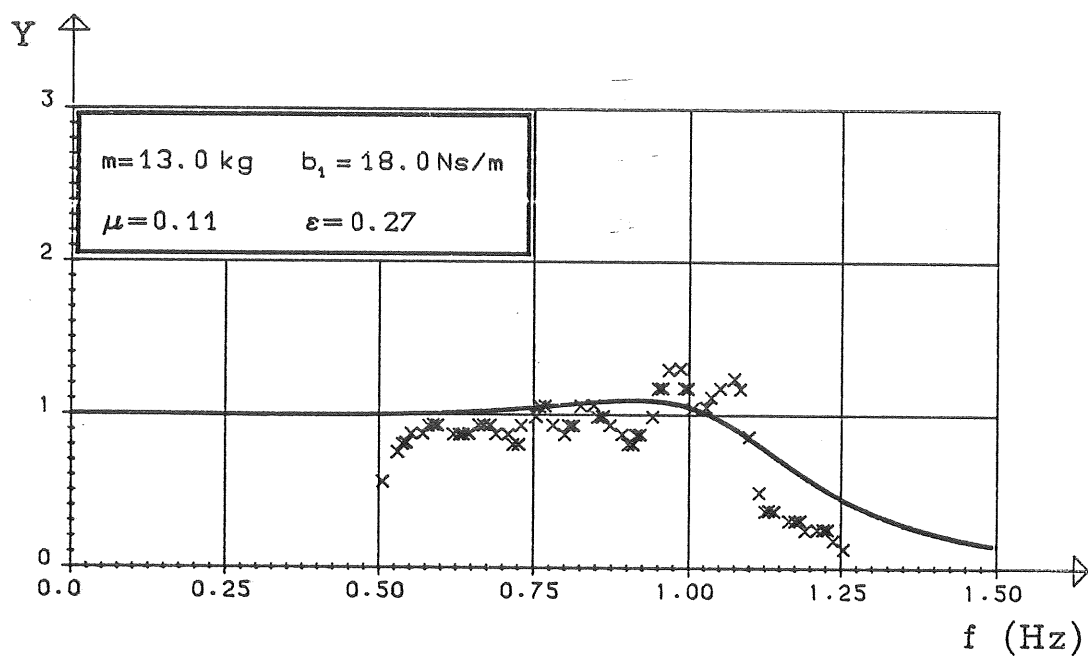


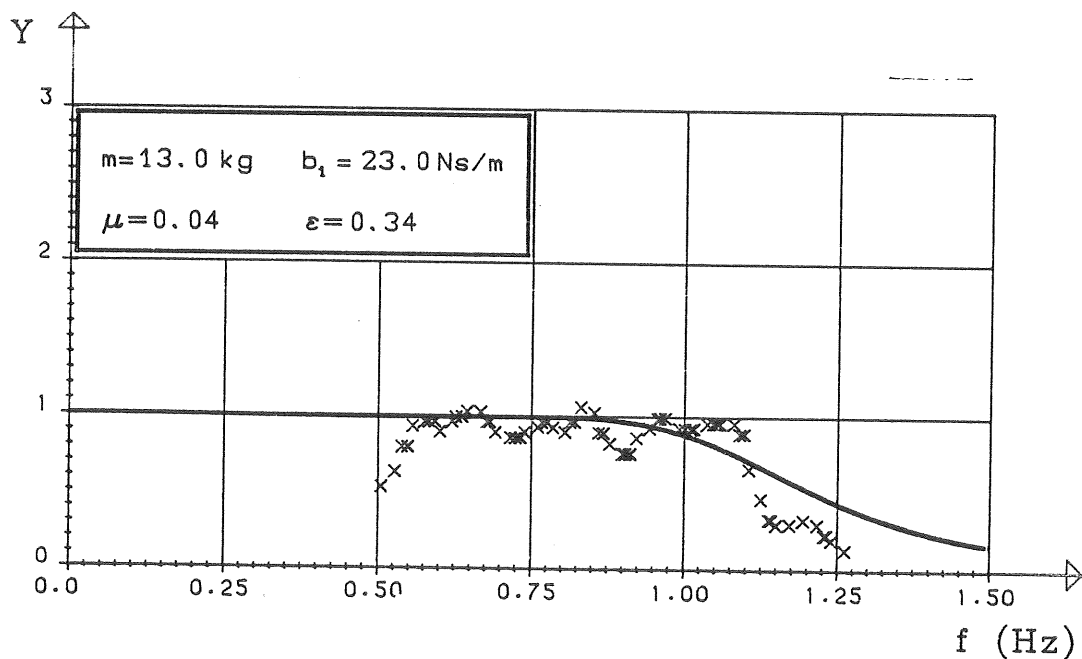
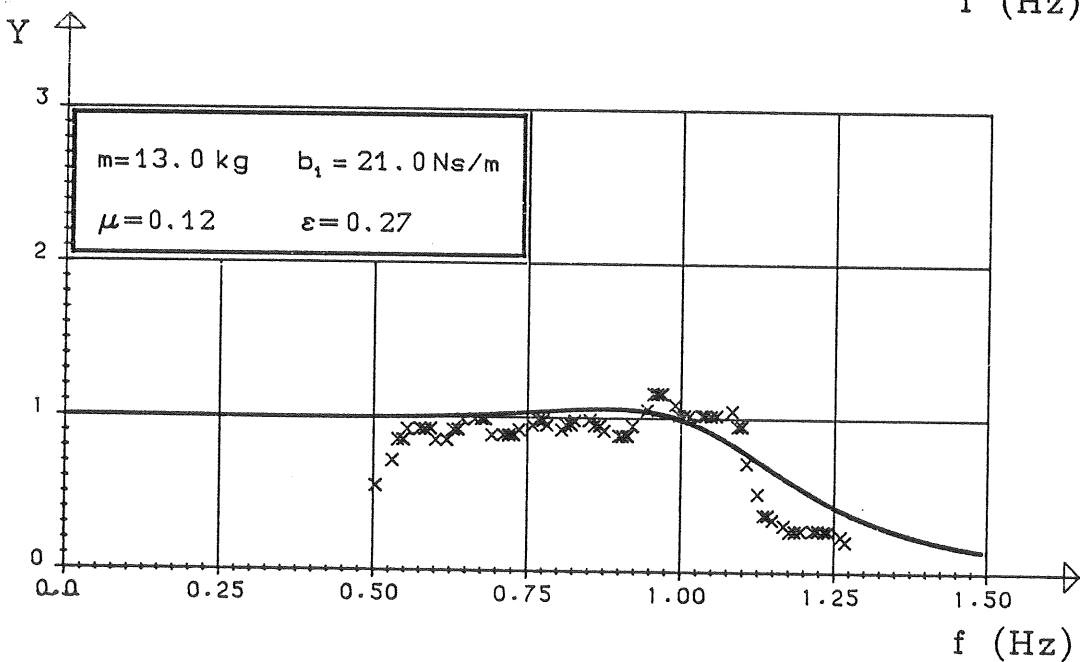
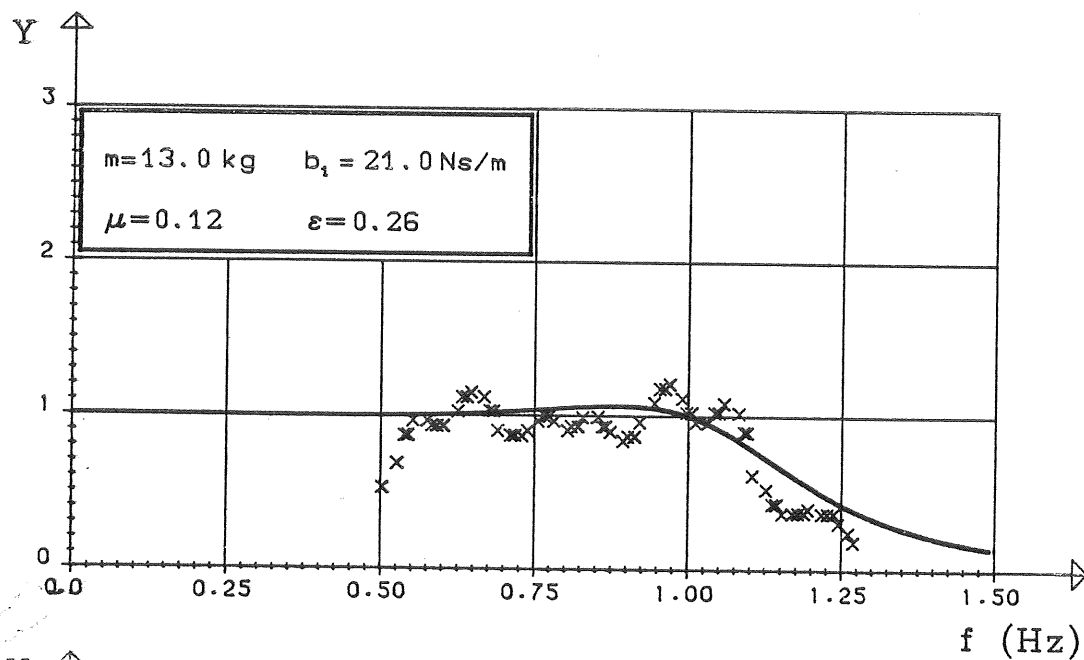
A1.12 BOJMASSA: 13, KG

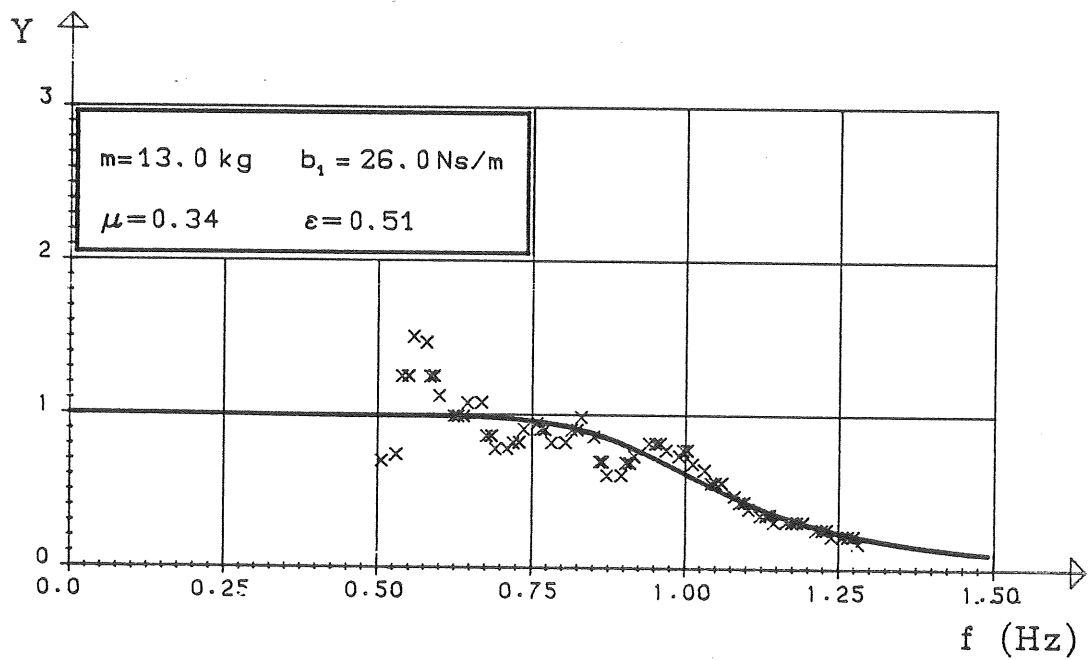
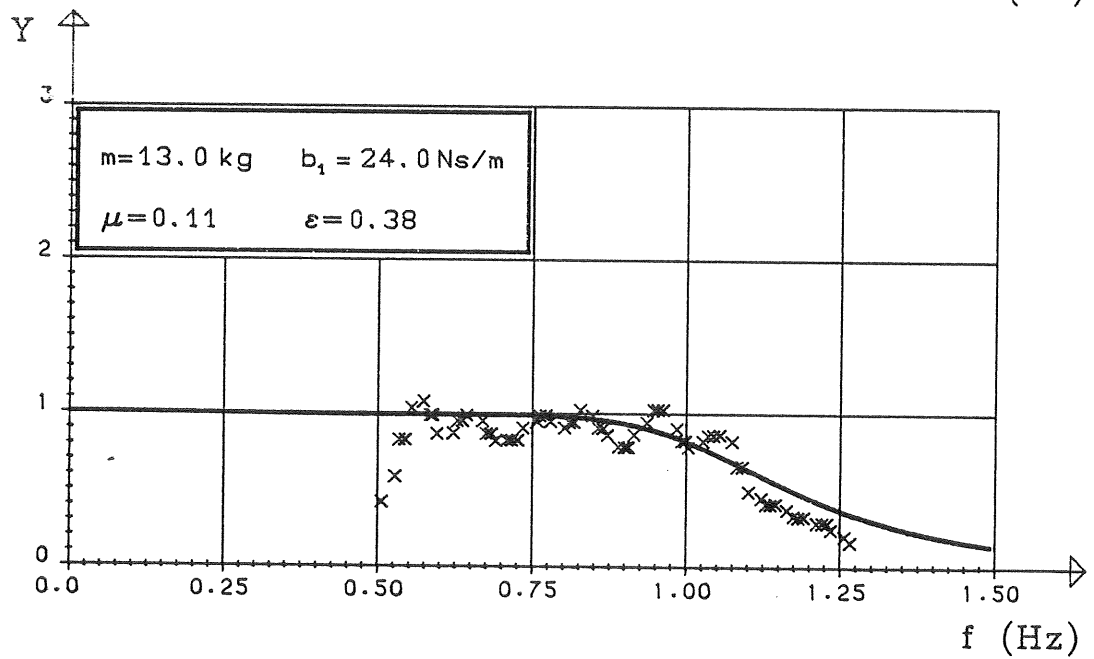
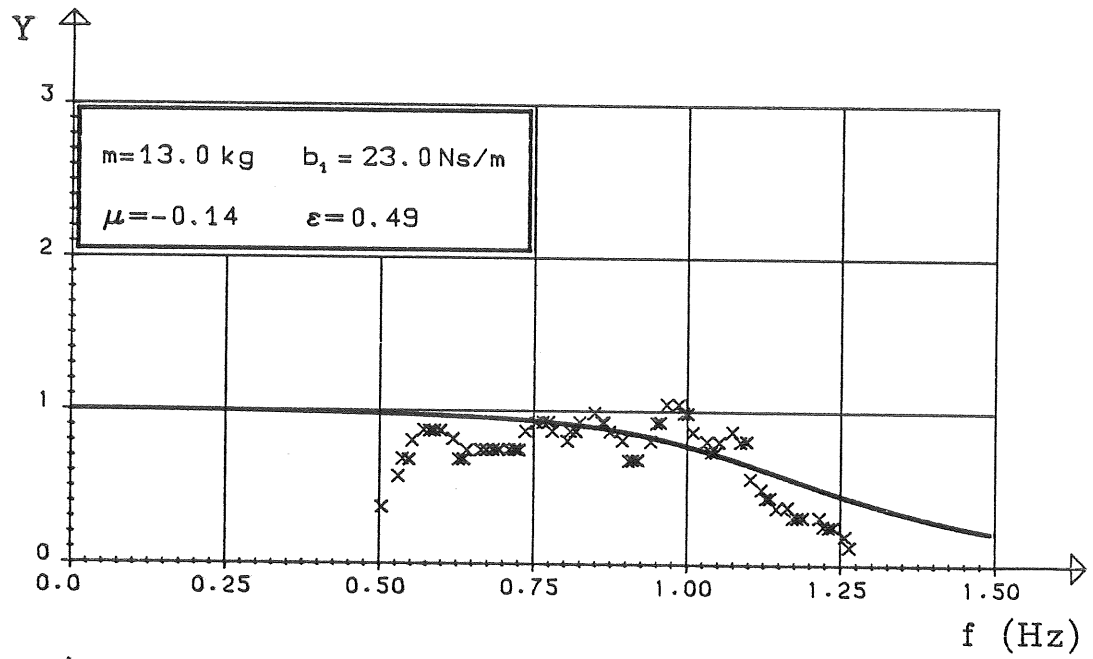
YTTRE DÄMPNING: 13 - 26 Ns/M





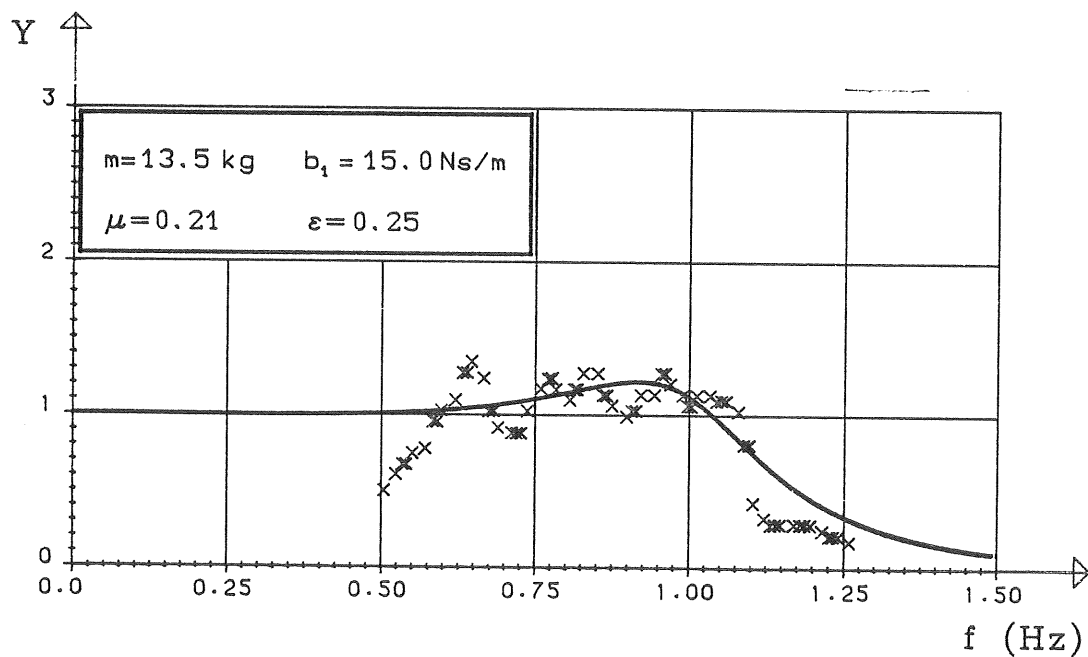
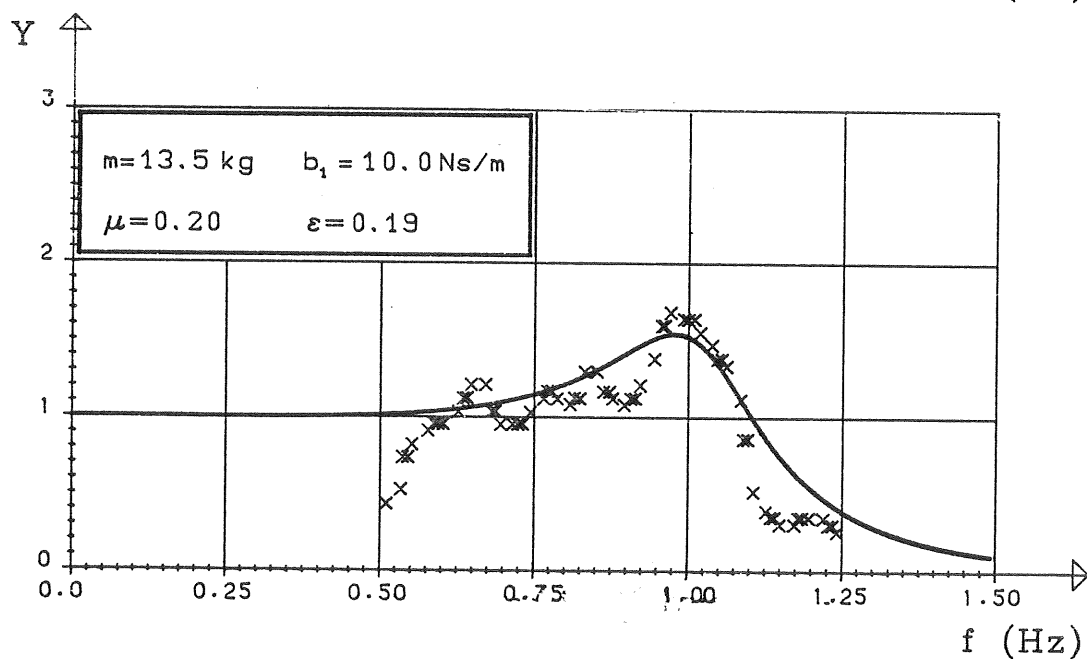
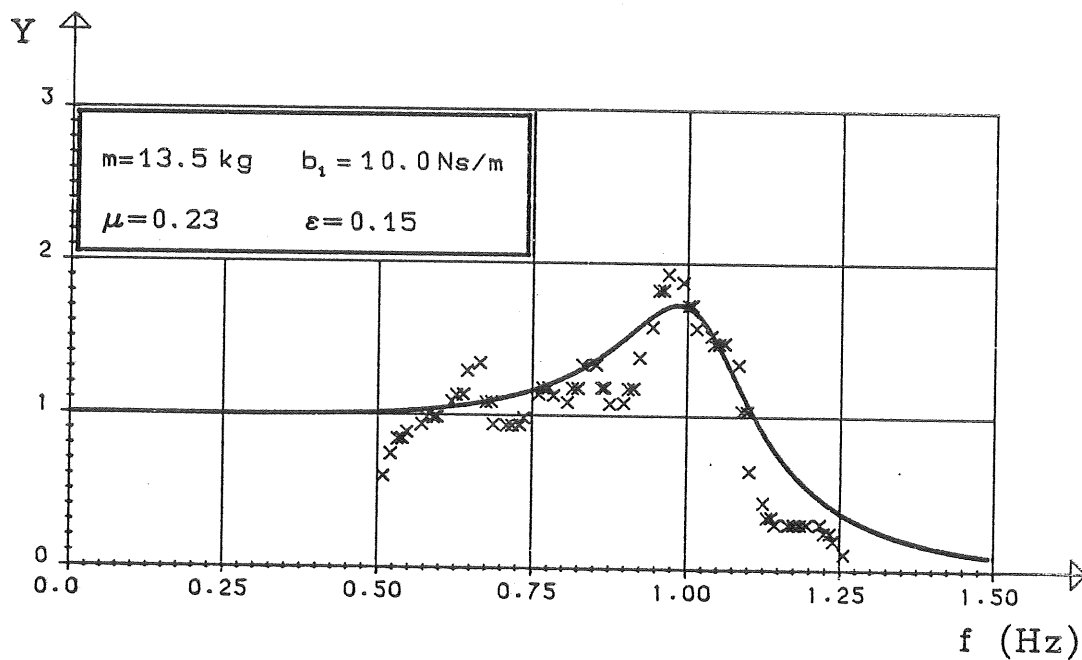


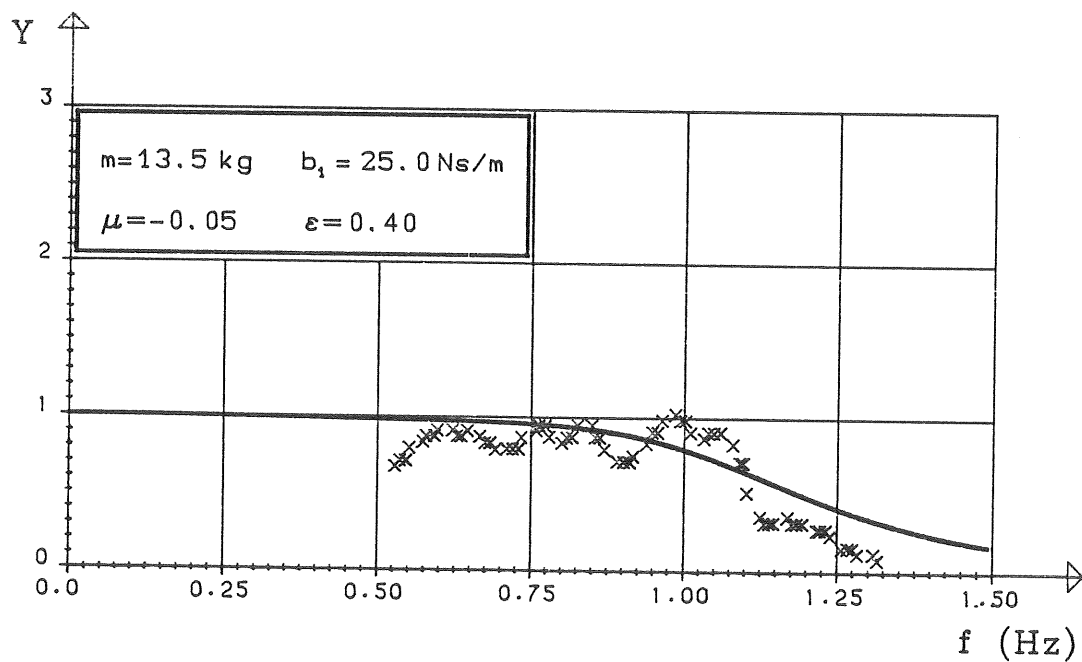
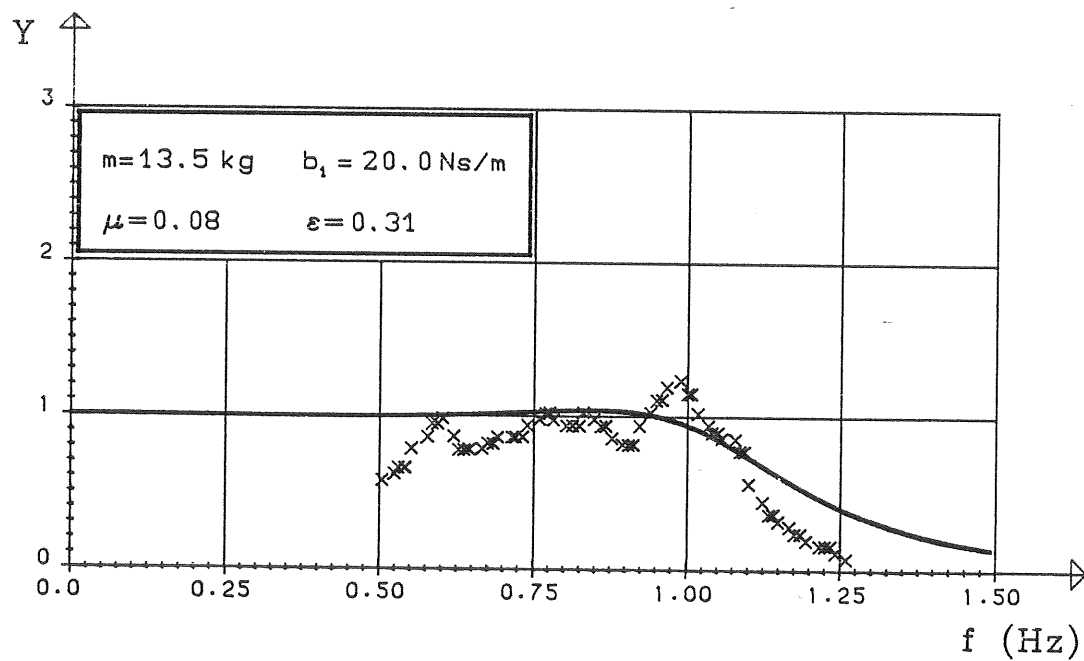
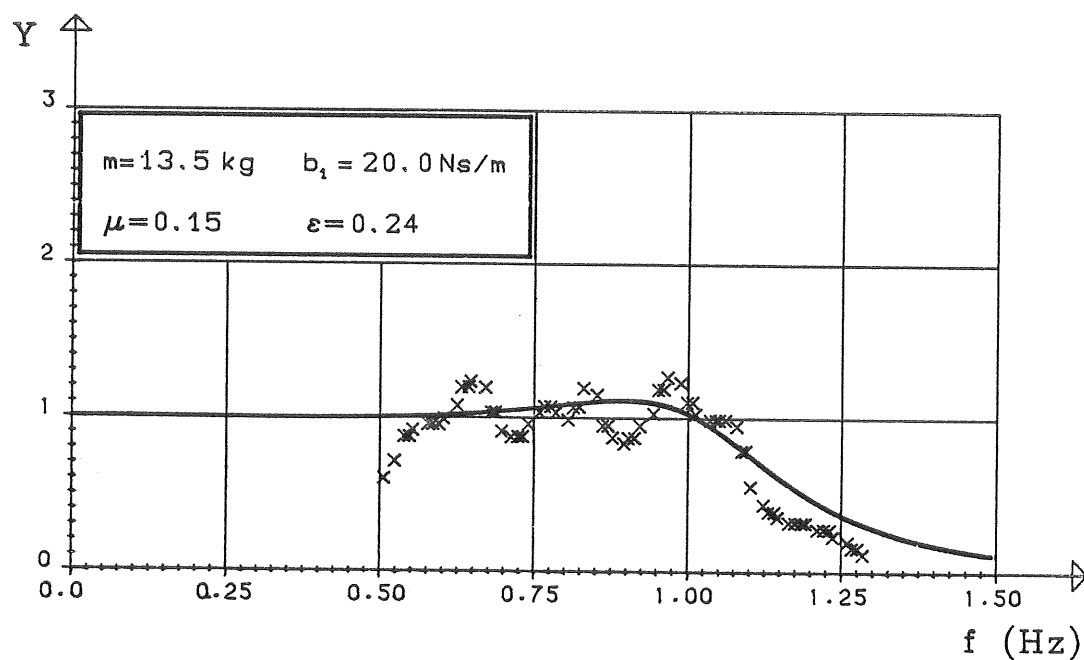


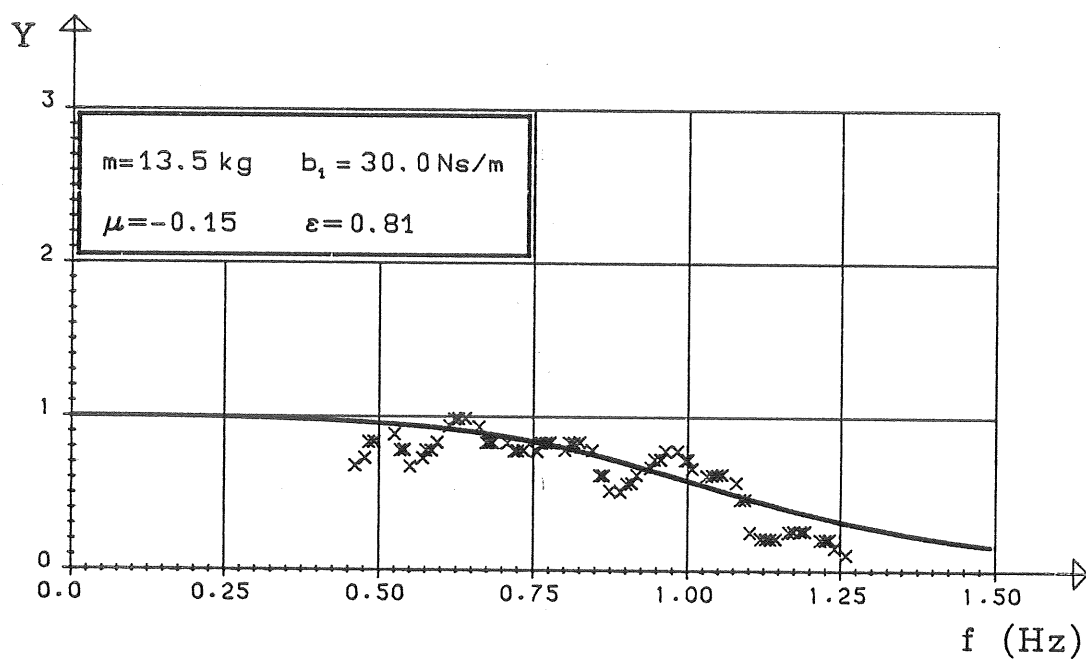


A1.13 BOJMASSA: 13.5 KG

YTTRE DÄMPNING: 10 - 30 Ns/M

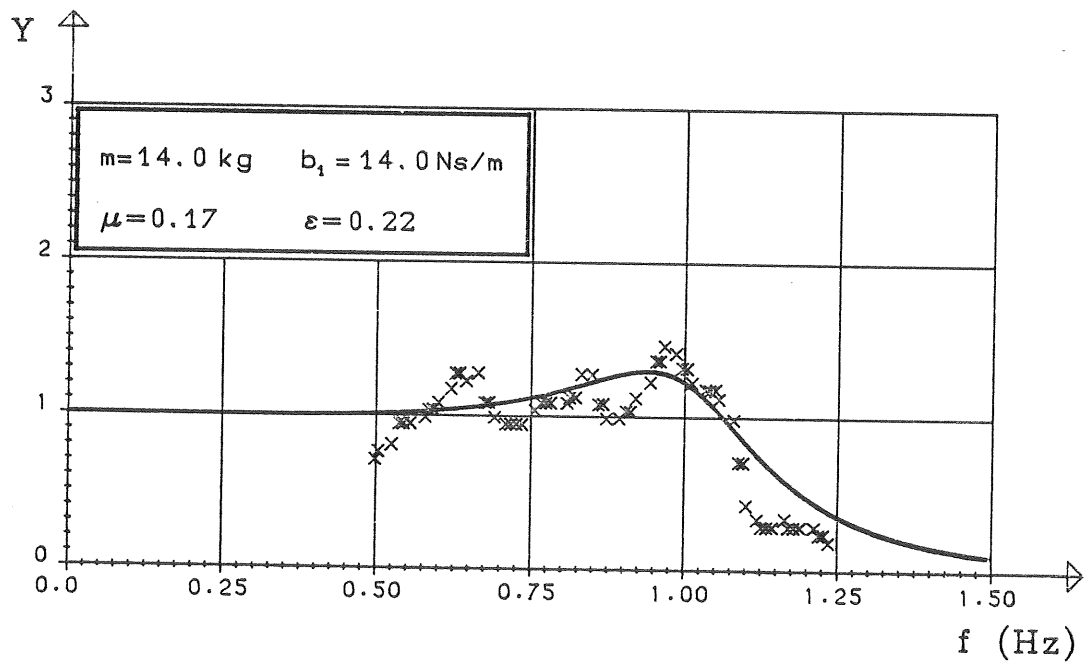
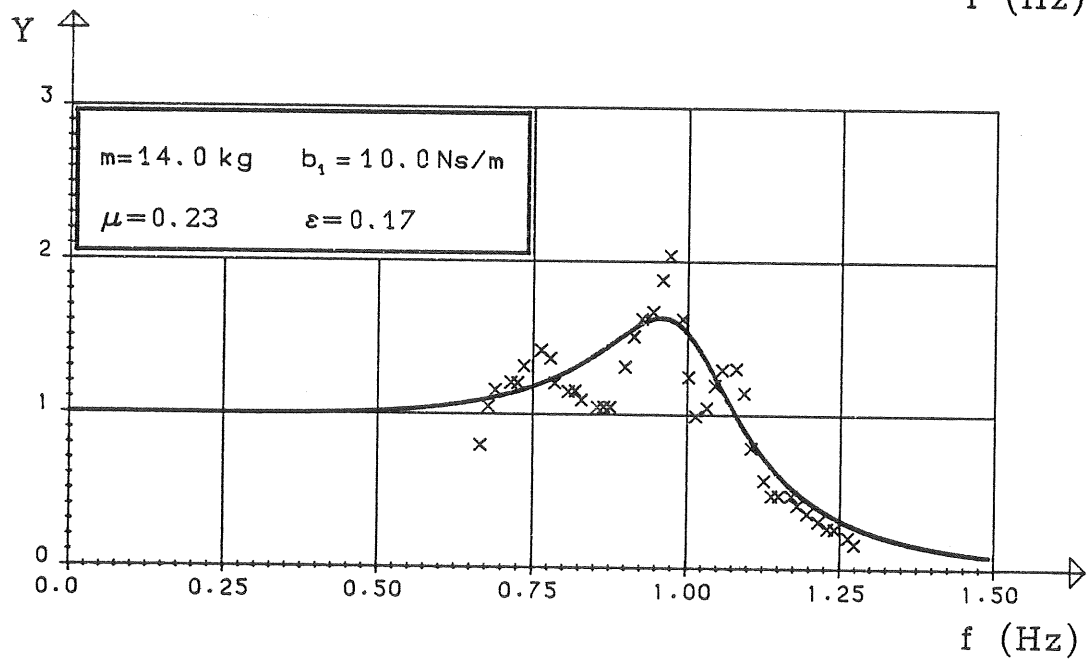
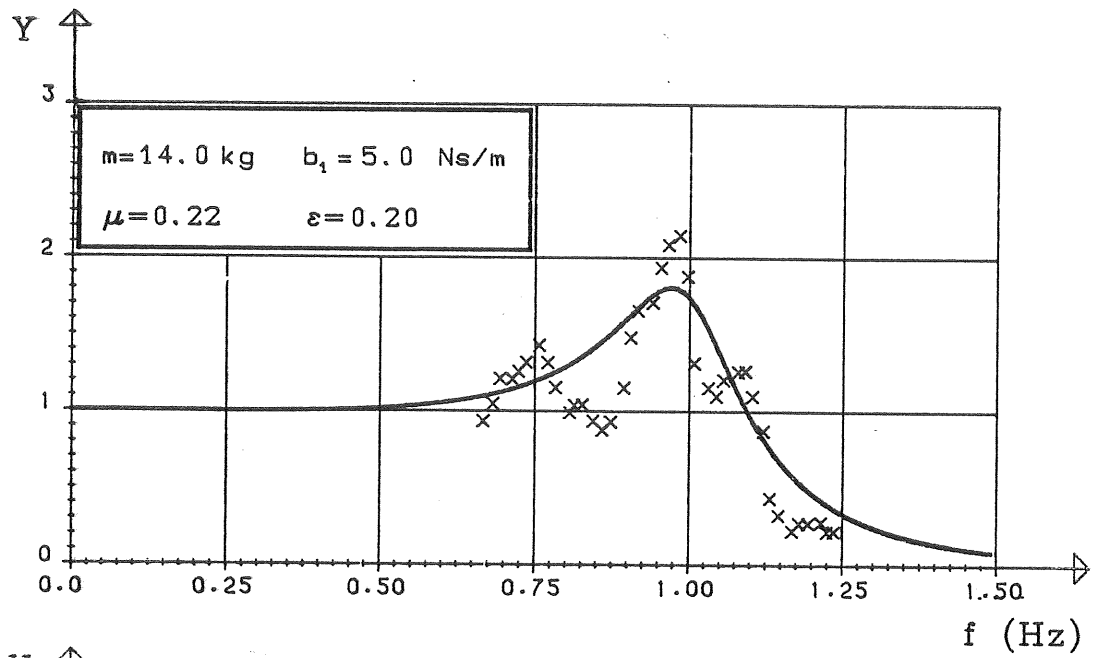


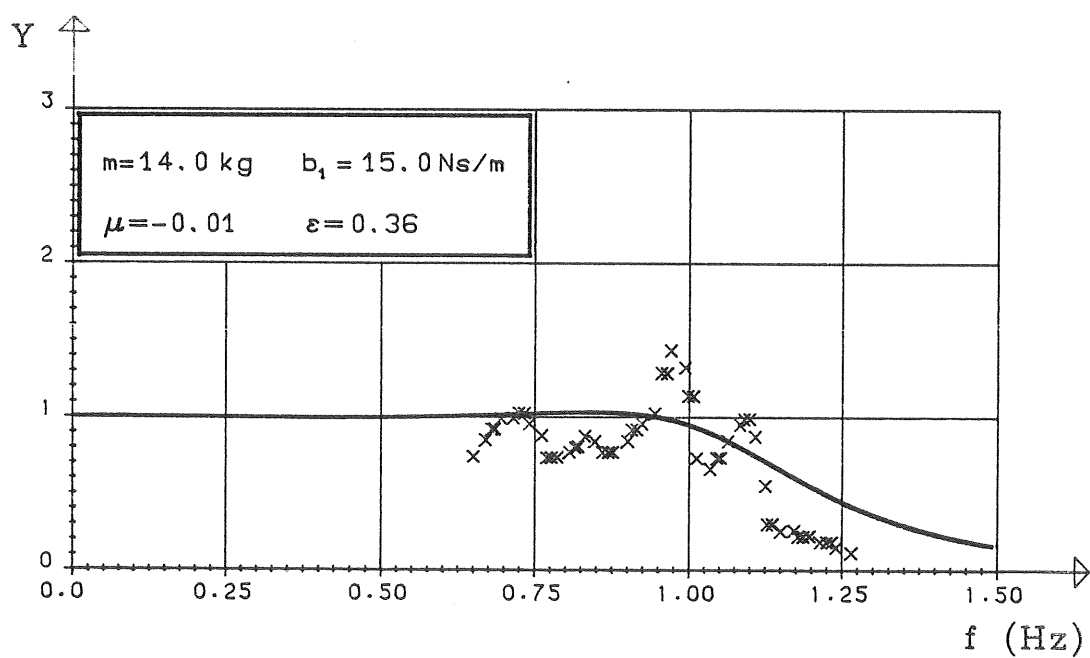
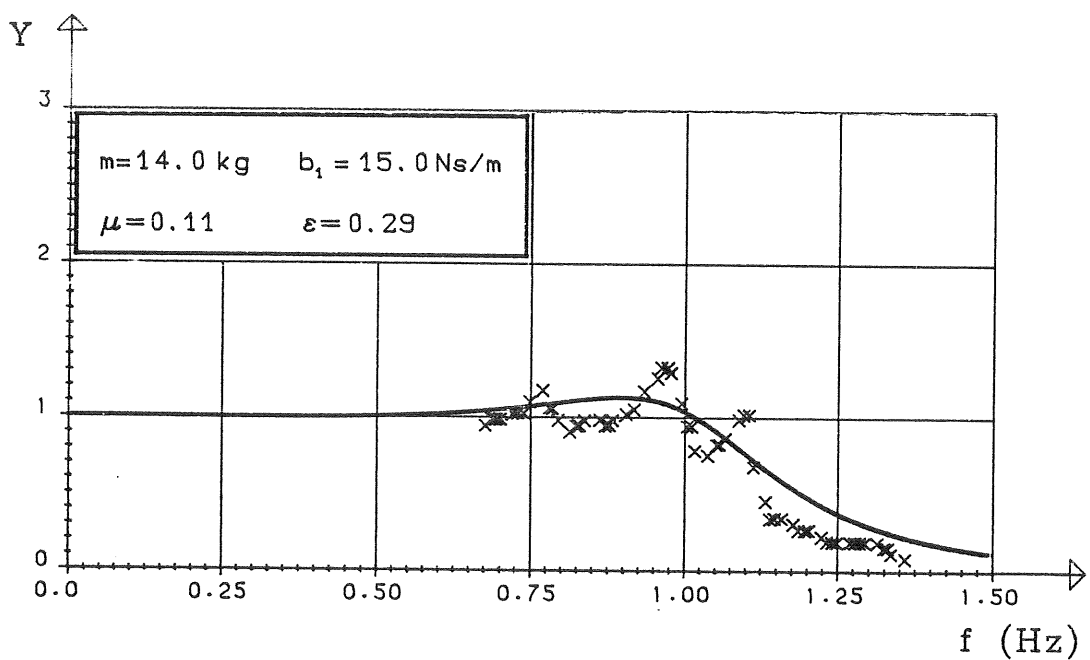
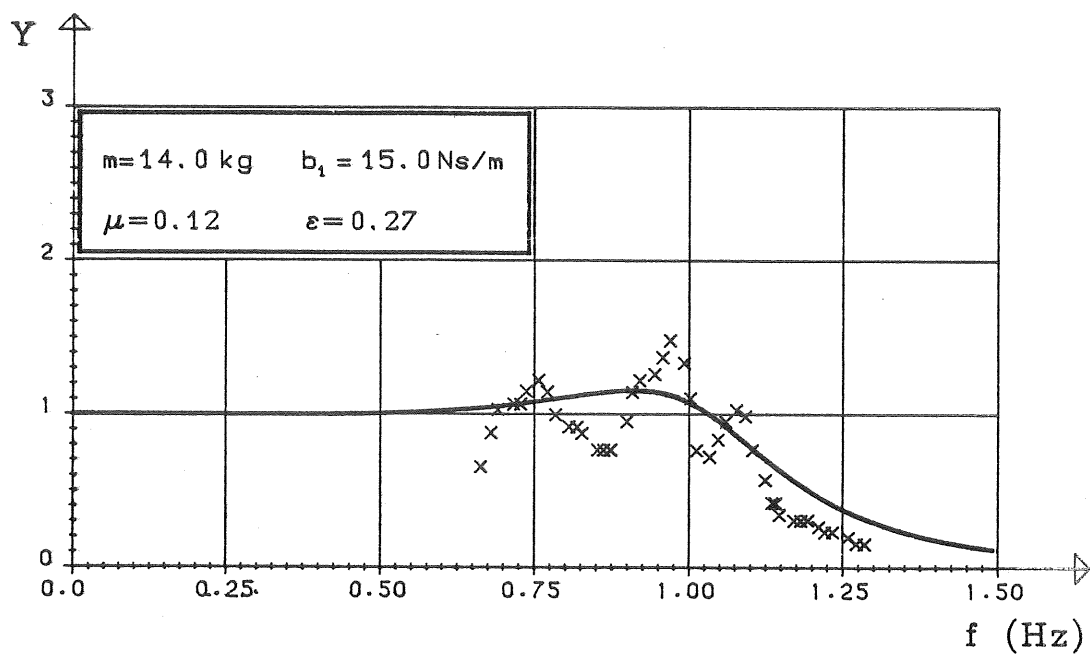


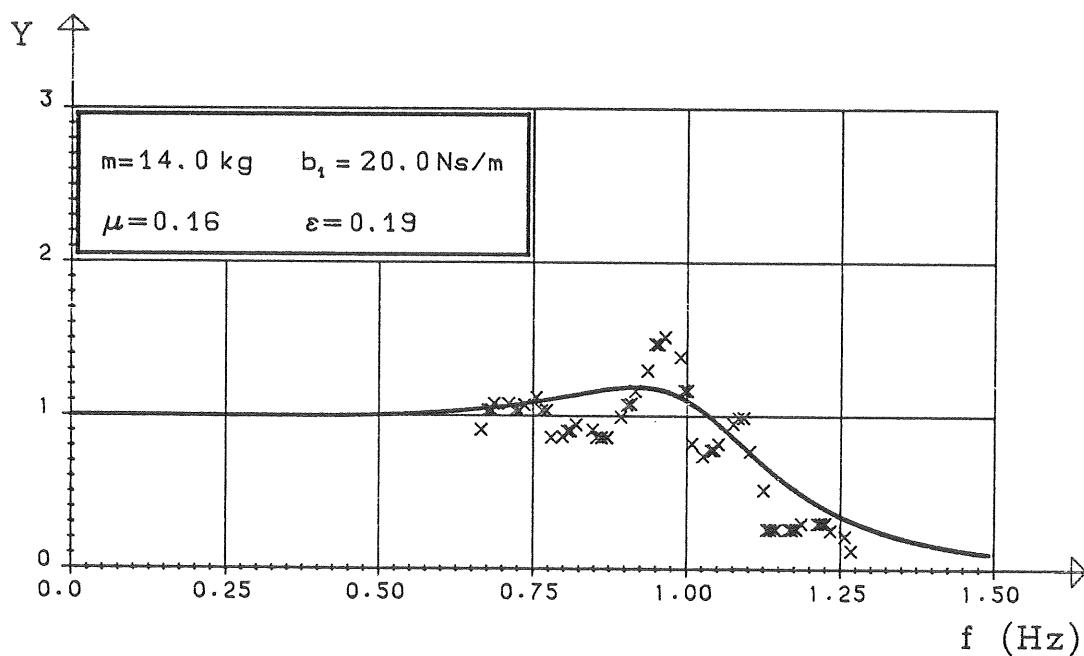
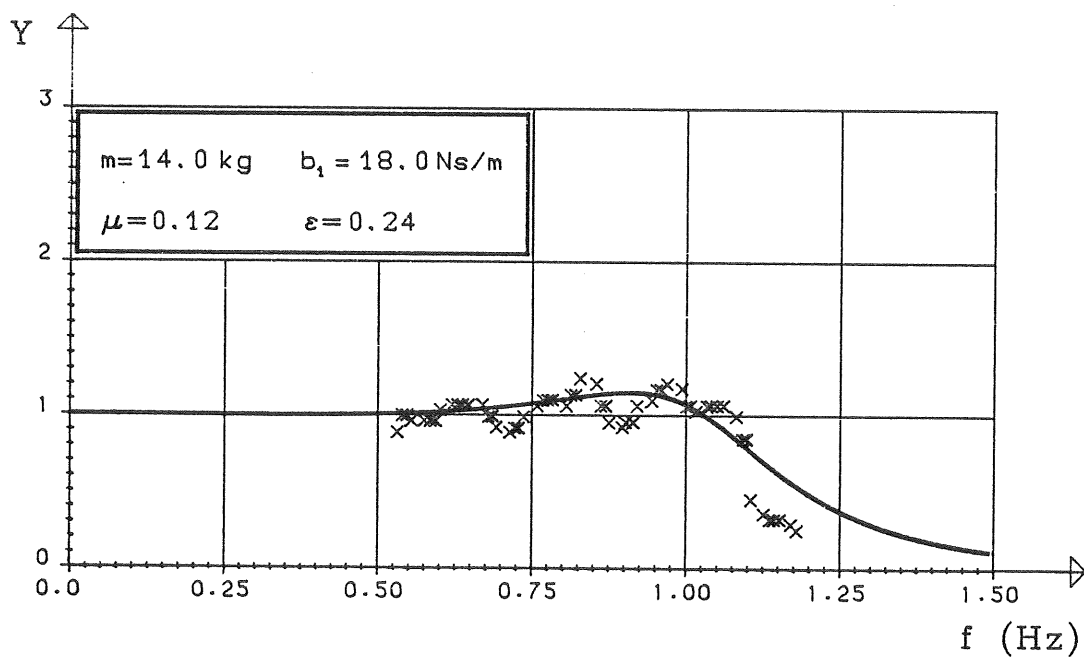
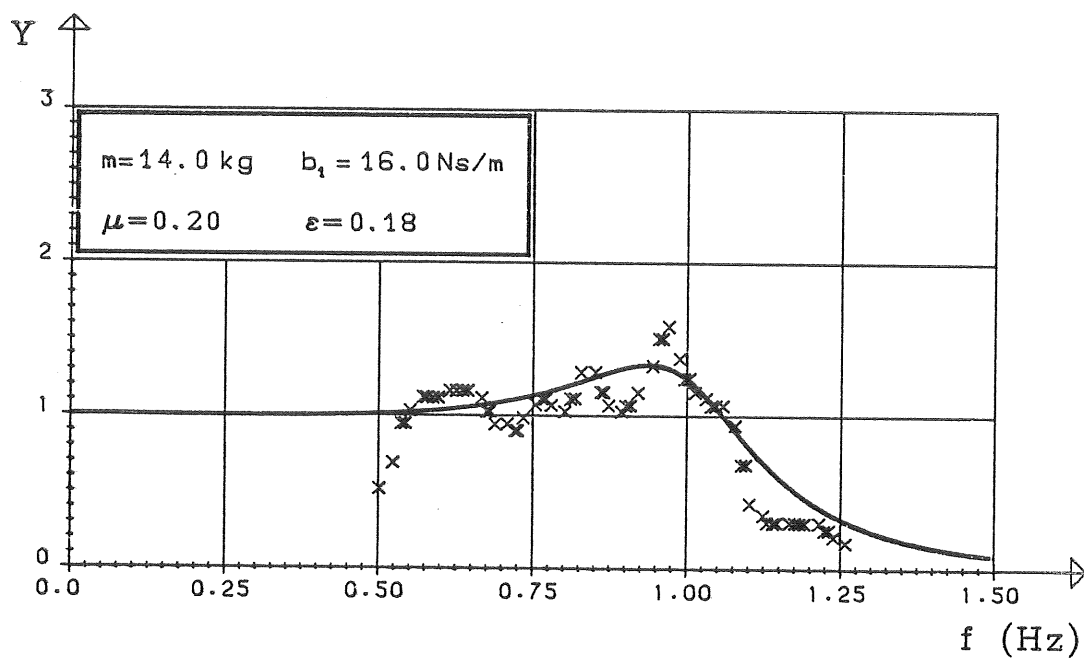


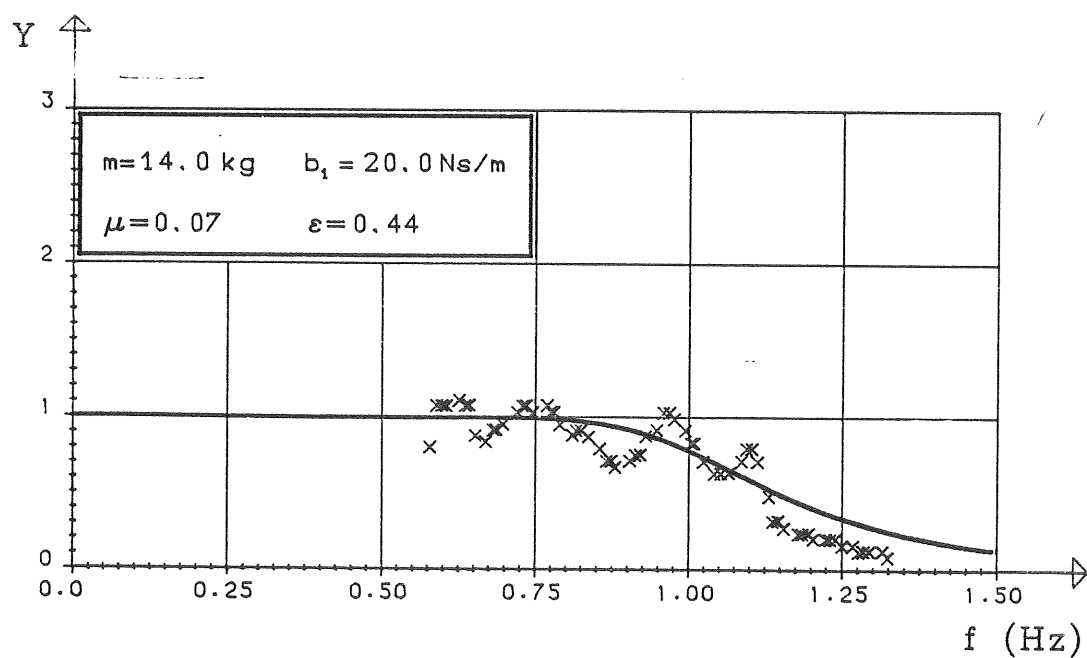
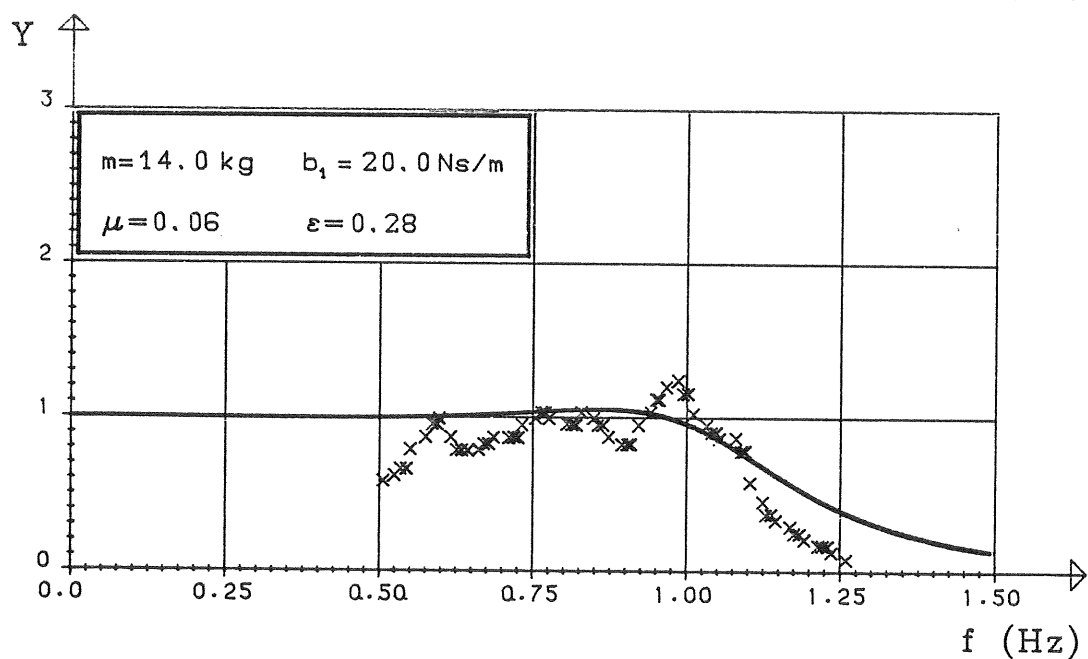
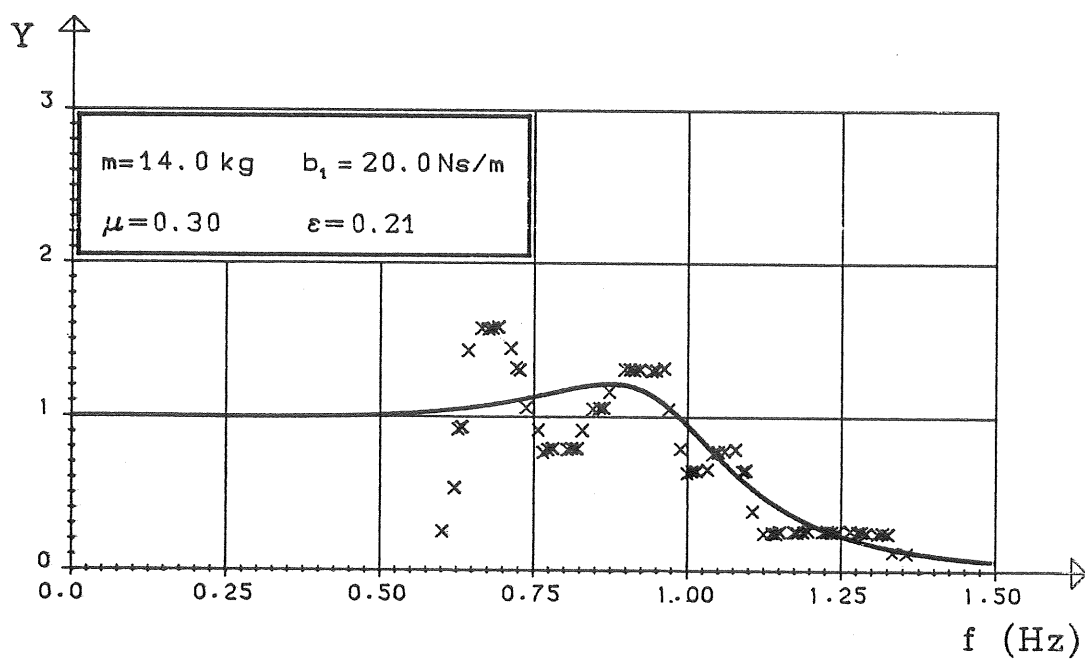
A1.14 BOJMASSA: 14, KG

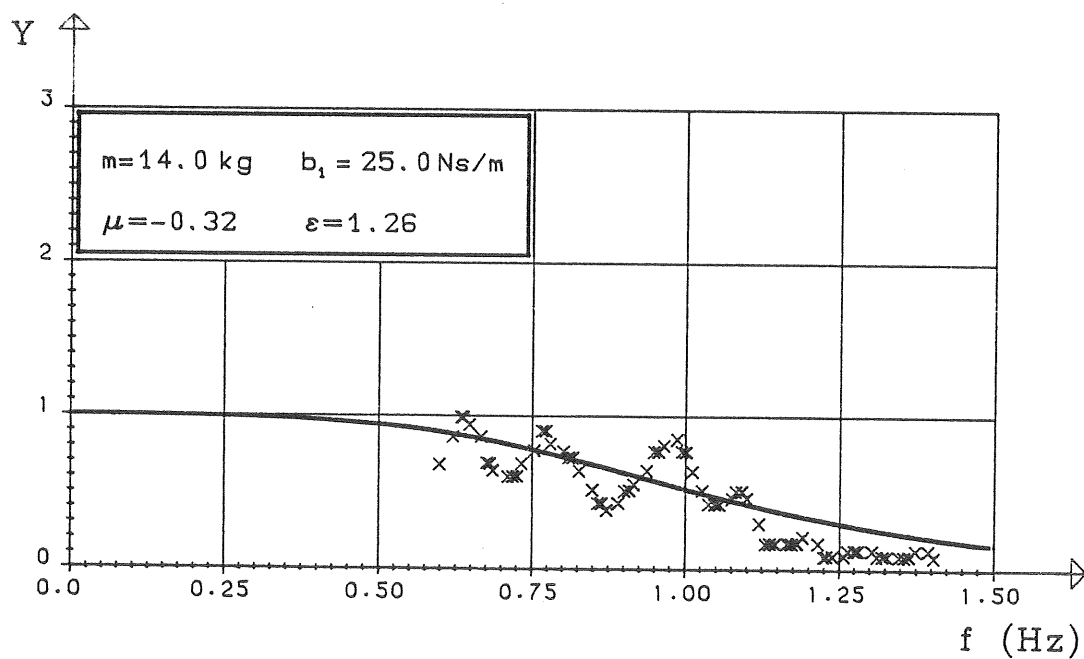
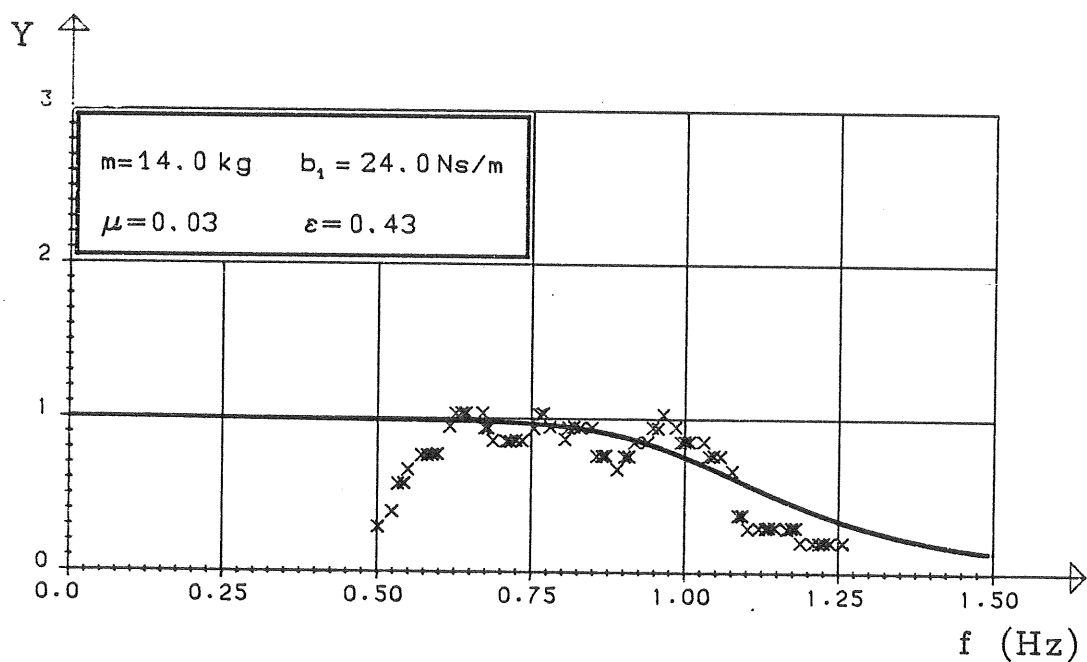
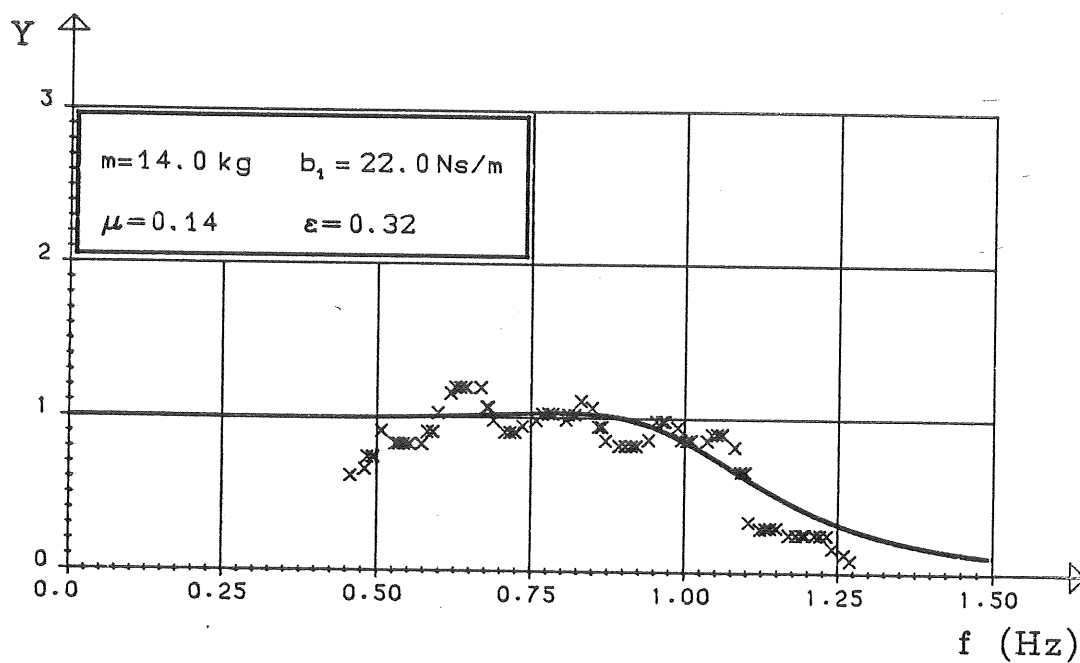
YTTRE DÄMPNING: 5 - 30 Ns/M

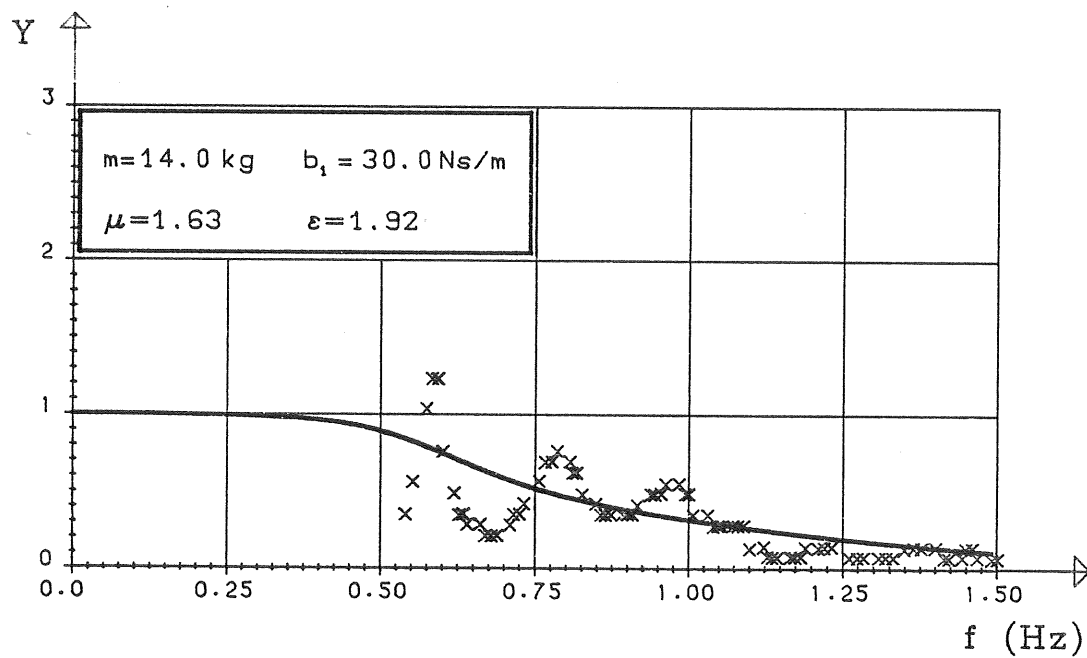
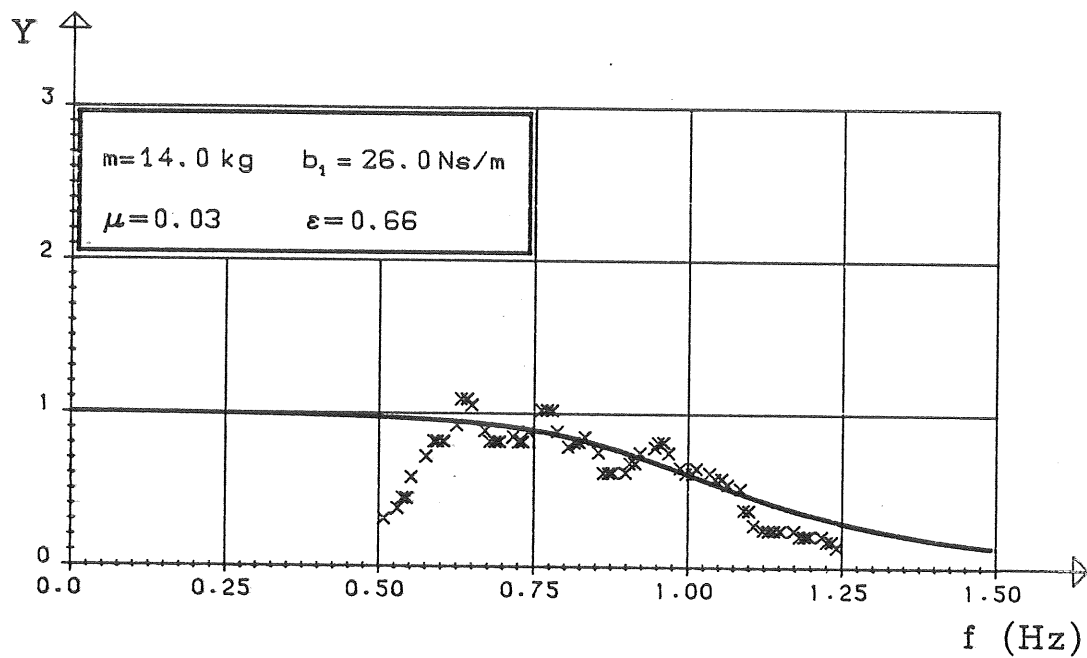






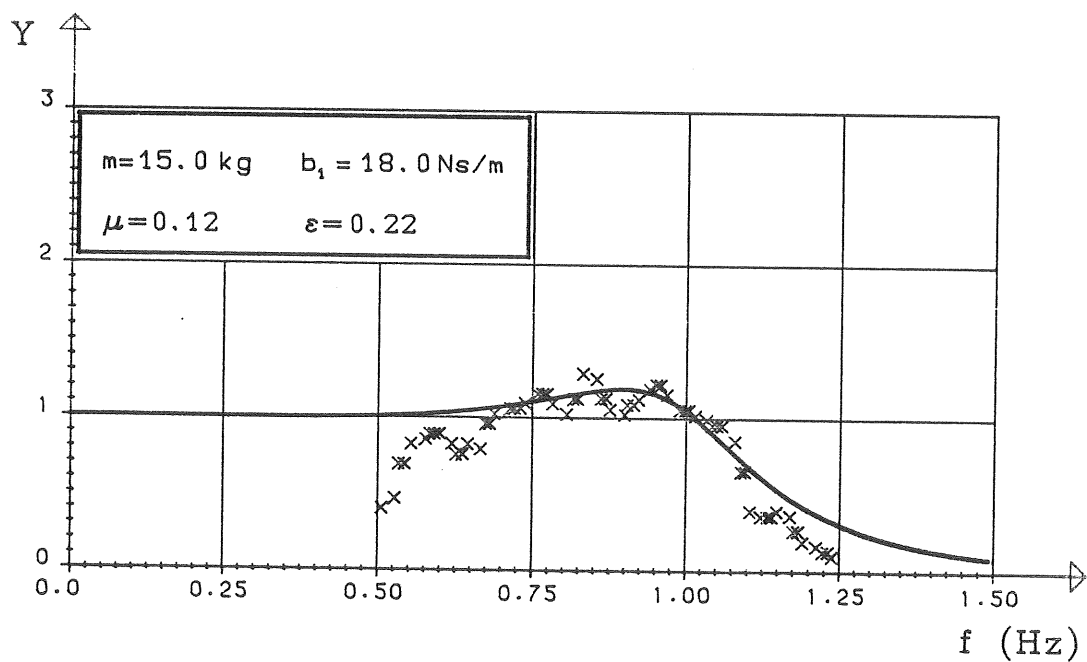
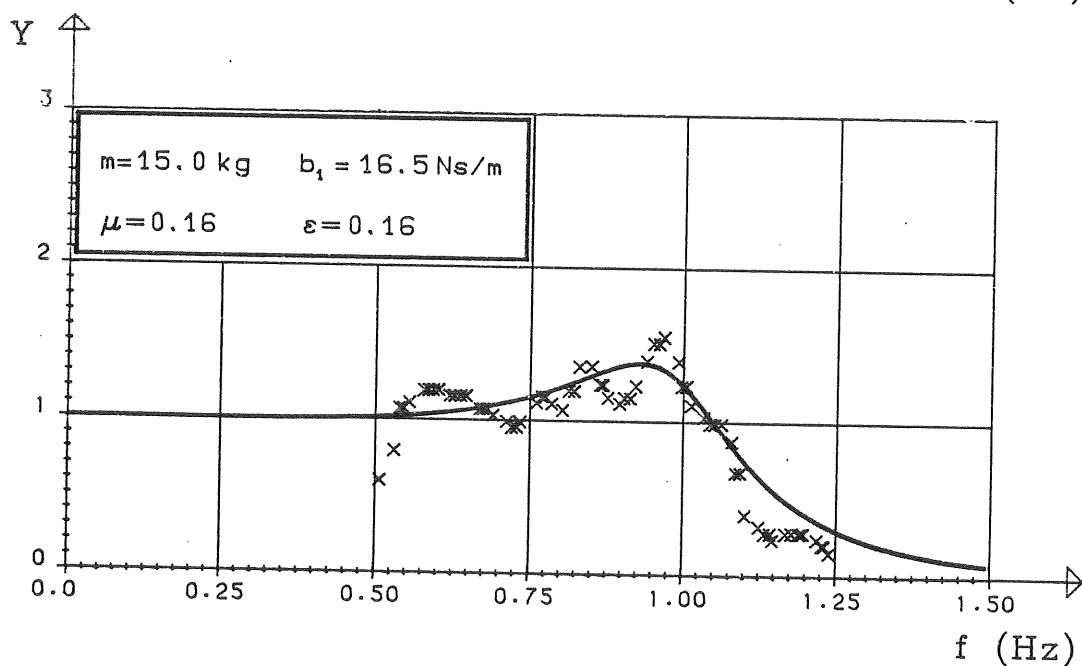
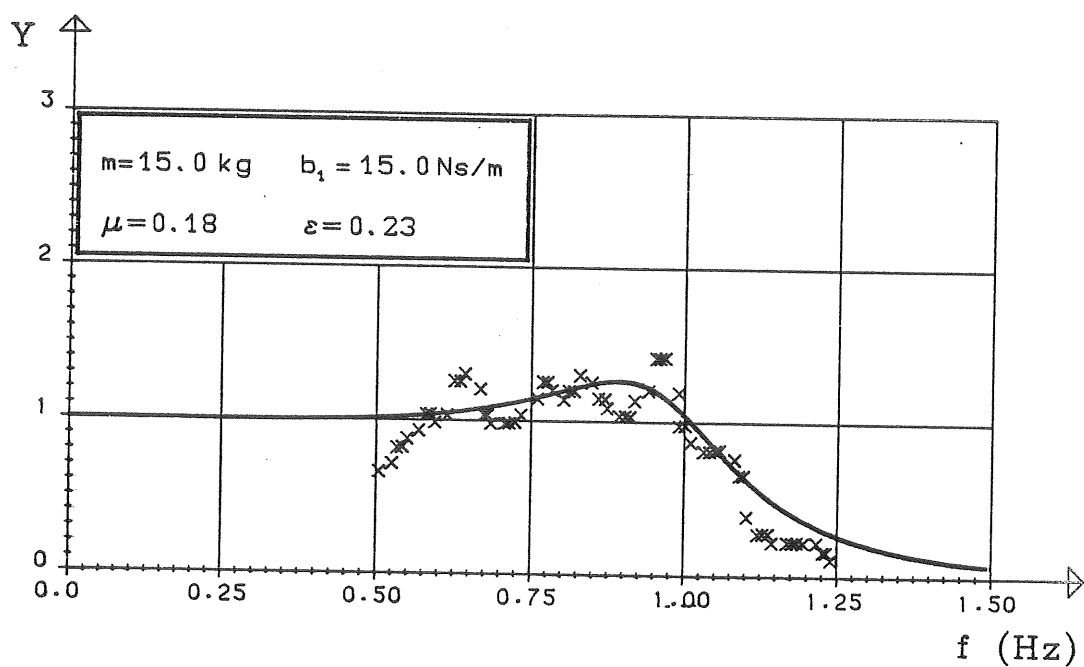


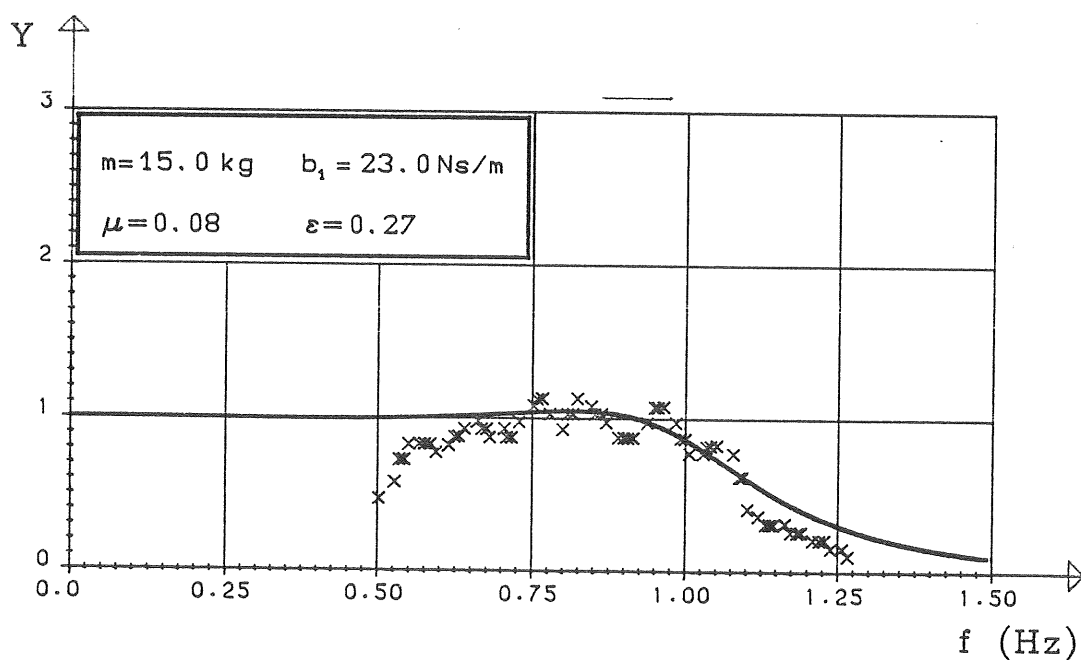
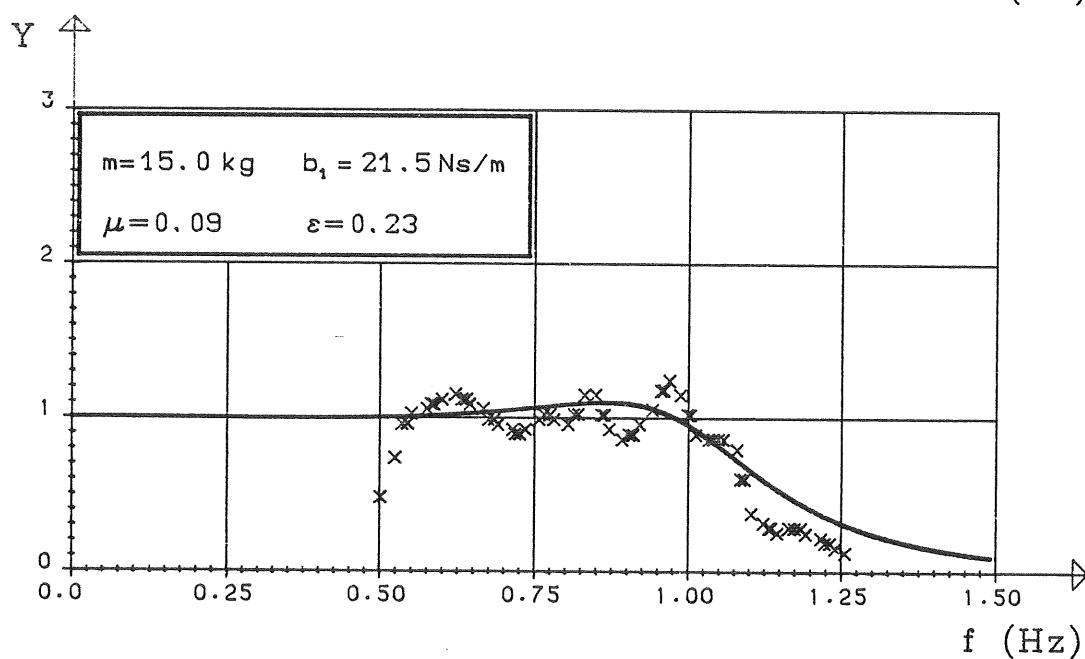
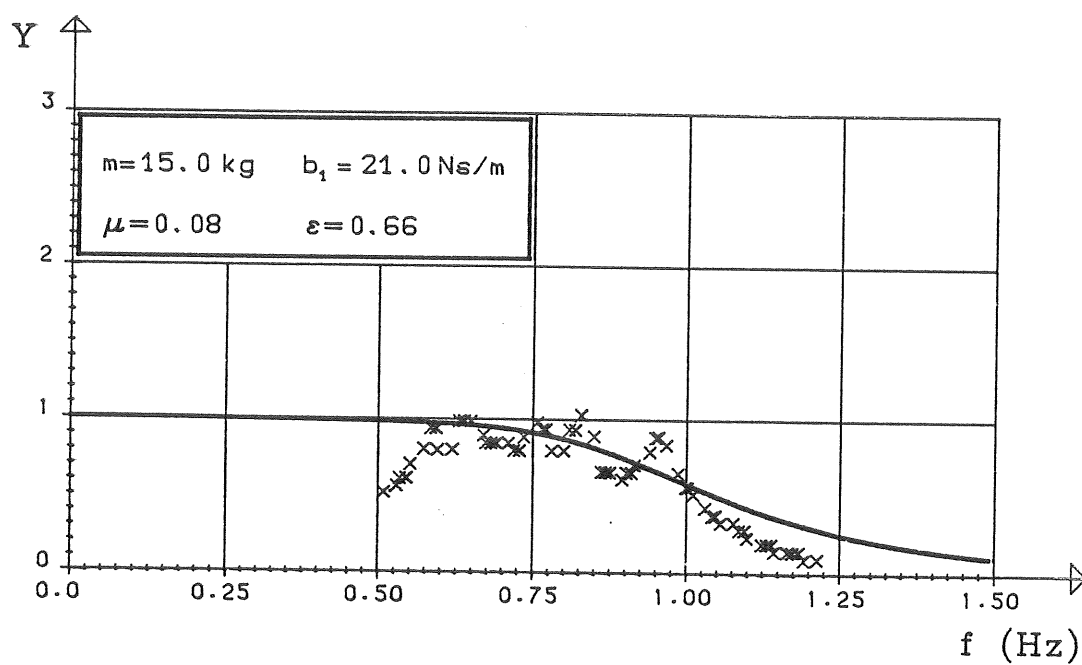


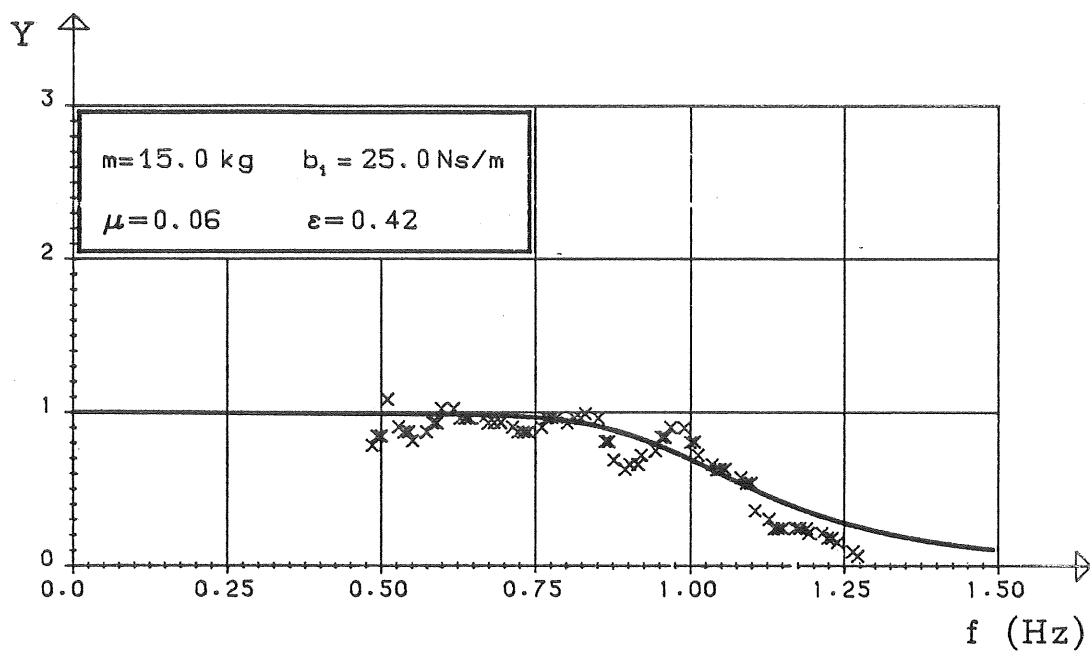


A1.15 BOJMASSA: 15, KG

YTTRE DÄMPNING: 15 - 25 Ns/M







A1.16 BOJMASSA: 16 KG

YTTRE DÄMPNING: 18 - 24 Ns/M

